Glaciers of Alaska:

Mapping and change detection using satellite data and geomatics

---

Dissertation

zur

Erlangung der naturwissenschaftlichen Doktorwürde

(Dr. sc. Nat.)

vorgelegt der

Mathematisch-naturwissenschaftlichen Fakultät

der

Universität Zürich

von

Raymond Louis André Le Bris

aus

Frankreich

Promotionskomitee

Prof. Dr. Wilfried Haeberli (Vorsitz)
Dr. Frank Paul (Leitung der Dissertation)
Dr. Étienne Berthier

Zürich 2013

Summary

Glaciers and ice caps are among the most evident natural features affected by atmospheric conditions (i.e., temperature and precipitation) and their changes through time. They are key indicators of climate change, as their ice is in most regions of the world close to the melting point, i.e. a large part of energy input is used to melt the ice. Accordingly, strong changes in glacier geometry are observed since the end of the Little Ice Age (LIA) around the 1850s in many regions of the world. This is especially the case for the maritime glaciers located around the Gulf of Alaska, where a strong mass loss with an accelerating rate for the last few decades is reported for many glaciers. Assessments of the overall impact of climate change on glaciers in Alaska and accurate estimation of their past or future contribution to global sea-level rise requires a complete and accurate inventory of all glaciers in this region. Unfortunately, large data gaps existed in the available databases (i.e. World Glacier Inventory and Global Land Ice Measurements from Space), which hampered precise analysis and calculation of future changes so far.

This thesis presents the results of a large-scale glacier mapping effort for an important part of western Alaska (from the Chugach to the Chigmit Mountains) to improve its poor representation in the database mentioned above. The thesis is also a contribution to the European Space Agency (ESA) GlobGlacier project, which is part of an international effort to map all glaciers globally.

Only glacier inventories in a digital format (vector outlines) allow for assessment of geometry changes and digital modelling in a consistent and reproducible manner. Several previous studies have already demonstrated the usefulness of optical satellite images and Digital Elevation Models (DEMs) to compile such an inventory. In this thesis the well-established semi-automated band ratio method (TM3/TM5) with manual threshold selection is applied to map all glaciers and ice caps in the study region using Landsat scenes from 2004 to 2009 that were freely available in the glovis.usgs.gov archive. In total, ten scenes with USGS Level 1T processing covering the study region have been selected. All processing steps were performed within a geographic information system (GIS) including calculation of topographic parameters from a DEM.

With the new glacier outlines and a DEM, the further work focuses on the development of an automatic method to create central flow lines of glaciers to determine their length and length changes at the terminus. The developed approach is based on a "2D glacier axis" concept written in an open source programming language (Python). The final part of this thesis is related to the determination of glacier-specific volume change over a 50 year period using a former glacier dataset and topographic maps from the USGS. With this study, the representativeness of the two glaciers with long-term mass balance measurements (Gulkana and Wolverine) is determined for all glacier of the region.

The main results of this thesis are:

- A new glacier inventory has been compiled for Western Alaska including 8,800 glaciers larger than 0.02 km^2 covering a total area of 16,250 km^2.
- This new dataset revealed that 86% of all glaciers are smaller than 1 km^2 (covering 7.5% of the total area) while glaciers larger than 10 km^2 cover 75.6% of the area but only 2.4% by number.
- The mean glacier elevation increases from ca. 100 m a.s.l. at the coast to 3000 m a.s.l. in the interior of Alaska.
- Glaciers lost 23% of their area from the 1950s to 2007 for a subsample of 347 selected glaciers.
- Glacier outlines digitized from other sources (e.g. maps) require careful inspection and adjustments before they can be used for change assessment.
- The new algorithm developed to automatically create glacier central flow lines was applied to a subset of 400 glaciers of the new inventory and a historic one to also derive length changes.
- Length values computed with this algorithm are close to the mean value (±5%) of manual digitizations.
- The derived cumulative length changes for a subsample of 400 glaciers is -277 km (or -700 m per glacier or -15 m per year).
- The glacier-specific elevation changes for a sample of 3180 glaciers gives a mean rate of -0.6 m/year for calving and tide-water glaciers, -0.25 m/year for land-terminating glaciers and -0.63 m/year for Gulkana and Wolverine glaciers.
- Despite their different elevation, size and topographic setting, the mass balance values obtained for the two benchmark glaciers are thus representative for the entire region.
- The ASTER GDEM is suitable to derive elevation change when the total changes are sufficiently large.

Zusammenfassung

Gletscher und Eiskappen gehören zu den offensichtlichsten natürlichen Erscheinungen die durch atmosphärische Bedingungen (d. h. Temperatur und Niederschlag) und deren Änderungen in der Zeit geprägt sind. Sie gelten als Schlüsselindikatoren für den Klimawandel, weil sich ihr Eis in den meisten Regionen der Welt nur knapp unterhalb des Schmelzpunktes befindet, d. h. ein Grossteil des Energieeintrags für die Eisschmelze verwendet wird. Dementsprechend werden seit dem Ende der Kleinen Eiszeit in den 1850er Jahren in vielen Regionen der Erde starke Geometrieänderungen der Gletscher beobachtet. Dies trifft insbesondere für die maritimen Gletscher rund um den Golf von Alaska zu, wo für viele Gletscher während der letzten Jahrzehnte ein grosser Massenschwund mit steigender Verlustrate beobachtet wird. Abschätzungen des Einflusses der Klimaänderung auf die Gletscher in Alaska und genaue sowie des vergangenen und zukünftigen Beitrages dieser Eismassen zum globalen Meeresspiegelanstieg benötigen ein komplettes und genaues Inventar aller Gletscher dieser Region. Leider wiesen die existierenden Datenbanken (das World Glacier Inventory sowie die Global Land Ice Measurements from Space Initiative) grosse Datenlücken auf, was eine präzise Analyse und Berechnungen zukünftiger Veränderungen bisher verunmöglichte.

Diese Arbeit stellt die Resultate einer grossräumigen Gletscherkartierung für einen wichtigen Teil Westalaskas (von den Chugach- bis zu den Chigmit-Mountains) vor, die unter anderem auch der Verbesserung der Datenlage in den oben genannten Datenbanken dient. Zudem ist diese Arbeit auch ein Beitrag zum Projekt GlobGlacier der Europäischen Weltraumorganisation (ESA), welches Teil der internationalen Anstrengungen zur weltweiten Kartierung aller Gletscher ist.

Abschätzungen von Geometrieänderungen von Gletschern sowie konsistente und nachvollziehbare digitale Modellierungen sind einzig mit Gletscherinventaren in digitaler Form (Vektorumrisse) möglich. Zahlreiche frühere Studien haben die Nützlichkeit von optischen Satellitenbildern und digitalen Geländemodellen (DGM) zur Erstellung solcher Inventare belegt. In dieser Arbeit wird die etablierte halbautomatische Methode mit Verhältnisbildern (TM3/TM5) und manueller Bestimmung eines Schwellenwertes verwendet, um alle Gletscher und Eiskappen des Untersuchungsgebietes mit Landsat-Szenen von 2004 bis 2009 zu kartieren, welche im GLOVIS Archiv (glovis.usgs.org) frei verfügbar sind. Insgesamt wurden zehn Szenen verwendet die dem USGS Level 1T entsprechend vorprozessiert sind und das Untersuchungsgebiet abdecken. Alle Bearbeitungsschritte wurden in einem Geographischen Informationssystem (GIS) durchgeführt, einschliesslich der Bestimmung toppgraphischer Gletscherparameter aus einem DGM.

Ein weiterer Schwerpunkt bildet die Entwicklung einer Methode zur automatischen Erzeugung von zentralen Gletscherfliesslinien, die – unter Verwendung der neuen Gletscherumrisse und eines DGMs – zur Bestimmung von Gletscherlängen und

Gletscherlängenänderungen dienen soll. Der entwickelte Ansatz basiert auf einem „2D Gletscherachsen"-Konzept und wurde in einer Open-Source Programmiersprache (Python) geschrieben. Der letzte Teil dieser Arbeit steht im Zeichen der Berechnung gletscherspezifischer Volumenänderungen während der letzten 50 Jahre, basierend auf einem Datensatz früherer Gletscherumrisse und topographischen Karten des USGS. Mit dieser Studie wurde die Repräsentativität der beiden Gletscher mit Langzeit-Massenbilanzmessreihen (Gulkana und Wolverine) für alle Gletscher der Region bestimmt.

Die Hauptergebnisse dieser Arbeit sind:

- Ein neues Gletscherinventar für Westalaska wurde erstellt, bestehend aus 8'800 Gletschern die grösser als 0.02 km^2 sind und insgesamt eine Fläche von 16'250 km^2 bedecken.
- Dieser neue Datensatz zeigt, dass 86% aller Gletscher kleiner als 1 km^2 sind und 7.5% der Gesamtfläche bedecken, während die Gletscher grösser als 10 km^2 75.6% der Gesamtfläche, aber nur 2.4% der Anzahl ausmachen.
- Die mittlere Gletscherhöhe steigt von ca. 100 m ü. M. an der Küste bis 3000 m. ü. M. im Landesinneren von Alaska.
- Die Gletscher verloren zwischen 1950 und 2007 23% ihrer Fläche für eine Stichprobe von 347 Gletschern.
- Gletscherumrisse von anderen Quellen (z.B. Karten) benötigen einer sorgfältigen Überprüfung sowie Anpassungen bevor sie für Änderungsabschätzungen verwendet werden können.
- Der neu entwickelte Algorithmus zur automatischen Erzeugung zentraler Gletscherfliesslinien wurde auf eine Auswahl von 400 Gletschern des neuen sowie eines historischen Inventars angewendet um die Längenänderungen zu bestimmen.
- Die mit diesem Algorithmus berechneten Gletscherlängen kommen dem Mittelwert von handdigitalisierten Gletscherlängen nahe (±5%)
- Die berechneten kumulativen Längenänderungen für eine Auswahl von 400 Gletschern beträgt -277 km (bzw. -700 m pro Gletscher, bzw. -15 m pro Jahr)
- Die gletscherspezifischen Höhenänderungen für eine Auswahl von 3180 Gletschern ergibt eine mittlere Änderung von -0.6 m/Jahr für kalbende Gletscher und Gezeitengletscher, -0.25 m/Jahr für Festlandgletscher und -0.63 m/Jahr für Gulkana und Wolverine, die über Langzeit-Massenbilanzmessreihen verfügen.
- Trotz ihrer unterschiedlichen Höhenlage, Grösse und Exposition sind die gemessenen Massenbilanzen dieser beiden Referenzgletscher daher repräsentativ für die gesamte Region.
- Das ASTER GDEM ist zur Bestimmung von Höhenänderungen geeignet sofern die Gesamtänderungen genügend gross sind.

Sommaire

Les glaciers de montagnes et les calottes glaciaires font partie des composantes naturelles les plus visiblement affectées par les conditions atmosphériques (i.e. température et précipitation) et leurs changements. Ils représentent des indicateurs clef du changement climatique car leurs glaces sont, dans la plupart des régions du monde, proches du point de fusion, i.e. une large part de l'énergie incidente est utilisée pour fondre la glace. En conséquence, un important changement dans la géométrie des glaciers est observé depuis la fin du Petit Âge Glaciaire (PAG) - aux alentours des années 1850 - dans beaucoup de régions du monde. Ceci est spécialement le cas pour les glaciers maritimes situés autour du Golf de l'Alaska où une forte perte de masse ainsi qu'une accélération de celle-ci est observée pour de nombreux glaciers depuis quelques décennies. L'analyse générale de l'impact du changement climatique sur les glaciers de l'Alaska ainsi qu'une estimation précise de leur contribution passée et future sur la hausse du niveau des mers requière un inventaire complet et précis de tous les glaciers de cette région. Malheureusement, d'importantes lacunes existent dans les bases de données disponibles (i.e. World Glacier Inventory and Global Land Ice Measurements from Space), ce qui pénalisait jusqu'à présent, l'analyse fine et les calculs des changements futurs.

Cette thèse présente les résultats d'un travail de cartographie des glaciers à grande échelle pour une importante partie de l'ouest Alaska (des Monts Chugach aux Monts Chigmit) afin d'améliorer leur faible représentation dans les bases de données mentionnées auparavant. Cette thèse est également une contribution au projet GlobGlacier de l'Agence Spatiale Européenne (ESA) qui fait lui-même partie d'un effort international pour la cartographie des glaciers du monde entier.

Seuls les inventaires des glaciers sous forme numérique (lignes vectorielles) permettent l'analyse des changements géométriques ainsi que la modélisation de façon cohérente et reproductible. De nombreuses études ont d'ores et déjà démontré l'utilité des images optiques satellitaires et des Modèles Numériques de Terrain (MNT) pour la compilation desdits inventaires. Dans cette thèse, la semi-automatique méthode de rapport de bandes (TM3/TM5) avec sélection manuelle- par seuillage est appliquée pour cartographier les glaciers et les calottes glaciaires de la région d'étude en utilisant des images Landsat acquises de 2004 à 2009 et gratuitement disponibles dans les archives du glovis.usgs.gov. Au total, dix scènes pré-traitées (USGS Level 1T) et couvrant- la région d'étude ont été sélectionnées. Toutes les étapes du traitement ont été réalisées avec un Système d'Information Géographique (SIG) incluant notamment les calculs des paramètres topographiques dérivés des MNT.

En s'appuyant sur les nouveaux contours des glaciers ainsi créés et sur les MNT disponibles, la poursuite des travaux de cette thèse se porte sur le développement d'une méthode automatique pour la création des lignes d'écoulement des glaciers en ayant pour but de déterminer la longueur et les changements de longueur dans la partie frontale de ceux-ci. L'approche de ce développement est basée sur un concept bidimensionnel d'axe

des glaciers (2D Glacier Axis) retranscrit avec le langage de programmation open source Python. La dernière partie de cette thèse est dédiée à l'analyse et à la détermination du changement du volume glaciaire sur une période de 50 ans en utilisant des données pré existantes sur les glaciers couplées à des cartes topographiques de l'USGS. Grâce à cette étude, la représentativité des deux glaciers de référence (Gulkana et Wolverine) pour lesquels des mesures de bilan de masse sur une longue période sont disponibles, est déterminée pour l'ensemble des glaciers de la région.

Les principaux résultats de cette thèse sont:

▪ Un nouvel inventaire des glaciers a été créé pour la région ouest de l'Alaska, comprenant plus de 8800 glaciers supérieurs à 0.02 km^2 et couvrant une superficie totale de 16 250 km^2.

▪ Ce nouveau jeu de données révèle que 86% des glaciers sont inférieurs à 1 km^2 (couvrant 7.5% de la surface totale) alors que les glaciers plus larges que 10 km^2 couvrent 75.6% de la surface mais seulement 2.4% en nombre.

▪ L'altitude moyenne des glaciers s'accroît progressivement en s'éloignant des côtes (altitude moyenne d'environ 100 m près des côtes et de plus de 3000 m à l'intérieur de l'Alaska).

▪ Les glaciers ont perdu près de 23% de leur surface entre les années 1950 et 2007 pour un sous-ensemble de 347 glaciers sélectionnés.

▪ Les contours des glaciers numérisés à partir d'autres sources d'information (e.g. Cartes topographiques) requièrent une attention particulière ainsi que des ajustements avant qu'ils ne puissent être utilisés pour l'analyse des changements.

▪ Le nouvel algorithme développé pour la création automatique des lignes d'écoulement? des glaciers a été appliqué à un sous-ensemble de 400 glaciers – issu du nouvel inventaire et d'un inventaire historique - afin de déterminer également les changements de longueurs.

▪ Les longueurs des glaciers calculées avec l'algorithme sont proches de valeurs moyennes (±5%) dérivées manuellement.

▪ Le changement cumulé de longueur calculé pour un sous-ensemble de 400 glaciers est de -277 km (soit -700 m par glacier ou -15 m par an).

▪ Le changement spécifique d'élévation par glacier donne pour un ensemble de 3180 glaciers une valeur moyenne de -0.6 m/an pour les glaciers de vêlage et lacustre, -0.25 m/an pour les glaciers de vallée et -0.63 m/an pour les glaciers Gulkana et Wolverine.

▪ Malgré leurs différentes altitudes, tailles et caractéristiques topographiques, les deux

glaciers de référence (Gulkana et Wolverine) sont représentatifs pour la région entière au regard des mesures de leurs bilans de masses.

▪ Le modèle numérique de terrain ASTER GDEM est approprié pour dériver les changements d'élévation lorsque ces changements totaux sont suffisamment larges.

Table of content

List of Figures:

List of Tables:

Abbreviations:

AAR	Accumulation-Area Ratio
ALOS	Advanced Land Observing Satellite
ASCII	American Standard Code for Information Interchange
ASTER	Advanced Space-borne Thermal Emission and Reflection Radiometer
CCD	Charge Coupled Device
dbf	database file
DEM	Digital Elevation Model
DLG	Digital Line Graph
DN	Digital Number
DRG	Digital Raster Graph
DUE	Data User Element
ECV	Essential Climate Variables
EE	Earth Explorer
ELA	Equilibrium Line Altitude
ERDAS	Earth Resources Data Analysis System
ESA	European Space Agency
ESRI	Environmental Systems Research Institute
ETM+	Enhanced Thematic Mapper Plus
FCC	False Colour Composite
FLA	Flow Line Algorithm
FOG	Fluctuations Of Glaciers
GCOS	Global Climate Observing System
GDAL/OGR	Geospatial Data Abstraction Library – Open source Geospatial Resources
GeoTIFF	Geographic Tag Image File Format
GIS	Geographic Information System
GLAS	Geoscience Laser Altimeter System
GLIMS	Global Land Ice Measurements from Space
GLOVIS	USGS Global Visualization Viewer
GNIS	Geographic Names Information System
GTN-G	Global Terrestrial Network for Glaciers
HRG	High Resolution Geometric
HRVIR	High Resolution Visible Infra Red
ICESat	Ice, Cloud and land Elevation Satellite
InSAR	Interferometry Synthetic Aperture Radar
IPCC	Intergovernmental Panel on Climate Change
IPY	International Polar Year
JPL	Jet Propulsion Laboratory
L1T	Level-one terrain-corrected

LIA	Little Ice Age
MSS	Multi-Spectral Scanner
NASA	National Aeronautics and Space Administration
NED	National Elevation Dataset?
NGA	National Geospatial Agency
NIR	Near Infra-Red
PAEK	Polynomial Approximation with Exponential Kernel (algorithm)
PALSAR	Phased Array L-band SAR
RADAR	RAdio Detection And Ranging
shp	Shapefile format
SLC	Scan Line Corrector
SPIRIT	SPOT 5 stereoscopic survey of Polar Ice: Reference Images and Topographies
SPOT	Satellite pour l'Observation de la Terre
SQL	Structured Query Language
SRTM	Shuttle Radar Topography Mission
STD	Standard Deviation
SWIR	Short Wave Infra-Red
TIN	Triangular Irregular Network
TIR	Thermal Infra-Red
TM	Thematic Mapper
UNEP-DEWA	United Nations Environment Programme, Division of Early Warning
UNESCO-IHP	United Nations Environment Programme, International Hydrological Programme
UNFCCC	United Nations Framework Convention on Climate Change
USGS	U.S. Geological Survey
UTM	Universal Transverse Mercator
VIS	Visible
VNIR	Visible and Near Infra-Red
WGI	World Glacier Inventory
WGMS	World Glacier Monitoring Service
WGS 84	World Geodetic System 1984
WP	Work Packages

Part I

1 Introduction

1.1 Background

Among evidences of climate change, mountain glaciers are certainly one of the most visible natural features affected. In fact, under the ongoing and fast air temperature increase recorded for more than a century now, glacier changes became perceptible even within a human life span. Sensitivity of glaciers to atmospheric warming results from their ice being close to melting point. In response to climate forcing (e.g. the observed temperature increase since the end of the Little Ice Age (LIA) around the 1850s), glaciers act by adjusting their area, length and volume (e.g. FOG; Fluctuations Of Glaciers reports). This implies that glacier changes need to be determined precisely in order to assess climate change impacts. This is particularly true for temperate glaciers that are located in maritime environments such as in the Alaska Range, Scandinavia, New Zealand and Patagonia because glaciers in these regions are even more sensitive to climate changes (Braithwaite 2009). Indeed, one of the most important aspects of glaciological studies is related to sea-level rise assessment. In this regard, southern Alaska represents a most important key region (Radić and Hock 2010) as its mountains are largely covered by ice.

As an illustration of this sensitivity, many studies (e.g. Wood 1988; Andreassen *et al.* 2005) reported a short advance phase that occurred during the 1980s as a reaction to a slight decrease in global mean annual air temperature (MAAT). Over the last few decades glaciers have shown an accelerating rate of retreat (Dyurgerov 2003). Considering future climate change scenarios showing temperatures increasing by 2 to 4°C before the end the

21st century (Parry *et al.* 2007), it is expected that in the European Alps, more than 75% of all glaciers will vanish within the coming decades (Paul *et al.* 2007; Raup *et al.* 2007; Radić and Hock 2010).

Glaciers and ice caps have been defined as Essential Climate Variables (ECV) in the Global Climate Observing System (GCOS) implementation plan for the United Nations Framework Convention on Climate Change (UNFCCC, 2004). In fact, the GlobGlacier project played a key role for the task to collect glacier data from satellites within the multi-level strategy of the Global Terrestrial Network for Glaciers (GTN-G) which is operated by the World Glacier Monitoring Service (WGMS) in close collaboration with the Global Land Ice Measurements from Space (GLIMS) initiative.

To help decision makers, scientists have developed a range of strategies to monitor the cryosphere within the framework of international efforts such as the GTN-G of GCOS (Haeberli *et al.* 2007). In this regard, completion of glacier inventories accounts for one of the most urgent tasks to get a more accurate vision of the amount of ice stored in glaciers and ice caps. The World Glacier Inventory (WGI) has been created with a hydrologic purpose in the 1970s and includes information for ca. 71,000 glaciers. Dyurgerov (2003) estimated that 160,000 glaciers exist worldwide by scaling indicating that the WGI was incomplete. Although the WGI has been widely applied, this dataset is not practical for change analysis as it only represents glaciers as point features without knowing their shape (Paul *et al.* 2011). For Alaska in particular, the database is poor and the glacier inventory is largely incomplete. Therefore, the key aim of this thesis is to close the gap in knowledge for a large part of western Alaska.

1.2 Key objectives and research framework

The first objective of this thesis is to create a new glacier inventory for western Alaska and compare it with earlier data available from the US Geological Service (USGS) for this region. The determination of glacier specific changes in area, length and volume constitutes a second objective and the development of an automatic method to assess length changes represents the final purpose of this study.

The thesis presented here is based on the GlobGlacier project. This project was launched in 2007 by the European Space Agency (ESA) as part of its Data User Element (DUE) programme (Fig. 1.1A). It lasted for three years and ended with a final meeting in Zermatt (Switzerland) in August 2010. The aims of this project were to monitor glaciers and ice caps from space by implementing a network and to contribute to an international effort in maintaining and developing data exchange between user groups.

The GlobGlacier project was divided into five Work Packages (WPs) in order to dispatch the tasks and produce a set of glacier specific data. This apportioning between participants is depicted in Fig. 1.1B and 1.1E. Figure 1.1C lists some of the key regions

around the world that have been selected according to the user group requirements. The main goals were to complete the existing World Glacier Inventory (WGI) and GLIMS database with a particular emphasis on regions with missing data. Figure 1.1D synthesizes the elements of this thesis.

1.3 Research questions

Several research questions related to Alaskan glaciers emerge from the aspects mentioned above:

- What is the glacier area in Alaska?

Detailed glacier extents remained unmapped (especially in a digital format) and particularly for a large part of western Alaska the precise glacierized area is still unknown. Glacier outlines created during this thesis will contribute to complete the existing inventory and serve as an input for different applications (e.g. change assessment or glacier modelling).

- Can glacier specific drainage divides be derived from the USGS National Elevation Dataset (NED)?

DEMs are needed to compute drainage divides which in turn are required to separate contiguous ice masses into individual glaciers. The NED DEM is available for the complete region, but needs to be evaluated and compared with others DEMs in order to choose the most appropriate one.

- Can the Digital Line Graph (DLG) be used for area change assessment?

A digital dataset for Alaska representing glacier extents from the 1950s exists from the USGS (DLG). Therefore, coupling this old information with a new glacier inventory would permit the assessment of glacier changes.

- Why and how to create glacier flow lines automatically?

Glacier flow lines (vector) and glacier length (scalar value) represent important parameters to study glacier response to climate variations. Unfortunately, these parameters are mainly absent from glacier inventories as they demand a considerable workload to be generated. Hence, an automatic method to derive glacier flow lines and glacier length is needed.

- How to derive glacier length changes automatically?

Glacier length change analysis helps to better understand the past and also to predict

future glacier behaviour resulting from climate forcing. They are also compiled in the Fluctuation Of Glaciers publications from the World Glaciers Monitoring Service (WGMS 2008). A specific part of this thesis will illustrate a method to automatically derive this information.

- How to upscale mass balance measurements from Gulkana and Wolverine glaciers to the entire region?

The determination of the past contribution to sea-level change from all glaciers in Alaska is difficult as the representativeness of the Gulkana and Wolverine glaciers, where long-term mass balance measurements are available, is not known (Kaser *et al.* 2006). An assessment of this representativeness will be performed in this thesis by determination of their cumulative elevation change over a 50 year period.

- How to eliminate Columbia glacier from the calculation?

Columbia glacier represents a considerable part of the total ice volume loss occurring in Alaska (Berthier *et al.* 2010) which is not only due to climate forcing. Its contribution strongly influences the mean value and has to be eliminated from calculations. A methodology is presented to remove lacustrine and tide-water glaciers from the sample.

1.4 Datasets

The study presented in this thesis is based on a limited amount of input data. Most of this data is freely available for researchers in vector and/or raster format (see § 5.1.1). We used (a) optical satellite scenes, (b) digital glacier outlines and (c) various digital elevation models to perform our analysis.

A) Optical satellite scenes

The key factors when selecting optical satellite scenes are their suitability to map glaciers under optimal snow conditions and without cloud cover. To delineate glacier outlines, Landsat Thematic Mapper (TM) scenes from 2004-2009 were used (see Appendix A1).

B) Digital glacier outlines

Former digital outlines describing glacier extents from the 1950s were used to perform change assessments. In this regard, the Digital Line Graph (DLG) from USGS represents a valuable and very important dataset. Though available for the complete study region, the DLG requires some manual editing for which the Digital Raster Graph (DRG) maps are used.

C) Digital elevation models

Digital elevation models (DEM) are used to compute topographic glacier parameters (e.g. minimum and maximum elevation), to derive drainage divides and to automatically create glacier flow lines (see § 4.4.6 and 5.2.3). The DEMs used in this study are the NED DEM, the Shuttle Radar Topography Mission (SRTM DEM) (up to 60°N), the Advanced Space-borne Thermal Emission and Reflection Radiometer Global DEM (ASTER G-DEM) and the SPOT-SPIRIT DEM. The latter is already a difference between the NED and the SPOT DEMs performed by Berthier *et al.*, (2010) and covers the period 1962-2006 (see § 4.2).

1.5 Methodological approaches

Glacier mapping for western Alaska:
High mountain regions such as in western Alaska provide several challenges in terms of snow, shadow and cloud conditions when it comes to glacier mapping. To properly delineate glacier extents, a well-established semi-automated band ratio method as described in Paul and Kääb, (2005) is applied. This is an efficient and reproducible way to map glaciers from optical satellite data. The method takes advantage of the special spectral properties of ice and snow to discriminate them from the surrounding terrain.

Creating drainage divides:
Drainage divides represent an important element of glacier inventories. The aim is to use them to divide contiguous ice masses into individual glaciers and then, to derive glacier specific topographic parameters with GIS tools (zonal statistics). A method detailed in Bolch *et al.*, (2010) is applied to create them from hydrological watershed analysis using the DEM (see § 5.2.2). Particular attention is given to the selection of DEMs according to their accuracy and potential artefacts. In this regard, the NED DEM has been selected as it is slightly more suitable than the ASTER G-DEM.

Determination of area changes:
One of the main aspects analysed in this thesis concerns glacier changes. Using a former glacier outlines dataset (DLG) and our new satellite-derived outlines a glacier area change analysis has been performed. In a first approach the DLG outlines appear extremely useful for this purpose, but quantitative and qualitative comparisons reveal that a direct comparison between the two datasets is not a straightforward solution. In fact, both datasets have inherent challenges when creating a glacier inventory due to the highly variable nature of glacier shapes, location and analyst interpretation differences. Careful visual and statistical inspections were made before assessing glacier changes.

Confronting the DLG outlines with the Digital Raster Graph (DRG):
The DRG, which depicts the published paper topographic maps in a high-resolution scan raster format was used to assess the DLG accuracy. Digital overlapping of the DLG and

DRG showed mismatches of glacier extents for several cases which were mainly in the ablation region. Manual corrections were applied for ca. 400 glaciers before computation of changes.

Glacier flow lines:
A new algorithm allowing to automatically generate flow lines in vector format has been developed in this thesis. It is based on Python programming plus additional libraries (GDAL and OGR (see § 5.2.3)) and requires only a DEM and glacier outlines as an input. The method is based on a glacier axis concept. Geometry rules such as the k-d Tree, Nearest Neighbour and crossing test theory are applied to create the vector lines and the terminus positions for 400 glaciers.

Length changes:
The flow line algorithm is applied to both the DLG and the satellite-derived outlines. Length changes are computed by a digital intersection of the vector line for the DLG outlines with the more recent glacier extent, representing glacier front variations rather than length changes.

$\Delta h/\Delta t$ raster maps:
This dataset represents glacier elevation changes (Δh) for the entire study region over the time period Δt. It is based on subtracting the NED DEM from a more recent DEM and divide by the time period. These sequential DEMs cover the period 1962-2006 and were provided by Etienne Berthier (Berthier *et al.* 2010).

Glacier-specific elevation changes:
The calculation of glacier-specific elevation changes is obtained by digital intersection of the $\Delta h/\Delta t$ raster maps with the drainage divide dataset created for the new Alaskan glacier inventory. Only glaciers with less than 20% of their area covered by data voids and larger than 0.05 km^2 are considered (they were deselected in the GIS).

Glacier classification:
Lacustrine and tide-water glaciers (especially Columbia glacier) hampered analysis of glacier changes that are due to climate forcing. Hence, these glacier types have to be removed from the calculation of elevation changes. We manually selected lacustrine and tide-water glaciers of the entire region and identified them in the attribute table of the database. A statistical analysis was performed to assess the representativeness of the two benchmark glaciers with long-term mass balance measurements (Gulkana and Wolverine).

1.6 Structure of the thesis

The thesis presented here is composed of five parts. The first part gives an overview on the glaciological background (Chapter 2) followed by a section on remote sensing and glacier mapping methods (Chapter 3). Chapter 4 gives an overview of digital elevation

models and their uses for this thesis whilst Chapter 5 focuses on Geographic Information Systems and applications for glacier mapping and change assessment. Chapter 6 is a summary of the key research papers listed below. Chapter 7 synthesizes the results through an extended discussion on main findings and potential future work and is followed by the conclusions (Chapter 8).

Research papers:

(1) Le Bris, R.; Paul, F.; Frey, H. and Bolch, T., (2011). *A new satellite-derived glacier inventory for Western Alaska*. Annals of Glaciology, 52(59), 135-143.

(2) Le Bris, R and Paul, F., (2012). *An automatic method to create flow lines for determination of glacier length: A pilot study with Alaskan glaciers*. Computers & Geosciences Journal.

(3) Le Bris, R. and Paul, F., (submitted). *Glacier-specific elevation changes in western Alaska.* Annals of Glaciology.

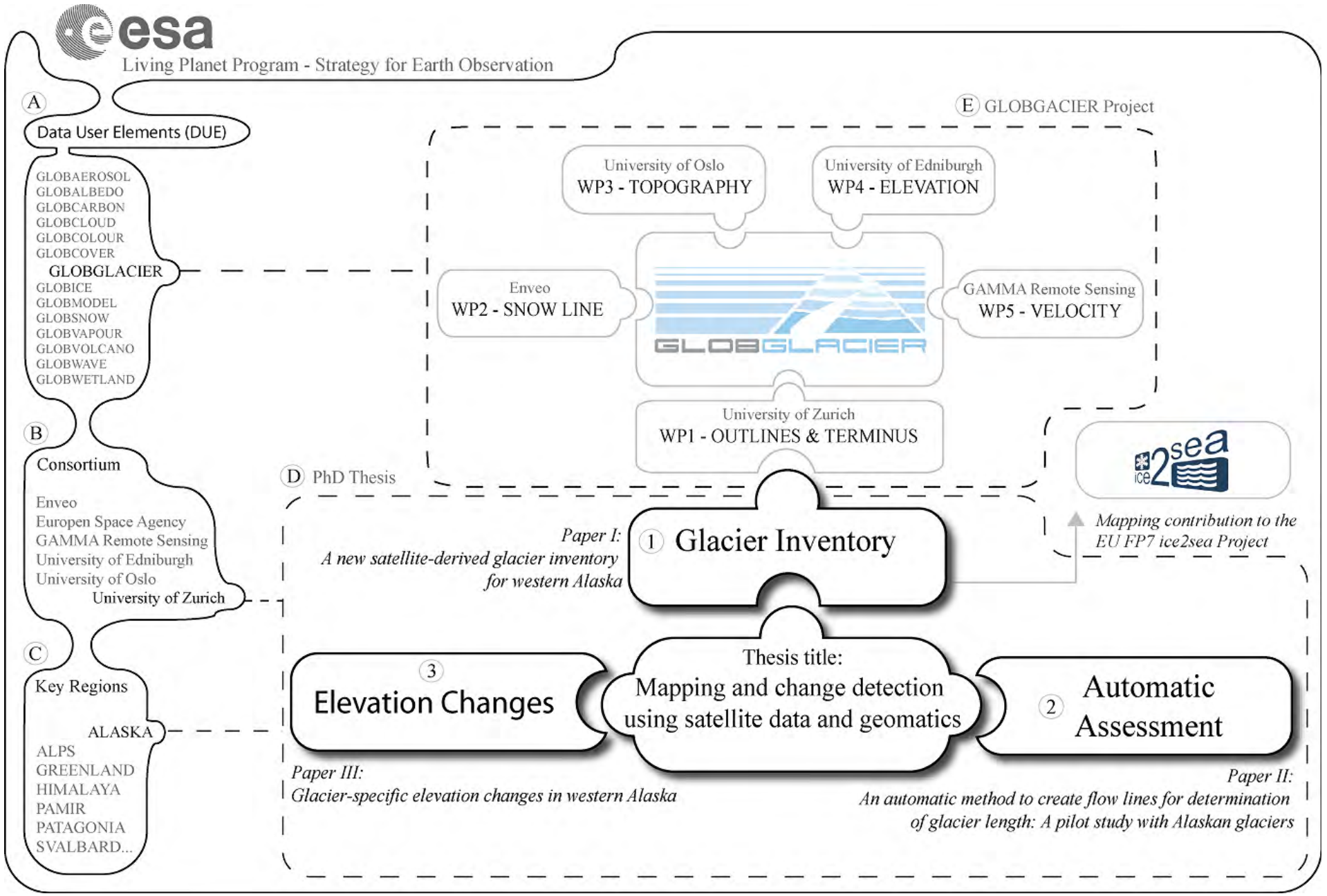

Figure 1.1: *PhD Framework*

2

Glaciological background

Glaciers and ice caps represent an important component of the cryosphere (Fig. 2.1) and a key element of the water cycle (UNEP 2007). Their cumulative extents are between 0.51 and 0.54 million square kilometres with an ice volume estimated from 0.05 to 0.13 million cubic kilometres (IPCC, 2007) excluding the peripheral (or local) glaciers and ice caps around Greenland and Antarctica. A more recent study by Huss and Farinotti (2012) used the data from the new Randolph Glacier Inventory (Arendt *et al.* 2012) giving an updated total glacier area of 786 882 km^2 and volume of $170 \times 10^3 \pm 21 \times 10^3$ km^3, or 0.43 ± 0.06 m of potential sea level rise. The proportion of water stored in glacierized regions across the world (including the two ice sheets - Greenland and Antarctica) is estimated at 1.7% of all water on Earth and accounts for 87% of the fresh water available (Van der Veen 1999).

From a human perspective, monitoring glaciers is important in terms of hazard mitigation (e.g. ice and snow avalanches, floods) (Huggel *et al.* 2004) and their impact on hydrology (e.g. water supply, hydropower) (e.g. Fountain and Walder 1998; Kaser *et al.* 2003; Moore *et al.* 2009), but these topics are not addressed here. However, assessing glacier changes is crucial to better understand the impacts of climate change and to determine future glacier evolution and sea-level rise. In this regard, glacier area, length and volume change assessments also constitute a fundamental objective of cryospheric research.

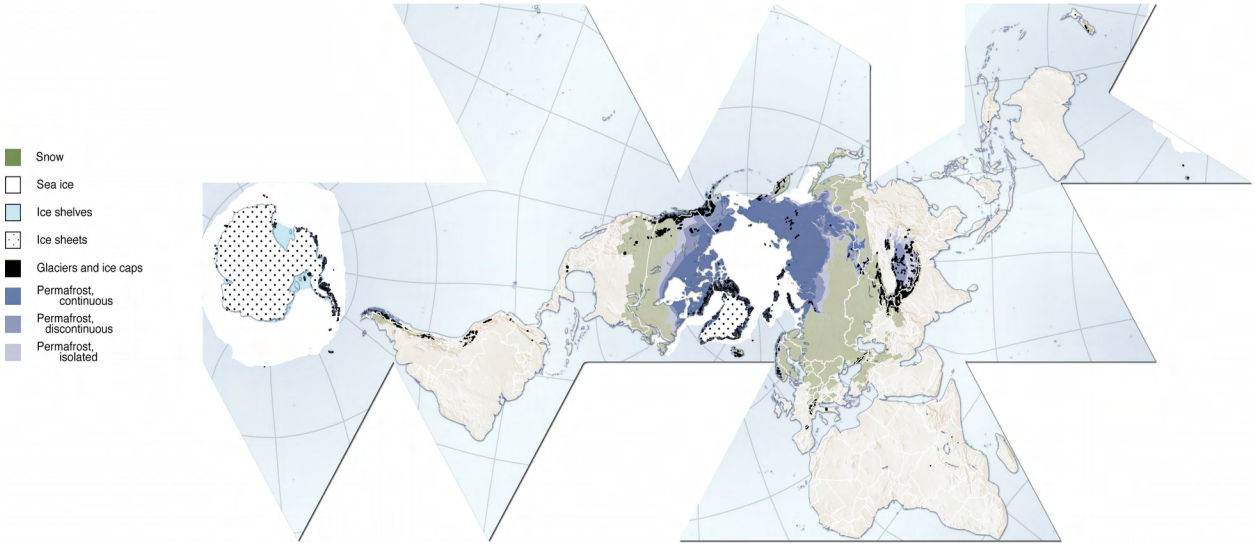

Figure 2.1: *The Cryosphere world map (from Hugo Ahlenius, UNEP/GRID-Arendal.)*

2.1 Definitions of glaciers and their genesis

At first glance, the notion of what a glacier is might be quite obvious. Nonetheless, a scientific definition is needed in order to avoid misunderstanding. In this regard, several definitions are available to describe glaciers based on their specific characteristics. A compilation of three of them is given below:

- *A glacier is a mass of surface-ice on land which flows downhill under gravity and is constrained by internal stress and friction at the base and sides. In general, a glacier is formed and maintained by accumulation of snow at high altitudes, balanced by melting at low altitudes or discharge into lakes or the sea (WGMS, 1989).*

- *A glacier is a perennial mass of ice, and possibly firn and snow, originating on the land surface by the recrystallization of snow or other forms of solid precipitation and showing evidence of past or present flow (Cogley et al. 2011).*

- *A glacier or perennial snow mass, […], consists of a body of ice and snow that is observed at the end of the melt season, or, in the case of tropical glaciers, after transient snow melts. This includes, at a minimum, all tributaries and connected feeders that contribute ice to the main glacier, plus all debris covered parts of it. Excluded is all exposed ground, including nunataks (Racoviteanu et al. 2009).*

From these examples it is clear that one of the main characteristics that define a glacier is its flow. As glacier flow is difficult to see on a single satellite image, a more morphological definition (n°3 in the list) was developed for the purpose of GLIMS. A second important

aspect to consider is related to the question which ice masses should be included in the glacier boundary (e.g. when tributaries are only in touch but not contributing to the flow) and how they can be identified and distinguished (e.g. debris cover or perinnial snow)? Those elements are important in regard to glacier mapping using optical satellite images since they exhibit specific patterns (e.g. medial, lateral and frontal moraines) and spectral properties (e.g. bare ice, snow and debris-cover parts).

Before a glacier starts to flow downward, a long natural process is involved. This process begins by accumulation of fresh snow from precipitation, wind drift, resublimation and condensation. Where favourable conditions prevail (topography, temperatures, etc…) a subsequent part of the snow pack will subsist after an ablation (melting) season leading to a compaction process. Slowly, snow grains will be compressed under the weight of fresh snow layers (which can be as thick as 6 to 10 m per year in maritime climates (Post and Mayo 1971) and the air contained between the snow grains is completely enclosed (close off). The resulting glacier ice is thus completely different in origin from sea, lake or river ice, which is just frozen water. Snow crystal metamorphism via rounded snow grains to firn - which is defined as snow that has survived at least one ablation season (Cogley *et al.* 2011) - and eventually to ice, can take several years to decades, depending on the climate regime. Figure 2.2 depicts the evolution of snow grains through time.

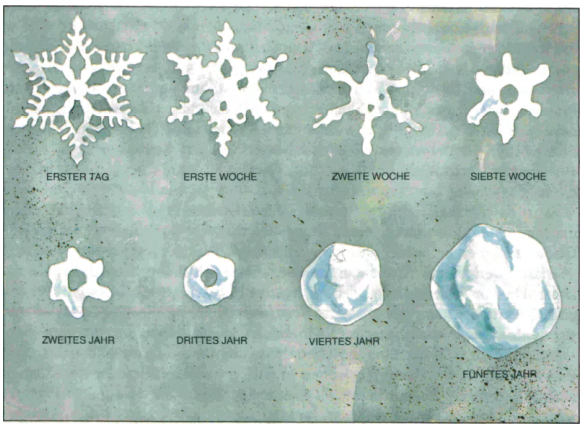

Figure 2.2: *Crystal snow metamorphism (Illustration from* R.H. *Bailey; Der Planet Erde-Gletscher; 1982. Time-Life Books)*

Depending on glacier bed topography (slope and roughness), glaciers start to deform under their own weight and flow downward to lower altitudes. Reaching warmer regions at lower altitudes, glacier extent is limited by the fact that melting (ablation) will overtake the amount of ice mass supplied by the flux from higher accumulation regions. Glacier ablation can also be driven by mechanical processes instead of pure climatic forcing. Calving or tidewater glaciers (largely present in Alaska) are a good example of such processes (see below). Glaciers covering active volcanoes are other examples where ablation can occur for reasons other than climate (e.g. geothermal heat flux, volcanic eruptions).

2.2 Glacier in the study region

2.2.1 Study region

The region considered in this thesis is located around the Gulf of Alaska (Fig. 2.3). This region encompasses large mountain ranges with many types of glaciers, from small cirques to large valley glaciers with multiple basins (Denton and Field 1975) ranging in altitude from sea level up to 4000 m a.s.l. For further information about this region, the satellite image atlas book represents an important source (Molnia, 2009). Near the coast, the climate is predominantly of maritime type while it is more continental further inland (e.g. http://climate.gi.alaska.edu). The mountain ranges, which act as a barrier for the westerlies, have an effect on precipitation with a high amount of annual sums especially along the coast. Accordingly, frequent clouds and seasonal snowfields often hamper visual interpretation of glacier boundaries and in turn strongly reduce the number of appropriate optical satellite scenes for glacier mapping. Volcanic activity can also impact glacier classification by changing the spectral properties of the ice and snow. Examples of ash and dust originated from volcanoes are visible on the Landsat TM scene from 2009 in the ablation region of some glaciers. For practical reasons and regionalized assessments, the region has been divided into seven subregions (see Fig. 2.3).

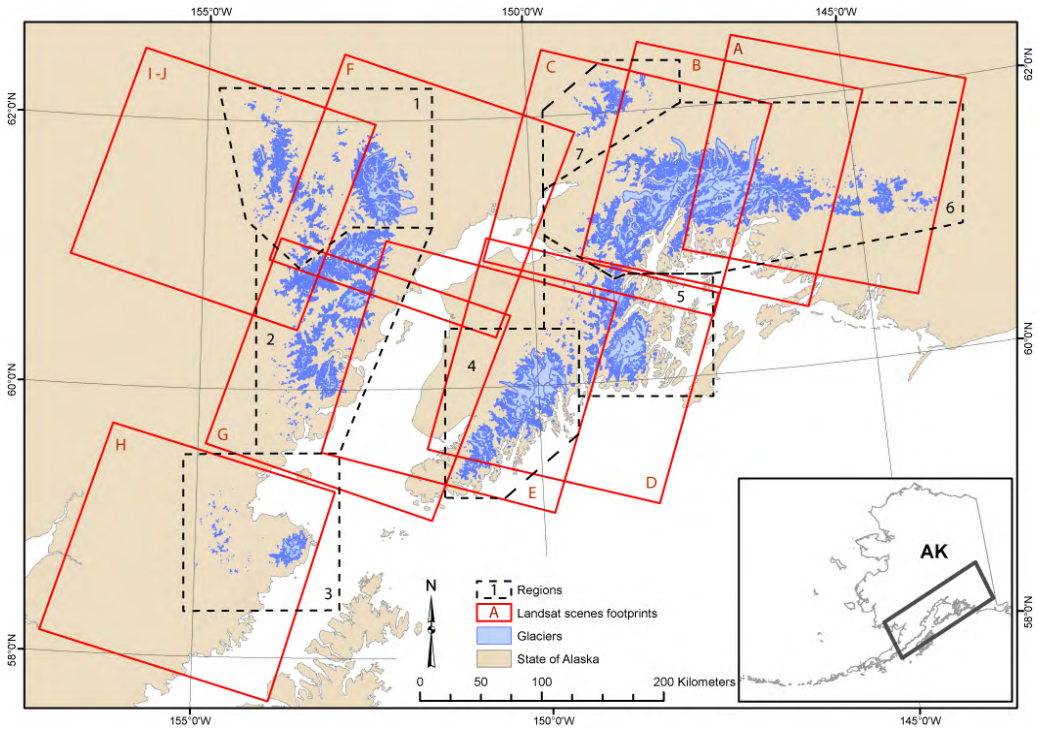

Figure 2.3: *Study region and Landsat scene footprints. The western part encompasses the Tordrillo Mountains (1) in the southern part of the Alaska Range, and Chigmit Mountains (2). The southern subregion is the Fourpeaked Mountain (3) and the eastern parts grouped the South and North Kenai Peninsula, the Chugach Mountains and the Talkeetna Mountains (4, 5, 6 and 7).*

2.2.2 Scene selection and archives

Most of the data produced by the sensors described below are freely available to scientists from online ftp servers. Landsat and ASTER data can be downloaded from the USGS Global Visualization Viewer (glovis.usgs.gov), the Earth Explorer (EE) or the Reverb systems. SPOT data can be found in the SPOTCatalog web-based client system and ordered at charges depending on data types and resolutions. Due to the failure (May 31, 2003) of the Scan Line Corrector (SLC) of the Landsat 7 ETM+ sensor (Markham *et al.* 2004), only Landsat 5 TM scenes were used in this thesis.
The most crucial elements when selecting suitable optical satellite scenes to map glaciers are the snow and cloud conditions. Particular attention must be given to select scenes from the end of the ablation period (August/September in the Northern hemisphere) in order to prevent the glacier boundaries from being obscured by seasonal snow. For humid regions like Alaska it is relatively difficult to find suitable scenes without clouds. A careful analysis of the Landsat archive between 1999 and 2009 has thus been performed. Unfortunately, it was not possible to get all scenes from the same year and the ten selected scenes used to create the inventory span a five year period. Table 1 lists the satellite scenes selected and gives a description of cloud and snow conditions. Quick-looks of all scenes are given in Appendix A1.

During the post-processing step (see § 3.3.1F), the visual interpretation of glacier delineations was improved by using higher spatial resolution data in Google Earth™. However, in many cases, snow conditions were quite poor and those higher spatial resolution data were only available for a few glaciers.

Id	Sensor	Path	Row	Date	Description
A	Landsat 5 TM	66	17	06.09.2009	Good conditions to map glaciers.
B	Landsat 7 ETM+	67	17	01.08.2002	Large amount of seasonal snow on glaciers.
C	Landsat 5 TM	68	17	03.08.2009	Some snow. Heavy clouds in south but no over gl.
D	Landsat 5 TM	68	18	12.09.2006	Some on glacier. No clouds.
E	Landsat 5 TM	69	18	09.07.2009	Large amount of seasonal snow on glaciers.
F	Landsat 5 TM	70	17	28.08.2007	Some snow on gl. Few clouds over gl. in the west.
G	Landsat 5 TM	70	18	28.08.2007	Snow on gl. Heavily cloudy in the south-eastern.
H	Landsat 5 TM	71	19	14.09.2005	Heavily cloudy over gl. in south and snow on gl.
I	Landsat 5 TM	72	17	20.08.2005	Heavily cloudy at the west. No snow on gl.
J	Landsat 5 TM	72	17	26.08.2007	Some cumulus over gl. in south. No seasonal snow.

Table 1: *List of satellite scenes used and description of cloud and snow conditions. Id refers to the Landsat scenes footprint (Fig.2.3) and 'gl' means 'glaciers'.*

2.2.3 Glacier morphology and type

The study region covers most of the glacier types from the UNESCO (1970) primary classification. These types range from small cirques to mountain glaciers of highly variable shapes, to valley glaciers of all sizes, to ice capped volcanoes and ice fields with outlet glaciers. The glaciers also show a wide range of surface characteristics ranging from clean ice to being heavily debris covered, and from prominent medial moraines to complex parallel bands of moraines for glaciers with multiple tributaries. In part, moraines are looped or otherwise distorted due to surging activity of some glaciers. Frontal characteristics range from normal land-terminating to multi-lobate, to calving into lakes or ocean (tide-water) glaciers. Also, the topographic structure can be highly-complex, ranging from simple downward flow to multi-tributary glaciers forming dendritic networks (Bahr and Peckham 1996). Some typical examples from Alaska are shown in Figure 2.4 (along with their respective satellite images). Figure 2.4D shows an example of a glacier tongue disconnected from the accumulation area (regenerated glacier) but still supplied with ice from above (Northwestern Fjord in the South Kenai Peninsula).

In regard to the work performed in this thesis, these characteristics are related to various challenges. For example, debris covered regions cannot be mapped automatically as they exhibit the same spectral properties as the surrounding terrain. The terminus of calving glaciers (into lakes and tide-water) needs to be corrected manually as ice being in the water as well as the turbid water itself is wrongly classified. The multi-tributary and/or multi-lobate glaciers cause problems in clearly assigning a length value or the terminus position.
Frequent seasonal or perennial snow fields cause difficulties in glacier boundary indentification that make proper change assessment difficult, in particular when outlines are compared to already existing datasets. How these various challenges are handled within this thesis is described in Chapters 3 to 5 and in the three research papers. A summary of glacier classification is available in the document "Illustrated GLIMS Glacier Classification Manual" and downloadable from the GLIMS website at http://www.glims.org/MapsAndDocs/assets/GLIMS_Glacier-Classification-Manual_V1_2005-02-10.pdf.

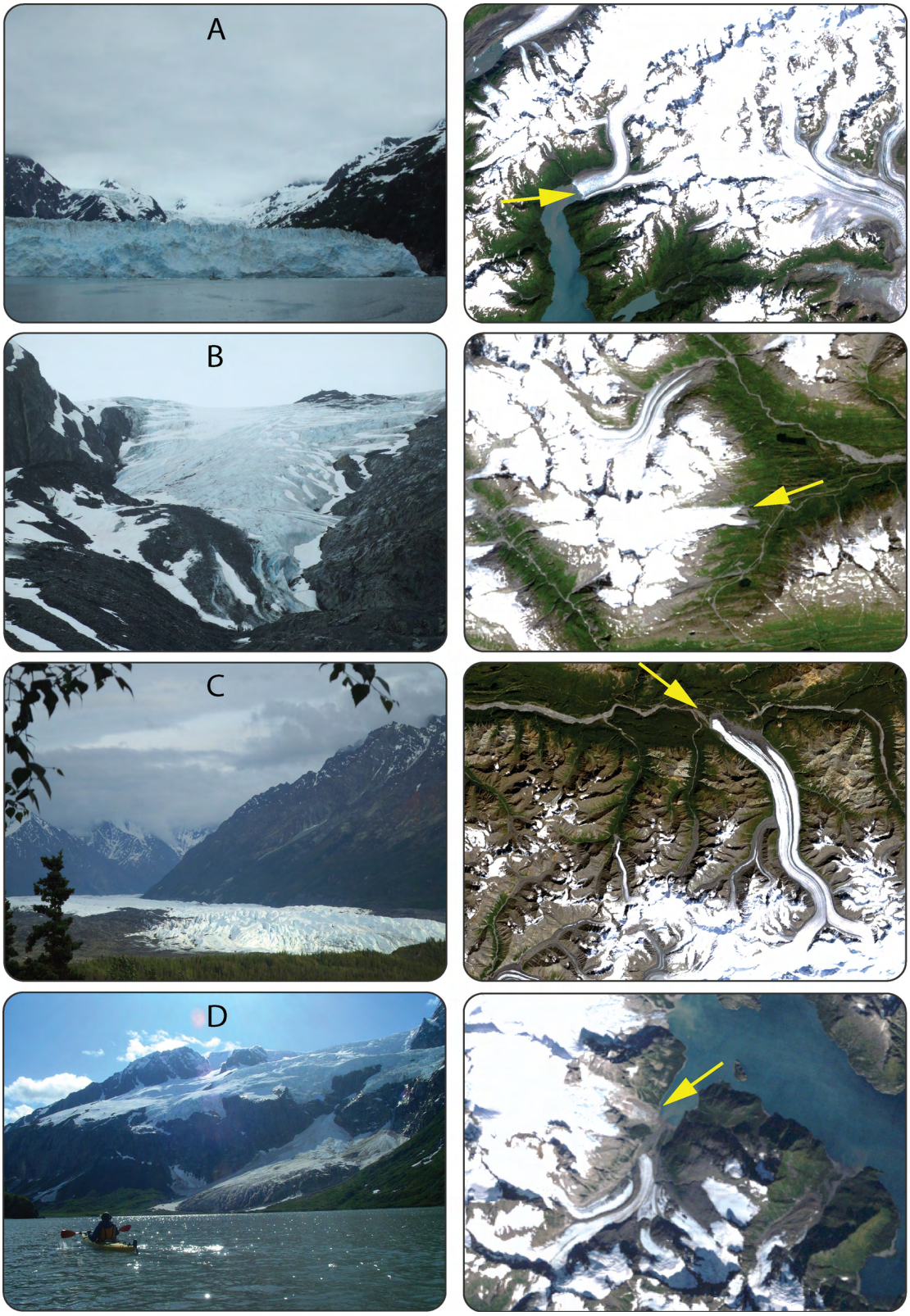

Figure 2.4 : *Examples of glacier types with their respective views on satellite images. Yellow arrows indicate the glaciers as well as the view directions. (A) Meares glacier, (B) Whorthington glacier, (C) Matanuska glacier, (D) Unnamed regenerated glacier in the Northwestern fjord (Kenai Peninsula). Photo A, B and C: R. Le Bris; photo D: L. Dale.*

2.3 Glaciers and climate

2.3.1 Glacier reaction to climate change

Adjustments in glacier length, area and volume following a specific climate forcing are strongly influenced by the particular topographic environment. Naturally, a glacier will adjust its shape to reach a new balance with climatic conditions so that gain and loss of mass are similar. In this process, temperature and precipitation are key factors driving glacier response. Accumulation (i) and ablation (ii) zones are clearly visible on most glaciers and involve several processes. While (i) is dominant at high elevation areas, where a glacier gains mass by solid precipitation (snow fall) or avalanches and wind drift, (ii) dominantes at low elevations where mass loss by melting or dynamical events (i.e. iceberg discharge) occur. While ablation regions are mainly dependent on increasing or decreasing temperatures, accumulation regions are mostly affected by a change in the amount of precipitation. Thereby, glacier flow is transporting the mass gained in the accumulation region to the ablation region. So, glaciers can only exist where temperatures are sufficiently low and precipitation is high.

The Equilibrium Line Altitude (ELA) is the altitude where accumulation equals ablation. When temperatures increase, the ELA is shifted to higher elevations, the accumulation zone decreases and the ablation area increases which in turn reduces the ice mass input by a reduction of glacier flow (Ohmura *et al.* 1992). Figure 2.5 shows the approximate conditions at the ELA as function of mean air temperature and average annual precipitation (UNEP 2007). For the typical maritime glaciers in Alaska, the high amount of precipitation and the relatively high temperatures along the coast induce a significant mass turnover with fast flow and strong melting. Further inland, where precipitation amounts decline, the reduced accumulation is compensated by lower temperatures, i.e. mean glacier elevation increases. Such a strong relation between glacier mean elevation and distance from the coast is also found in the study by Le Bris et al. (2011). Thus, when any of these parameters change, glaciers will adjust to the new conditions. However, as the glacier response times are often longer than climate fluctuations, changes for the largest glaciers will mostly be elevation change rather than changes in area or length. This down wasting is already observed for many large glaciers in the world including glaciers in Alaska (VanLooy *et al.* 2006).

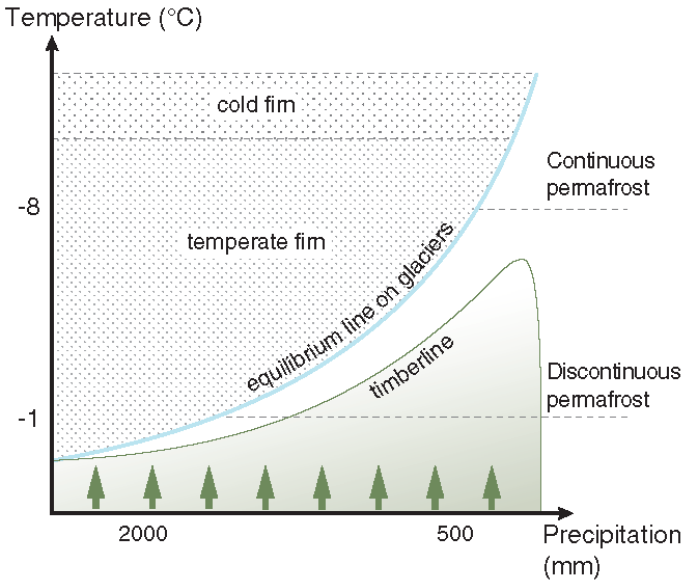

Figure 2.5: *Cryospheric diagram (UNEP 2007).*

2.3.2 Mass balance measurements

Mass balances are measured on more than fifty glaciers each year (WGMS 2008) reaching back to 1947 for entire glaciers (Zemp *et al.* 2009). In a first approach glacier mass balance can be defined as the mass gain over a year subtracted by the mass loss for a given glacier (Paterson 1994). In this way, glacier mass balance is the direct expression of annual climatic conditions (Haeberli *et al.* 2003).

Glaciological method

The direct glaciological method is used to estimate glacier mass balance in the field (Kaser *et al.* 2003). It uses in-situ measurements and requires that a given glacier has to be surveyed at different locations and zones of its surface. Measurements of surface elevation change and density are usually undertaken twice a year at the end of the accumulation and ablation periods. This gives the winter balance (end of April) and the summer balance (end of September) in the Northern Hemisphere. Summing these two balances up leads to the annual mass balance. In the accumulation area, several snow pits are dug until the last observed horizon is reached. Accumulated snow thickness and snow density are directly measured at the pit wall (Fig. 2.6). In the ablation area, stakes are drilled into the glacier and reveal the amount of ice loss. The density of ice is assumed to be 900 kg m^{-3} (Paterson 1994). Mass gain or loss in units of metre water equivalent (m w.e.) is calculated by multiplying the thickness differences by the ice or snow density. Interpolation over the entire glacier and division by the glacier area gives the specific mass balance (e.g. Cogley 2009). The fact that the mass balance values are defined per unit area allows for comparison with other glaciers from different regions in the world. The direct glaciological method is seen as a reference method but demands are high in terms of time

expenses and labour so that only a few glaciers (about 50) worldwide are investigated each year with this method (WGMS 2008). This method also requires calibration with the geodetic method (see next point) to compensate for systematic errors and volume changes that are not visible at the surface (e.g. internal melt or collapse).

Figure 2.6: *Measurement of snow thickness and density in a pit wall. (Photo taken by H. Frey)*

Geodetic method

Cumulative and overall mass balance estimates derived from the geodetic method are based on the subtraction of sequential DEMs of two epochs yielding elevation changes (Δh) over the respective glaciers. The resulting volume changes are converted to mass changes by multiplication with an appropriate value for density. This technique is now widely applied to estimate glacier volume and mass changes, in most cases using the SRTM DEM for one point in time (VanLooy *et al.* 2006; Larsen *et al.* 2007; Paul and Haeberli 2008; e.g. Schiefer *et al.* 2008; Berthier *et al.* 2010) and earlier national DEMs or more recent DEMs derived from airborne laser scanning (e.g. Andreassen *et al.*, 2012). The precision of the geodetic method is mainly related to DEM accuracy. For example, in the case of a DEM derived from photogrammetric techniques, the low contrast in optical imagery over accumulation areas (saturation of the sensor by snow) or in regions of cast shadow can introduce significant errors in the estimated elevations (Kääb *et al.* 2002). Other effects play a role for the accuracy of InSAR derived DEMs (e.g. radar shadow and layover), partly even causing data gaps (e.g. voids in the SRTM DEM).

When elevation or volume changes have to be converted to mass changes, assumptions about the density of the material have to be made. Depending on the time period considered, the climatic regime, and the general trend of the changes, this can be difficult

as density can only be determined in the field and has locally a high variability (Escher-Vetter *et al.* 2009; Kuhn *et al.* 2009). Using the density of ice for conversion will thus only provide an upper bound estimate so that density is in most cases approximated (a value of 850 kg/m^3 is often used). Furthermore, only signals of in the range of a decimetre per year can reliably be measured (Bamber and Rivera 2007). In fact, geodetic mass changes only reflect the changes that occurred over a certain period of time and do not provide information on shorter term changes. Moreover, it also considers internal or basal melting and is thus different from the cumulative values obtained at the glacier surface from the direct glaciological method (Fischer 2011).

Direct and geodetic measurements are thus two complementary methods to estimate glacier mass balance. The former offers well defined results in a year or even at a seasonal time scale for specific glaciers while the latter provides a large scale assessment (e.g. complete mountain region) over a longer time scale.

The geodetic method is thus most efficient to estimate volume changes of glaciers located in remote and difficult to access regions or huge glaciers. This method is thus of particular interest in this thesis as it has been used to evaluate elevation change occurring for glaciers in the western Alaska (see Chapter 4).

2.3.3 Length and area changes

In order to understand how glaciers react to climate forcing, glaciologists have been measuring length changes for more than 110 years (e.g. Reid 1901). First systematic measurements of length changes started in 1895 and represent an invaluable dataset for climate-related studies. For instance, length changes can be converted to temperature changes (Leclercq and Oerlemans 2012), to sea-level contribution (Oerlemans *et al.* 2007) and also serve to calibrate glacier flow models. Today, satellite data are also used to derive them (Paul *et al.* 2011). These measurements nevertheless require, an intensive effort as they are made manually. In this thesis a new method is presented to accomplish this task automatically.

Glacier length change is the most visible glacier reaction to climate forcing. It constitutes a key element in terms of interpretation of the past temperature and precipitation conditions. However, in contrast to glacier mass balance, length changes are a delayed and filtered signal to climate change (Haeberli 1995). In fact, length changes are delayed by glacier response times which are influenced by several parameters including glacier size, slope and climate regime (Hoelzle *et al.* 2003). Glacier area change is also an "easy" parameter to assess from remote sensing, but its relation with climate forcing is difficult to establish. So, area changes should always be analysed collectively (e.g. for entire mountain ranges as a mean signal).

3

Remote sensing

One definition of remote sensing is "measuring physical properties of an object at the Earth's surface without contact". Sensors are instruments able to measure the quantity of energy reflected by an object for specific electromagnetic wavelengths. Basically, sensors can be of two types: passive or active. Passive sensors take advantage of solar energy reflected from the Earth's surface to characterize objects, while active sensors like RADAR (RAdio Detection And Ranging) emit their own source of energy (microwaves) to "illuminate" their target. In view of the applications performed in this thesis, the focus of the following more detailed descriptions is on the sensors and techniques of relevance. This includes the Landsat TM/ETM+ sensors (glacier mapping) and the SPOT5 and Terra (ASTER) platforms providing DEMs for elevation change assessments. The glacier mapping section describes the workflow applied to create the glacier inventory.

3.1 Platforms

3.1.1 Landsat

The National Aeronautics and Space Administration (NASA) and U.S. Geological Survey (USGS) Landsat Program started in 1972 with the launch of the first satellite. The aim of this program was to survey the Earth's surface from space. From the six satellites that composed this program, only two were still operational (Landsat 5 and 7) at the beginning of the study described here. Unfortunately, Landsat 5 stopped working by the end of 2011 when technical problems in the satellite-to-ground transmissions data system occurred. Three main sensors are onboard Landsat satellites. The Multispectral Scanner System (MSS) and the Thematic Mapper (TM) for Landsat 1 to 5 and the Enhanced Thematic Mapper (ETM+) for Landsat 7 with multispectral capabilities designed to survey land surface properties in different spectral bands.

Over the last four decades, Landsat sensors have acquired a large image archive that is extremely useful to study glacierized regions and to perform change analysis. In fact, despite their relatively low spatial resolution compared to some other sensors, Landsat sensors are well suitable to study glaciers. For instance, the 30-m resolution of TM is sufficient to map glaciers with a minimum size of 0.01 Km^2 which is equivalent to 11 pixels (Paul *et al.* 2009). The resulting Landsat satellites scenes cover the Earth's surface between 81 degrees North and South and are available online from glovis.usgs.gov. (Wulder *et al.* 2012).

3.1.2 SPOT

The Satellites Pour l'Observation de la Terre (SPOT) is a French program initiated in 1978. Up to now, this program encompasses five satellites (SPOT 1-5) that have been launched in 1986, 1990, 1993, 1998 and 2002. Since the failure of SPOT 2 in 2009, only SPOT 4 and 5 remain operational. To ensure persistence of the program, SPOT 6 was launched in September 2012 and SPOT 7 is planed to be launched in 2014.

Sensors onboard SPOT 4 and 5 are named High Resolution Visible Infra Red (HRVIR) and High Resolution Geometric (HRG). Both of these sensors have a capability to record data with an oblique viewing angle of ±27 degrees from the vertical. The steering possibility is remotely controlled from the ground depending on scientific requirements and allows reducing of the temporal resolution to 4-5 days. SPOT 5 HRG is able to acquire stereopairs enabling the generation of DEMs. Those products are very useful and have been applied for detailed glaciological studies (for example in the IPY SPIRIT project which focused on Arctic glaciers including Alaska; (Korona *et al.* 2009)). These DEMs are made available for free for IPY participants.

3.1.3 Terra

The Advanced Space-borne Thermal Emission and Reflection Radiometer (ASTER) is a sensor onboard the Terra satellite launched in 1999. The satellite is a result of collaboration between the Japanese governments Ministry of Economy, Trade and Industry (METI) and the National Aeronautics and Space Administration (NASA). The three different spectral ranges covered by the sensor are: (i) the VNIR (Visible and Near Infra-Red); (ii) the SWIR (Short Wave Infra-Red) and (iii) the TIR (thermal Infra-Red). As with SPOT 5, the ability to acquire three-dimensional images (from an along-track with a nadir and backward looking telescope) makes the ASTER sensor useful to generate high-precision DEMs (Kääb *et al.* 2002; Toutin 2008). The SPOT 5 satellite is mainly dedicated to land surface surveying such as the study of vegetation, land temperature, glaciers or snow cover. Table 2 and 3 summarize some technical characteristics of those platforms and sensors.

Satellite	Landsat 5	Landsat 7	SPOT 5	Terra
Sensor	TM	ETM+	HRG	ASTER
Launch date	01.03.1985	15.04.1999	03.05.2002	18.12.1999
Earth distance [km]	705	705	822	705
Revisiting period [days]	16	16	26	16
Image size [km x km]	185 x 170	185 x 170	60 x 60	60 x 60
Spatial resolution [m]	30, 120 (T)	30 (15), 60 (T)	5 (P), 10 (V), 20 M)	15 (V), 30 (M), 90 (T)

Table 2: *Platforms and sensors characteristics. (V=visible, M=middle infrared, T=thermal infrared). After* Paul (2007).

3.2 Sensors

The optical sensors applied in this thesis differ in spectral, spatial, temporal and radiometric resolution. The specific characteristics of these resolutions are described below. They refer to the capability for a given sensor to properly discriminate objects at the ground among surrounding elements.

3.2.1 Spectral resolution

Multispectral sensors have the ability to record radiation reflected by objects at the surface in different parts of the electromagnetic spectrum. More specifically, a multispectral sensor can register data in discrete spectral bands. The number and the width of those individual bands define the spectral resolution of the instrument (see Table 3). Only the Landsat TM/ETM+ sensors have a blue band which is important to create natural colour images and identify snow and ice in shadow. The wavelengths covered by optical sensors include visible, near-infrared, shortwave infrared and thermal infrared bands. In this regard, the ASTER sensor uses 6 bands to cover the SWIR part of the spectrum while

Landsat and SPOT use 8 and 5 bands respectively.

TM Band #	Landsat 5 TM	Landsat 7 ETM+	SPOT 5	ASTER
Band 1 (Blue)	0.45 - 0.52	0.45 - 0.515	-	-
Band 2 (Green)	0.52 - 0.60	0.53 - 0.61	0,50 - 0,59	0.52 - 0.60
Band 3 (Red)	0.63 - 0.69	0.63 - 0.69	0,61 - 0,68	0.63 - 0.69
Band 4 (NIR)	0.76 - 0.90	0.75 - 0.90	0,79 - 0,89	0.76 - 0.86
Band 5 (SWIR)	1.55 - 1.75	1.55 - 1.75	1,58 - 1,75	1.60 - 1.70
Band 7 (SWIR)	2.08 - 2.35	2.09 - 2.35	-	2.15 - 2.43[1]
Panchromatic	-	0.52 - 0.90	0,51 - 0,73	-

Table 3: *Spectral bandwidths from different sensors in µm. [1]=summary of 5 individual bands. After Paul (2007).*

3.2.2 Spatial resolution

The spatial resolution of a sensor is related to the smallest ground area that can be resolved in an image. This image is defined in a two-dimensional form where its pixel (picture element) size approximates the spatial resolution of the instrument (Pellikka and Rees 2010). High spatial resolution satellites like ASTER, Landsat and SPOT (see above), are able to distinguish ground features at 15, 30 and 20 m (SPOT panchromatic also 10, 5 and 2.5) resolution respectively. It should be noted that the spatial resolution also depends on the spectral band considered. For example, the panchromatic band of ETM+ has a resolution of 15 m, bands 1-5 and 7 have 30 m, band 6 has 60 m. All very high spatial resolution satellites (e.g. Ikonos and QuickBird) have a ground resolution of 1 m or even higher (Huggel *et al.* 2004).

3.2.3 Temporal resolution

Temporal resolution is an important factor to find suitable images for change detection. It refers to the frequency of image acquisitions and relates directly to the orbital characteristics of satellites and the location on Earth. In fact, the time between successive images of the same location is determined by the repetition cycle of orbits around the globe and the swath width of the sensor. In general, the larger the swath, the higher the temporal resolution. As the lines of longitude converge towards the poles, the temporal resolution of a sensor will increase in these regions (Pellikka and Rees 2010). Moreover, when a specific sensor has a short temporal resolution, its spatial resolution is coarser (Huggel *et al.* 2004). The repeat cycle, which corresponds to the time taken by a satellite to resurvey the same area, is 16 days for Landsat but only 4 to 5 days for SPOT and 5 days for ASTER as their mirrors can be pointed to a target (non-nadir acquisition).

3.2.4 Radiometric resolution

The radiometric resolution defines the capability of an instrument to record brightness values (or levels of reflectance) in each individual band. The level of reflectance is stored

in computer binary digits modes. For example, in 1-bit mode, each pixel can receive 2 levels of reflectance (0 and 1) and an 8-bit mode offers 256 possible values (0 to 255). These values are named Digital Number (DN) and have integer format. Most of the sensors have a pre-defined radiometric resolution, but the sensitivity of the ASTER and the Landsat ETM+ can be shifted up and down to adjust for the wide range of spectral reflectances on Earth (Huggel, 2004). For normal, the setting is low gain over ice and snow and high gain over other land. This parameter needs to be taken into account when sensors sensitivity is saturated by snow or is close to 0 over shadow. In cast shadow for example, few details can be seen with low gain setting but better contrast in the ASTER 3N/3B over snow for DEM generation can be expected.

3.3 Glacier mapping

Glacier area is one of the most important parameters to be monitored from satellites. The high altitude of platforms allows for an extensive field of view (170 x 185 km in case of Landsat) which permits covering large regions or even entire mountain ranges. If weather conditions allow (cloud and free of seasonal snow), it is possible to map glacier extents by automatic delineation (i.e. band ratioing, see § 3.3.1C). The methodology used to create the inventory is described in the following in more detail.

3.3.1 Methodology

The method uses optical satellite data in a semi-automatic way and takes advantage of the spectral reflectance properties of ice and snow to map glaciers and ice caps (Paul and Kääb 2005). Steps A to H are visualized in Figure 3.2 and are explained in detail here:

A) Selection of satellite scenes

In some maritime regions like in Alaska, where cloudy conditions prevail, it is often difficult to find cloud free images. Therefore, merging two or more images from different years can be required to cover the complete region (see Quicklooks in Appendix A1). The snow conditions are also a key parameter when selecting images. Satellite scenes acquired at the end of the ablation period are the most suitable also regarding solar elevation as they offer a good trade-off between shadow and contrast. (See web link (http://academic.emporia.edu/aberjame/gage/glacier7.htm) for optimal dates for each region in the world).

B) Co-registration and georeferencing

To be digitally overlaid in a GIS, all data need to have a projection that can be transformed to the projection of choice. This implies mathematical transformations of the datasets and the use of projection and coordinate systems. Landsat scenes used in this

study have been orthorectified with a DEM and were downloaded as the standard terrain correction (Level 1T) product. After downloading all scenes were re-projected to the Universal Transverse Mercator (UTM) zone 5. DEMs were mosaicked and also re-projected to this UTM zone using a bilinear interpolation and 30 m cell size.

C) Main processing - Band ratioing

This processing step uses the multi-spectral capability of Landsat sensors to map glaciers and ice caps. With the respectively high and low reflectance of glacier ice and snow in TM3 (red) and TM5 (shortwave) bands (e.g. Dozier 1989), a simple band ratio (Red/SWIR) offers the possibility to efficiently discriminate clean ice from the surrounding terrain with a threshold in a reproducible and consistent manner (e.g. Albert 2002; Paul 2002) (Fig. 3.1). The band ratios TM4/TM5 or the Normalized Difference Snow Index (NDSI) were applied as well for glacier mapping (e.g. Sidjak and Wheate 1999), but here preference is given to the TM3/TM5 ratio (see D).

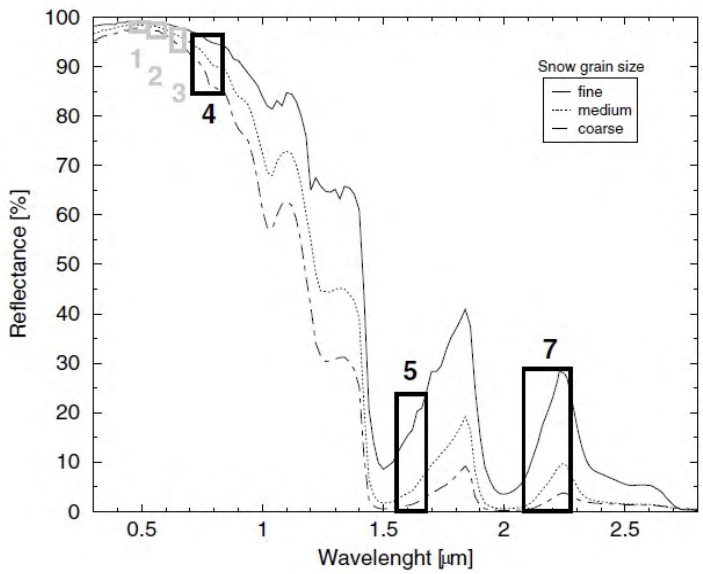

Figure 3.1: *Spectral reflectance curves of snow with varying grain sizes (from Paul, 2007)*

D) Classification – Threshold selection

The classification step is basically a selection of the threshold values on the raw ratio image (Rott 1994; e.g. Bayr *et al.* 1994; Dozier and Painter 2004). Several tests are made to find the most convenient results. In most of the cases values are set between 1.8 and 2.2. An additional threshold is applied on the blue band (TM1) to enhance the classification of glaciers in cast shadow regions. A low pass median filter (3x3) is finally used to remove isolated pixels (often snow patches). Even if the TM3/TM5 ratio also maps water bodies (which are easily recognized and removed in post-processing), it is still preferred over the TM4/TM5 ratio as this ratio failed to map glaciers in cast shadow (e.g. Andreassen *et al.*

2008). The choice of the band ratio depends on the study region and its haze conditions. For example, in one region of Alaska it was not possible to map the lower parts of the glaciers due to fog originating from fires. A second scene was used to map these parts (see Appendix A1-I-J).

E) Vector – Raster conversion

The raw classified map is converted from raster to vector format within the GIS or remote sensing software to obtain vector outlines and allow manual editing.

F) Post-processing (Manual corrections)

Misclassifications resulting from the band ratio technique need to be manually corrected in post-processing steps. Commissions errors (clouds, water bodies (lakes and/or rivers), snow patches) and omissions errors (debris-cover part of glacier, region in shadow) can be easily identified by visual interpretation of false colour composite (FCC) images in the background and manual digitizing. In this regard, band combinations normally used for visual identification are (i) 3-2-1, (ii) 4-3-2 and (iii) 5-4-3 as red, green and blue (RGB) respectively. The first combination (i) shows feature in natural colours while (ii) enhance vegetation (appearing in reddish colours) and water bodies (blue colours) and (iii) is the most appropriate combination to recognize glacier and cloud features (see Appendix A2).

G) Creation of drainage divides

The primary use of drainage divides is to separate contiguous ice masses into individual glaciers. The technique used to create them follows a method developed by Bolch *et al.*, (2010) (see § 5.2.2). The first step is to define a buffer zone (usually between 1000 to 1500 m) around each glacier and then apply hydrological watershed analysis using a DEM. Even if DEM accuracy influences the quality of the resulting drainage divides, this approach is recommended as it is more consistent and faster than a complete manual digitizing. However, manual corrections remain to obtain a high quality product.

H) Glacier parameters

Glacier specific topographic parameters (e.g. area, minimum and maximum elevations, slope, and aspect) are calculated within the GIS using zonal statistics tools (Paul *et al.* 2009) for details). These tools use a value grid (a DEM) to compute statistics over a defined digital polygon zone (i.e. the glacier boundary in vector format). Further details are given in the GIS section. Tabulated attributes are stored along with shapefiles to complete the inventory which is finally uploaded into existing glacier databases (GLIMS).

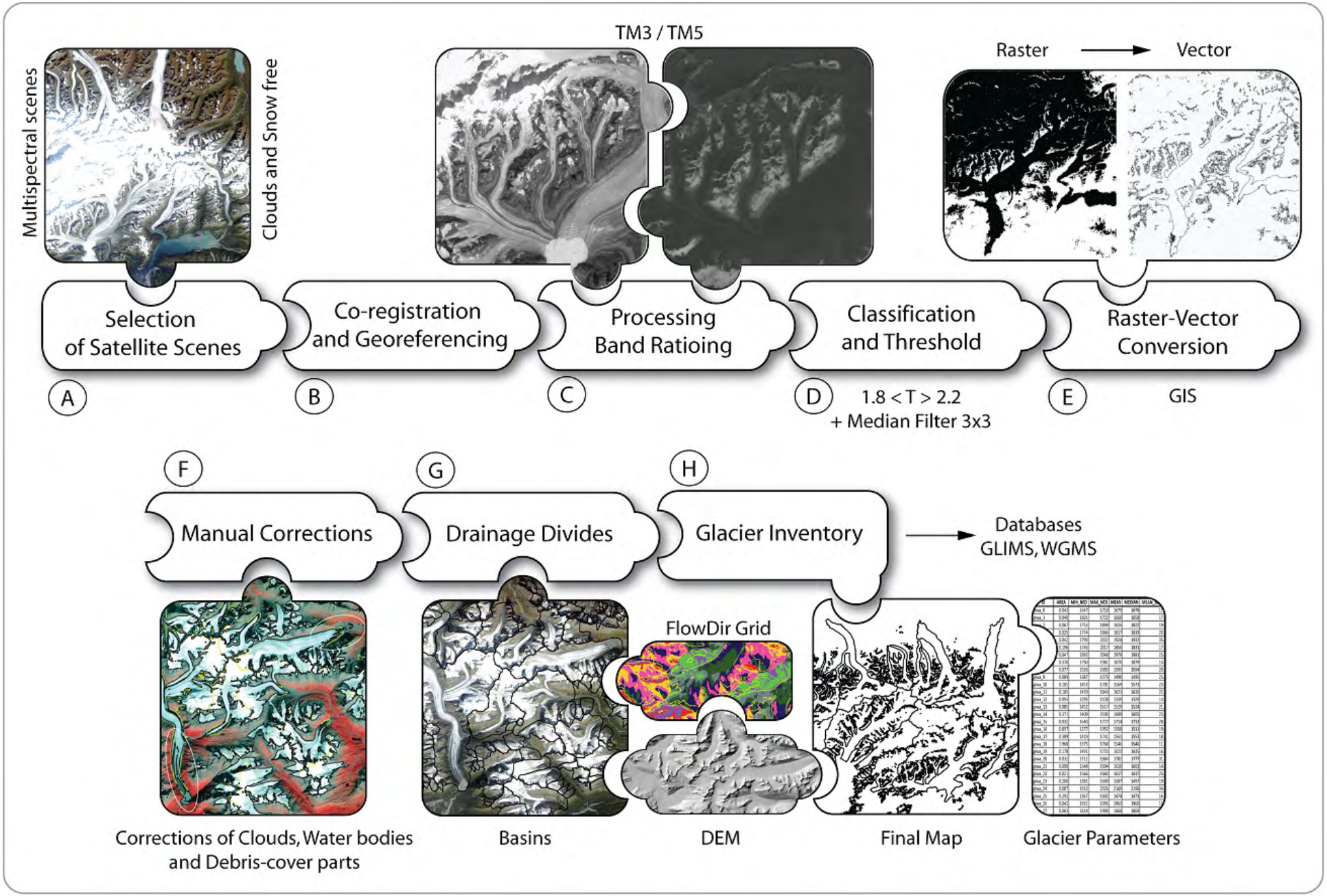

Figure 3.2: Flowchart of the glacier mapping process

3.3.2 Manual vs. automatic methods to map glaciers

Automatic methods to map glaciers (e.g. band ratioing) offer several advantages compared to complete manual digitizing of the outlines. It is a much faster, more robust and also reproducible method. The first point is especially important for large regions like Alaska with several thousand glaciers. In terms of accuracy, it is for clean ice at least as accurate as manual digitizing (see below). For satellite data that do not offer a band in the SWIR (e.g. many very high-resolution sensors or aerial photography) manual digitizing is the only way to create outlines. However, band ratioing also has some shortcomings. Water bodies, clouds, glaciers in cast shadow and debris-covered parts are not correctly mapped and represent a main drawback of this method and require corrections in the post-processing step.

3.3.3 PALSAR

The Synthetic Aperture Radar (SAR) is an active method using microwaves that illuminate the surface themselves. Although optical remote sensing is the key technique for mapping glaciers and obtaining glacier parameters, it comes with the important shortcomings of being dependent on solar illumination and thus daylight and cloud conditions, whilst microwaves penetrate through clouds and can also acquire images during night. Of specific importance in regard to glacier mapping is the Phased Array L-band SAR (PALSAR) of the Advanced Land Observing Satellite (ALOS). Though dielectric properties of glacier ice and snow are not sufficiently different from other material to map glacier extents directly (Hall *et al.* 2000), interferometric techniques offer an interesting potential to identify debris-covered parts of glaciers (e.g. Atwood *et al.* 2010). This technique is based on the loss of the coherence over interferograms (Paul *et al.* 2010) from two images acquired in summer due to glacier motion between the 46 days of the revisiting period. The coherence images can be used to improve delineation of the outline for debris-covered glaciers in regions with very low optical contrast (Frey *et al.* 2012).

3.4 Accuracy of glacier outlines

Assessing the accuracy of either manual or automatically derived glacier outlines is an important issue in particular for glacier area and length change studies. Obviously, the accuracy of glacier outlines showing glacier changes must be larger than the effective changes. To assess this accuracy, a round robin on glacier mapping was performed in the framework of the ESA Glaciers_cci project (http://www.esa-glaciers-cci.org/). The related paper gives an overview of the accuracy determination of glacier outlines and provides recommendations for accuracy determination using satellite data. Based on Paul *et al.* (2013), details of this analysis are given in this section.

3.4.1 Digitizing experiment

To determine the accuracy of glacier outlines created automatically and from manual digitization, a multiple digitizing experiment was performed by the participants of the round robin including the multiple digitizing of a few glaciers by the same and different analysts. The main issue when estimating accuracy is the lack of an appropriate reference dataset. To overcome this problem, the mean glacier area resulting from the multiple manual glacier delineations was computed and served as a reference data set.
The glaciers were selected from two different regions (eastern Chugach Mountains in Alaska and European Alps) and considered some of the main challenges related to glacier mapping and visual interpretation of satellites images: debris-cover, snow conditions and shadow. From the resulting dataset four types of comparisons were performed:

- the consistency of the manual digitizations by one person
- the determination of absolute differences to the automated method
- an overlay of all outlines for visual inspection of the problematic regions
- a comparison with an independently generated reference dataset

Three satellite scenes and aerial photography for three glaciers were used for the digitizing experiments. In total, 20 participants were involved in the round robin and had to manually delineate three times 21 glaciers from the two regions. In order to guarantee independent interpretation, no reference to the results of the previous sessions was allowed. Automated mapping of glacier outlines was performed with the band ratio method described above and applied to a Landsat TM scene.

Area differences for each glacier (mean values and standard deviation) are derived in comparison to the reference value. To illustrate the variability in glacier outline interpretation, an example showing overlays of the digitizations performed by the participants is given in Figure 3.3.

3.4.2 Results

Differences between the interpretations can be clearly seen from the overlays. For example, for glacier #8 (Fig. 3.3), the debris-covered parts show large differences from one analyst to another. In general, bare ice was correctly and consistently interpreted for all glaciers, but ice in cast shadow was omitted in several cases (glaciers 2 and 3).

The mean standard deviation (STD) of the derived glacier areas was 5.7% for all eight glaciers in Alaska using the QuickBird scene for digitization. Using the Landsat TM scene for the Ötztal Alps, STD values ranged from 2.7 to 14.6% with a mean of 3.5%. In the case of the automatically derived outlines the mean difference compared to the reference value is 3.1% (excluding the largest glacier). The STD of area differences is in general smaller than 5% for glaciers larger than 1 km^2 and between 1 and 18% for smaller glaciers (Fig. 3.4).

Glacier areas derived automatically from TM appear to always be slightly smaller than areas derived from the manually digitized outlines. This is likely due to full inclusion of mixed pixels in the manual digitization. However, the statistical results reveal that automated mapping of clean ice is as accurate as manual interpretation and that it is indeed a much faster, consistent and reproducible method for glacier mapping from optical satellite data. The analysis also revealed that a high spatial resolution does not necessarily result in a more accurate delineation of glacier outlines, as the correct interpretation of debris cover is still challenging.

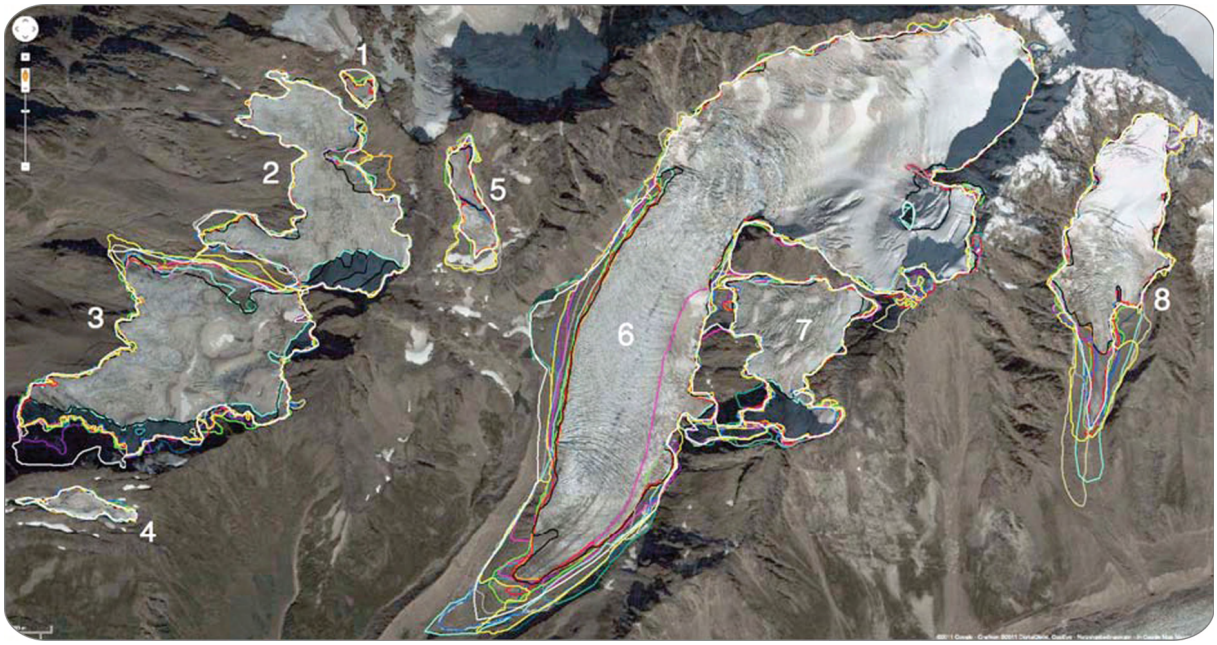

Figure 3.3: *Overlays of digitizations performed by the participants (After Paul et al., 2013)*

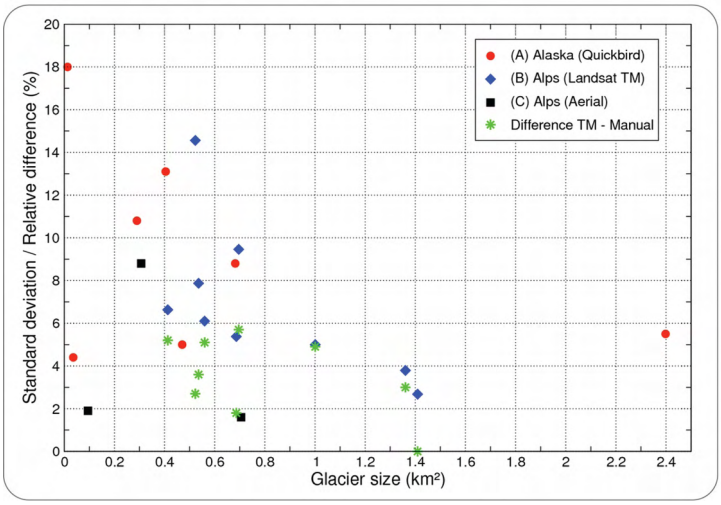

Figure 3.4: *Glacier size vs standard deviation for the test regions in Alaska, in the Ötztal Alps and in Switzerland. (After Paul et al., 2013)*

4

Digital Elevation Models

A Digital Elevation Model (DEM) is a digital and discretized representation of the Earth's surface. It can either be in vector format e.g. a so-called Triangular Irregular Network (TIN) representation (which is a set of contiguous non-overlapping triangles whose vertices are placed adaptively over the Earth's surface (Fowler and Little 1979)) or in raster format. In the latter case, a DEM is a regularly spaced matrix of cells (or pixels) over a specific region (Fig. 4.1) and quantifies terrain elevation on Earth from a set of points (x, y and z) (Burrough and McDonnell 1998). Satellite- and map-derived DEMs are a most important component to study a wide range of processes in remote regions (e.g. Huggel *et al.* 2004), as they provide crucial information about the variability of surface topography including glacier surfaces (details on DEMs are given in the next section). They are also a key element for a large number of calculations related to glaciers:

- orthorectification of satellite imagery,
- deriving drainage divides,
- calculating topographic parameters for each glacier,
- determination of elevation changes from two DEMs,
- and all kinds of distributed modelling (e.g. mass balance, glacier thickness)

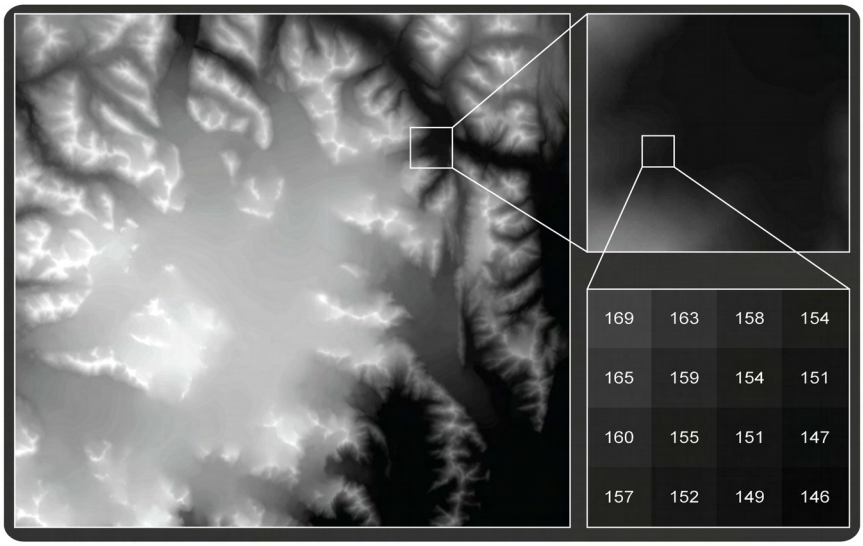

Figure 4.1: *Example of a DEM*

4.1 DEM generation

4.1.1 DEMs from optical sensors

The viewing angle for pixels that are not in the centre of a satellite scene (nadir) causes a shift of their location when they are placed at a certain elevation. This so-called panoramic distortion can be corrected with a DEM, but their elevation can also be derived from their shift when they are observed from two different angles. Stereo satellite sensors acquire such images of the Earth's surface from two viewing angles allowing for stereo pairs to be built. The different viewing angles are obtained from either two different sensor positions (across-track stereo) or from the same overflight with nadir- and backward-looking sensors (along-track stereo) (Kääb 2005). The main advantage of the along-track stereo is the short acquisition difference between the two images (from seconds to minutes) compared to the across-track stereo (from days to months), where conditions (e.g. snow, melting, clouds, shadow) could have changed in between. Automated stereo-correlation techniques (Hirano *et al.* 2003) are applied to the stereopairs to compute elevation values from the shift vectors of corresponding pixels (Colvocoresses 1982; Fujisada and Ono 1994; Toutin 1995, 2004). In regions where contrast is low (snow, shadow) it is difficult to find corresponding pixels and the matching might even fail, resulting in artefacts or even data voids.

The ASTER and SPOT5 sensors generate along-track stereo pairs. Across-track stereo pairs can also be generated from SPOT5 thanks to its steerable sensor (±27°) allowing acquisition of scenes from the same region using an adjacent track. The same sort of stereo pairs can be computed from adjacent Landsat paths for the region of overlap (Ehlers and Welch 1987), but this has never been done systematically and only works with the raw data.

4.1.2 InSAR-derived DEMs

The all-weather capability of active sensors represents an important advantage for DEM creation compared to optical sensors, because the emitted microwaves penetrate cloud cover and are day and night operational. However, measurements of the phase coherence from SAR techniques are sensible to the dielectric surface (ice and snow) conditions (Gens and van Genderen 1996). Indeed, SAR imagine techniques (side-looking) have the disadvantage of creating radar shadow, layover and foreshortening effects which hamper the monitoring of valleys (Kääb 2005).

Processing a pair of RADAR images taken from two slightly different positions, interferometric techniques (InSAR, Interferometric Synthetic Aperture Radar) can be used to reconstruct high-quality DEMs (e.g. Crosetto and Pérez Aragues 2000). InSAR exploit the coherence of SAR images to compute stereo parallaxes from phase differences resulting from terrain elevation (Bamler 1997) and convert the interferograms to elevation values. The Shuttle Radar Topography Mission (SRTM) DEM is likely the most prominent example of a DEM generated from InSAR techniques (Jordan *et al.* 1996; Rabus *et al.* 2003; Farr *et al.* 2007).

The choice between DEMs derived from maps, optical sensors or interferometric techniques mainly depends on the characteristics of the studied region (e.g. steep and rugged high-mountain topography, shadow or snow conditions) and data availability. In some regions several types of DEMs are available and it is advisable to directly compare them before one is selected and applied. An overview of DEM characteristics is given in Tables 4 and 5 below.

4.1.3 DEMs derived from topographic maps

DEMs can also be generated from topographic maps by interpolation of contour lines (Brown and Bara 1994; Guth 1999). The first step is to convert the topographic map into a raster format by scanning and georeferencing the resulting file. Contour lines and spot elevations are then digitized with their respective elevation values tagged to the vector data. Finally, the vector contour lines are converted back to a raster grid using an interpolation algorithm (e.g. Arrighi and Soille 1999). The USGS NED (National Elevation Dataset) DEM is an example of a DEM produced by this method.

4.2 DEM description and sources

The SRTM DEM is a product that was generated during an 11 day mission in February 2000 with the Space Shuttle Endeavour. This project was a collaboration between NASA's Jet Propulsion Laboratory (JPL) and the National Geospatial-Intelligence Agency (NGA) (Rodriguez *et al.* 2006). Using single-pass interferometry with two radar antennas of 60 m distance, almost 80% of the Earth's land surface was mapped and elevation values were

computed between 60° N and 57° S (http://www2.jpl.nasa.gov/srtm/index.html). The elevation values in the SRTM DEM have a good accuracy compared to various reference datasets around the world, for example Berry *et al.* (2007) found a mean deviation of ~ 3±15 m.

The ASTER GDEM is an elevation dataset generated from all available ASTER images acquired between 2000 and 2007. The resulting global DEM was released in June 2009 and covers nearly all of the Earth's land surface from 83° N to 83° S (http://asterweb.jpl.nasa.gov/gdem.asp). The GDEM is reported to have good quality (Hayakawa *et al.* 2008), with a vertical accuracy of 7~14 m (StDev) (ASTER GDEM Validation Team, (2009)) over various test regions, but strong artefacts over snow and shadow were reported as well (Frey and Paul 2012). The details visible are similar to the coarser resolution SRTM DEM, so the nominal resolution of 30 m does not reflect this.

The NED from USGS is a product created from contour lines compiled from topographic maps from the 1950s (Gesch *et al.* 2009). The related 1:63,360-scale 15-minute topographic quadrangle maps were derived from vertical aerial photographs (acquired between 1948 and 1957) via stereo-photogrammetric techniques. For Alaska, the NED DEM has a reported absolute vertical accuracy of 7 m (USGS, 1997).

The SPOT5 SPIRIT DEM is derived from the HRS sensor (Bouillon *et al.* 2006). The DEM was created in the framework of the International Polar Year (IPY) project "SPOT 5 stereoscopic survey of Polar Ice: Reference Images and Topographies (SPIRIT)" (Korona *et al.* 2009). The DEM has a reported absolute horizontal accuracy of 30 m, and a vertical accuracy between -5.5 and 3.5 m (compared to ICESat data). Over the entire studied area the elevation uncertainty is ±10 m (Korona et al. 2009). The SPOT5 SPIRIT DEM and the NED DEM were used to compute elevation changes for the entire region (Berthier *et al.*, 2010). The related $\Delta h/\Delta t$ raster maps were used in Paper III (Le Bris and Paul, subm.) to derive glacier specific elevation changes.

DEM	Type	Resolution [m]	Date	Sources
SRTM	InSAR	30	2000	http://www2.jpl.nasa.gov/srtm/index.html
ASTER G-DEM	Optical	30	1999-2007	http://asterweb.jpl.nasa.gov/gdem.asp
NED	Map based	60	1950's	http://seamless.usgs.gov
SPOT5 SPIRIT	Optical	40	2007	http://polardali.spotimage.fr:8092/IPY

Table 4: *Some DEM characteristics and data sources*

4.3 DEM characteristics for Alaska

In Table 5 we provide an overview of the pros and cons of the DEMs used in this study in regard to their suitability for glaciological studies in Alaska.

DEM	Pros	Cons
SRTM	▪ Usable for DEM comparison ▪ Sufficient spatial resolution ▪ Suitable to derive drainage divides ▪ Refers to the glacier topography in the year 1999	▪ Northern extent limitation (60°N), thus only available for the Kenai Peninsula ▪ Data voids due to radar shadow, layover and foreshortening effects
ASTER G-DEM	▪ Available for the complete study region ▪ Usable for DEM comparison ▪ Sufficient spatial resolution ▪ Suitable to derive drainage divides ▪ Fits better to the acquisition period of the Landsat data than the NED ▪ Used to calculate minimum glacier elevation	▪ Inaccuracies in steep slopes (Frey and Paul, 2012) ▪ Low contrast over fresh snow (Svoboda and Paul 2009) ▪ Northern slopes are distorted in the back-looking band 3B (Kääb 2005) ▪ Compiled from scenes acquired between 1999 and 2007 (glacier time stamp problem)
NED	▪ Available for the complete study region ▪ Sufficient spatial resolution ▪ Suitable to derive drainage divides ▪ Used to derive specific-glacier parameters (excluding minimum elevation) ▪ Used to perform an elevation change analysis	▪ Refers to the contour lines of the related topographic maps from the 1950s ▪ Maps are interpreted by cartographers (different purposes)
SPOT5 SPIRIT	▪ Availabile for the complete study region ▪ Sufficient spatial resolution ▪ Used to perform an elevation change analysis	▪ Available only for IPY participants ▪ Data voids in the resulting $\Delta h/\Delta t$ raster maps

Table 5: *DEM characteristics and suitability for Alaska*

4.4 DEM applications

4.4.1 Orthorectification

DEMs created by one of the techniques described above are used to correct the panoramic distortion and shifts each pixel in a position where it would be if seen from a nadir view point. This process is called orthorectification and normally also includes projection to a reference grid and datum. Afterwards, digital overlay with other geocoded datasets (e.g. the DEM itself or other satellite scenes) is possible (Paul 2007).

The Landsat scenes used to create the new Alaskan glacier inventory (Level 1 T product) are already orthorectified using commonly available DEMs (e.g. SRTM and NED) and projected to a reference grid (UTM projection with WGS84 datum). However, errors in these DEMs directly translate to wrong positions of the pixels which in turn cause problems when datasets are later spatially combined (Frey *et al.* 2012). For details on the Landsat orthorectification process refer to e.g. Gao *et al.* (2009) and Schowengerdt (2006).

4.4.2 Comparison of hillshades

Hillshade views of a DEM allow qualitative evaluation of DEM artefacts. In Figure 4.2 a comparison of the DEMs used is depicted for the McCarthy and Northwestern fjords. All DEMs were previously re-sampled to 30 m cell size by a bilinear interpolation. Pronounced differences between the DEMs are seen on this figure. For example, the NED DEM (Fig. 4.2a) reveals a very good quality and a regular smoothed surface throughout the Harding ice cap and even on steep slopes. White arrows indicate the 1950s front position of the Northwestern glacier which receded by more than 4 km since then. Figure 4.2b is the hillshade of the SRTM DEM which reveals a good quality for rather flat regions of the same ice cap and over glacier tongues, but also very large areas with data voids on steep slopes (white ellipses). The frontal moraine of the Northwestern glacier (white arrow) is also visible on this hillshade and indicates its maximum extent at the Little Ice Age. In the case of the ASTER G-DEM (Fig. 4.2c), the hillshade view reveals a rather speckled pattern mainly in flat accumulation regions (white ellipses).

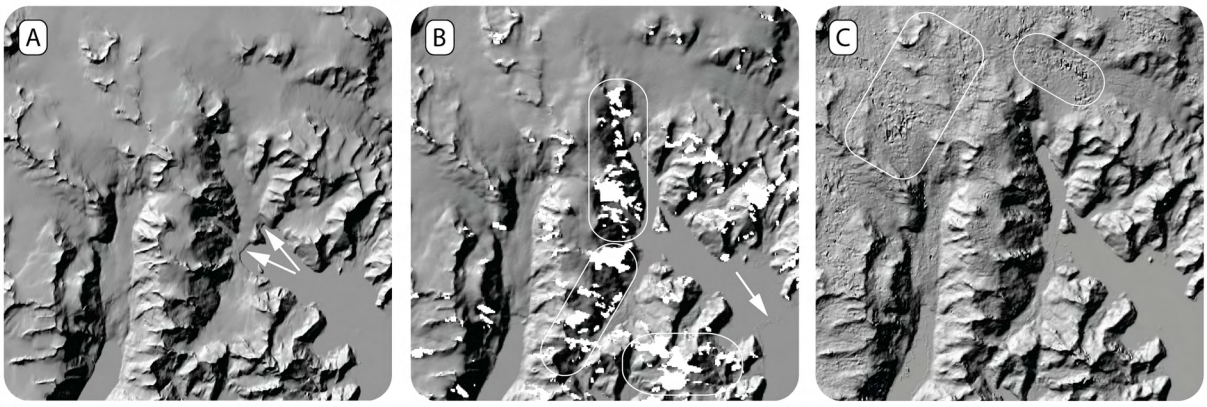

Figure 4.2: *Comparison of three digital elevation models (DEMs). (A) NED DEM, (B) SRTM DEM and (C) ASTER G-DEM.*

4.4.3 Drainage divides

A further important application of the DEM is related to the calculation of drainage divides from watershed analysis using a flow direction grid derived from the DEM (Racoviteanu *et al.* 2009). Following a method described in Bolch *et al.* (2010) and detailed in § 5.2.2, the NED DEM was used to obtain the drainage divides for the new Alaskan glacier inventory (cf. Paper I). In fact, these drainage divides also served to identify individual glaciers in the DLG dataset and to track changes in glacier separation/merging during phases of retreat and advance within the same basin. A comparison of drainage divides obtained from different DEMs is shown in Figure 4.3. Although all DEMs used in this comparison were suitable for this purpose, some distinctions can be observed, especially in the accumulation areas where the low contrast of the optical-derived ASTER G-DEM introduces large shifts (Svoboda and Paul 2009). As a consequence, all divides in accumulation regions were carefully checked before application. For this thesis the NED DEM was selected over the GDEM for this purpose as the artefacts in the GDEM would have caused a too high correction workload.

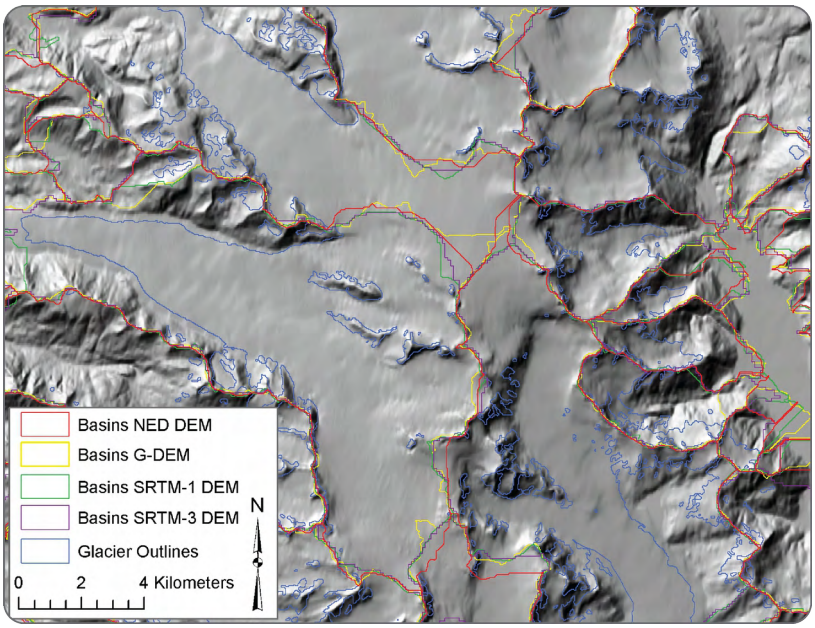

Figure 4.3: *Comparison of drainage divides derived from four different DEMs where the background is a shaded relief of the USGS NED (from Le Bris et al., 2011)*

4.4.4 Topographic parameters

One of the other main applications of DEMs for glacier inventory creation is to derive glacier-specific topographic parameters (e.g. Kääb *et al.* 2002; Paul *et al.* 2002). These parameters can be included for all inventories that are uploaded to the GLIMS database (Raup *et al.* 2007). Glacier area, elevations (max, min, mean, median), mean aspect, and mean slope (in degrees and as a sector) are the parameters that can be easily calculated from a DEM (Manley 2008; e.g. Paul *et al.* 2009). For the new Alaskan glacier inventory most of them were derived from the NED DEM using GIS-based scripts according to Paul *et al.* (2009).

As the NED DEM represents the surface topography from the 1950s, the minimum elevation was extracted from the more recent ASTER G-DEM. The SRTM DEM was not used due to its northern limitation (60° N). A study by Frey and Paul (2012) showed that the SRTM and the ASTER G-DEM are both suitable to compile topographic parameters required in glacier inventories.

4.4.5 Analysis of elevation changes

Sequential DEMs from different years have been used to estimate glacier volume changes in several regions around the world such as in North-West Canada and South-East Alaska (Berthier and Toutin 2008; Berthier *et al.* 2010), in western Alaska (Arendt *et al.* 2006), in the Swiss Alps (Paul and Haeberli 2008) and the Kerguelen Islands (Berthier *et al.* 2009). In this study the elevation change or $\Delta h/\Delta t$ raster maps from Berthier *et al.* (2010) are

used to determine glacier specific elevation changes over the 44 year period from 1962-2006 (see Paper III).

4.4.6 Flow line algorithm

A specific application of a DEM in this thesis was related to the development of an automatic method to create flow lines for determination of glacier length. This method computes from glacier outlines and the DEM the highest and lowest points of each glacier and provides elevation values of middle points along the flow line. More details on the method are given in Paper II (Le Bris and Paul, 2012).

4.4.7 Visualisations

DEMs are often used to produce oblique perspective views. When satellite scenes, glacier outlines and DEMs are correctly co-registrated, it is possible to create a pseudo 3D view which has the advantage of exhibiting the very steep topography around glaciers (Paul 2007). Visualisation of glacier changes and communications for wider public are also improved with such views. Examples of oblique views are given in Appendix A3-1 and A3-2.

5

Geographic Information System (GIS)

A Geographic Information System (GIS) is a computer structure able to acquire, store, manage and display referenced geographic information (Marble 1990; Bonham-Carter 1994; Burrough and McDonnell 1998). It represents an important component of the geomatic sciences as it permits the grouping and linkage of a large amount of heteroclite data.

The results of this thesis have largely been obtained by GIS-based processing combining several kinds of geographic data e.g. satellite images, scanned topographic maps, DEMs and tabulated information, within a unique environment. The geospatial analysis performed to monitor changes in glacier area, length and elevation were also accomplished within a GIS environment. Figure 5.1 gives a schematic overview of key input datasets (raster, vector, image) and the data layer concept of a GIS. In the following, data format definitions, main pre-processing steps and some example applications are described.

5.1 Description of data formats and processing

5.1.1 Data formats

Vector data describe graphic objects in a Cartesian plane with primitive geometric shapes such as points, lines and polygons (Star and Estes 1990). As a source of information for a GIS, those geometric data represent discretized geographic phenomenons of the real world. Geographic objects are composed of one (points), two (lines) or several (polygons) vertices or nodes. In the case of the latter two, the vertices are linked to each other with an arc (Figure 5.1A) and topological relationships. Unlike the raster format, geographic coordinates are stored for each vertex of the vector data.

The **raster** format is one of the two main models (along with the vector format) that can represent the land surface (Peuquet 1979). It might contain imagery or DEMs, but all other information that can be discretized in cells forming a continuous grid are stored as well. Composed by a matrix of cells organized in columns and rows (Figure 5.1C), a grid is an efficient means for describing the most often only gradual changes of the Earth's surface. A unique value, according to the represented element on the ground, is assigned to each cell of the matrix. Images from satellite data are usually provided with a header that gives information about the geographic location, the spatial resolution which is expressed by the cell size (e.g. 30 m for most of the Landsat scenes), as well as projection and datum. Image and raster data can be stored in different formats (GeoTIFF, ERDAS Imagine, ESRI GRID, ASCII) independently to the computer platform used. Satellite sensors are an important source of raster data.

Tabular information (Figure 5.1D) is used to characterize every object in a GIS project. This information is stored in the attribute table within a database file (.dbf) and associated to the vector data which represents the object's geometry with a dynamic link. For example, a single glacier represented by a polygon made of several vertices can receive numerous parameters like the area of the polygon, a unique identification, the mean elevation or its name. This makes this format particularly suitable for specific computer query language like the *Structured Query Language (*SQL) (Egenhofer 1994).

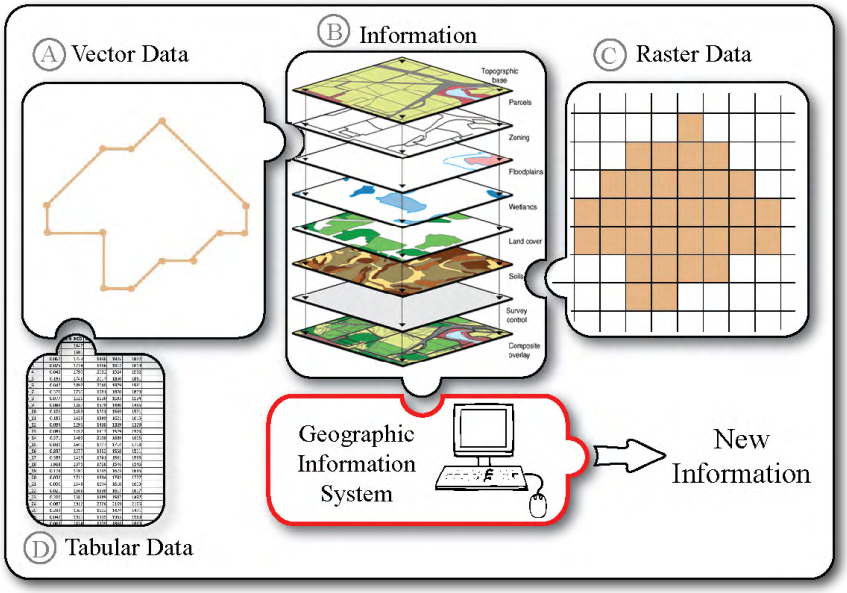

Figure 5.1: *Data format and structure of a GIS.*

Vector, tabulated and raster data are complementary and have been conjointly used in this thesis to perform spatial analysis (e.g. change assessment), create thematic maps, and perform modelling (i.e. the flow line algorithm to determine glacier length). The table below summarizes the data used according to their formats and applications.

Data	Description	Format	Application
Landsat scenes	Satellite imagery of Alaska	Image	Glacier Mapping
Digital Line Graph (DLG)	Digital outlines describing glacier extents from the 1950s	Vector	Change assessment
Digital Raster Graph (DRG)	Scan of topographic maps from the 1950s	Image	Change assessments
Digital Elevation Models (DEM)	Elevation datasets	Raster	Drainage divides, FLA, topographic parameters
Geographic Names Information System (GNIS)	List of glacier's names	Tabular	Identification of glaciers

Table 6: *Description, format and main applications of the various data sources (FLA: Flow Line Algorithm).*

Glacier outlines are created in the shapefile format (.shp) to facilitate data exchange and later incorporate the vector data into the GLIMS glacier database (Kargel *et al.* 2005; Raup *et al.* 2007). For the latter purpose some transformations have to be applied to the dataset as the GLIMS format has a rather specific set-up (see detailed description at: http://www.glims.org/MapsAndDocs/datatransfer/data_transfer_specification.html)

5.1.2 Co-registration of DEMs - A GIS computing perspective

Finding the problem

One key assessment of in this thesis is the computation of glacier-specific elevation changes for a large sample of glaciers in Alaska. By comparing the values derived for the two benchmark glaciers (Gulkana and Wolverine) to the mean value of the entire sample, we can determine the representativeness of them for the entire region over the time period of the DEMs. This analysis was performed by combining the difference of two DEMs (in this case from SPOT and the NED) acquired at two points in time (see Berthier et al. 2010 for details) with glacier outlines from the new inventory (see Paper III). Unfortunately, Gulkana glacier was not covered by the SPOT DEM and over Wolverine glacier the SPOT DEM had considerable data voids (>20%) as illustrated in Fig. 5.2. We thus had to compute the elevation changes for these two glaciers from other data sources. Despite the much better constraint acquisition date of the SRTM DEM, we decided to use the ASTER-GDEM2 here as the region is not covered by the SRTM DEM (which ends at about 60°).

Before the two DEMs can be subtracted, a good co-registration between them is required. The co-registration process guarantees that only spatially corresponding pixels in both DEMs are subtracted. This requires to find a potential (horizontal) shift between the coordinates and also to detect any vertical bias between the DEMs (Nuth and Kääb, 2011). The latter can be introduced when subtracting DEMs of different spatial resolution (Paul, 2008, Gardelle et al. 2012). The steps performed in the GIS to determine these shifts and correct them are illustrated in the following.

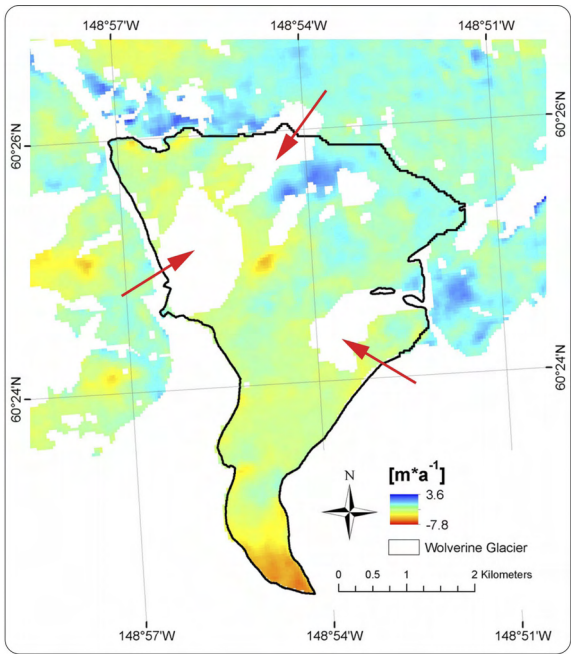

Figure 5.2: *Elevation changes over Wolverine glacier as derived from the NED and SPOT DEM. Red arrows show examples of data voids.*

Assessment of the co-registration (ASTER-GDEM2 vs NED)

In a first step we have computed the elevation differences between the GDEM2 and the NED DEM for flat terrain off-glaciers (with slopes less than 5°). This analysis did not show any systematic elevation changes for terrain outside glaciers (see Fig. 3 in Paper III). However, elevation differences on steeper slopes revealed a hillshade like rendering when coded in grey scale (Fig. 5.3, left) that is typical for a systematic shift between the two datasets. The co-registration between the two DEMs was achieved by following the method developed by Nuth and Kääb (2011). This analytic approach requires elevation differences and corresponding aspect values (at the same grid cell) as an input to quantify the offset values with an iterative approach. The correction vectors Δx and Δy were obtained after three iterations yielding values of 2.5 and 7.6 m respectively. The NED DEM was shifted accordingly using GIS tools with those correction vectors. A vertical bias for terrain off-glaciers was not found as both DEMs have about the same spatial resolution.

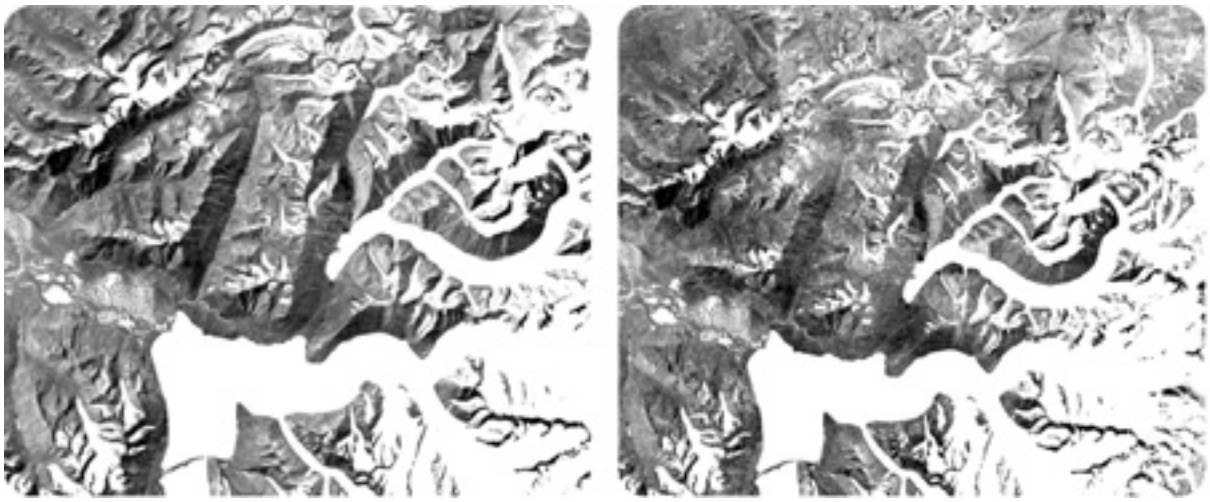

Figure 5.3: *Elevation differences between the ASTER GDEM and the NED DEM show a systematic shift (hillshade-like pattern) before x and y vector correction (left) and afterwards (right).*

Correction of the vertical bias

After both DEMs were aligned, we had to consider a potential vertical bias due to the different acquisition dates. For this purpose we compared the elevation changes derived over glaciers only from the NED/SPOT dataset with the NED/GDEM2 values. For glaciers in the same size class as Gulkana and Wolverine glaciers (10-20 km^2), we found mean differences of 0.09 m a^{-1} (see Table 2 in Paper III). These values were finally applied to both glaciers to obtain the final mean value. Figure 5.4 shows the resulting $\Delta h/\Delta t$ raster maps of Gulkana and Wolverine glaciers after horizontal co-registration of the two DEMs and vertical bias correction.

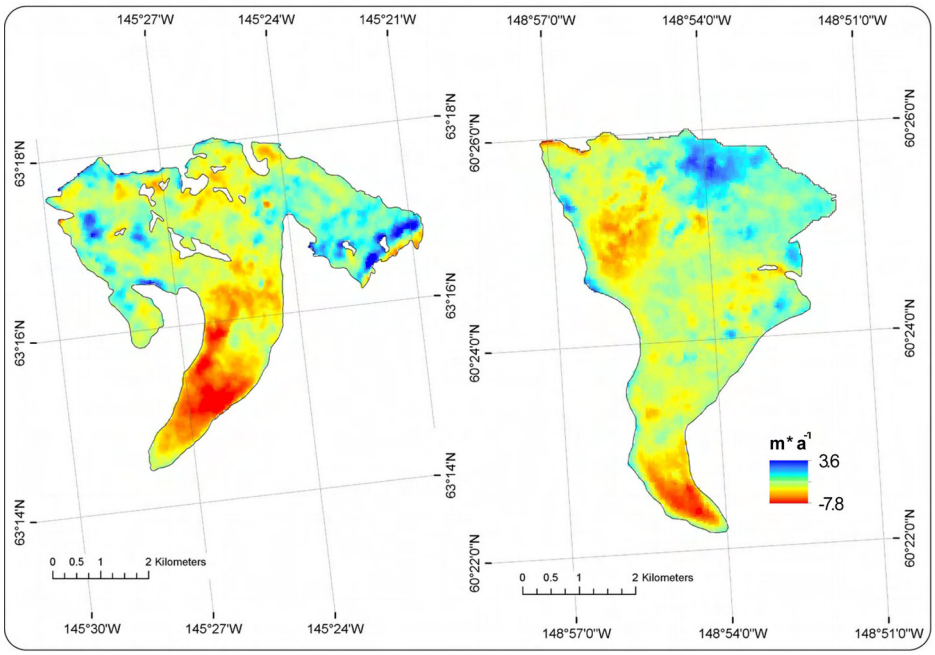

Figure 5.4: *$\Delta h/\Delta t$ raster maps of Gulkana and Wolverine glaciers.*

5.2 Applications

5.2.1 Manual digitizing

Glaciers in Alaska are located in steep, high-mountainous terrain and partly very close to the coast which results in several challenges for mapping glacier boundaries. Clouds and shadows are frequent and often hamper the interpretation of the glacier boundary. Other challenges are the dense smoke from wildfires that can cover large parts of the ablation region under otherwise optimal glacier mapping conditions, and volcanic ash hiding the glacier ice. To deal with the smoke problem, two Landsat scenes (from 2005 and 2007) were combined in one region (path-row 72-16) to properly map the lower parts of the glaciers (see Paper I).

The glacier outlines for the new inventory are created from the well-established band ratio method (e.g. Paul and Kääb 2005) with manual corrections in regions of misclassification (Fig. 5.5) following the mapping strategy of the GlobGlacier project (Paul *et al.* 2009).

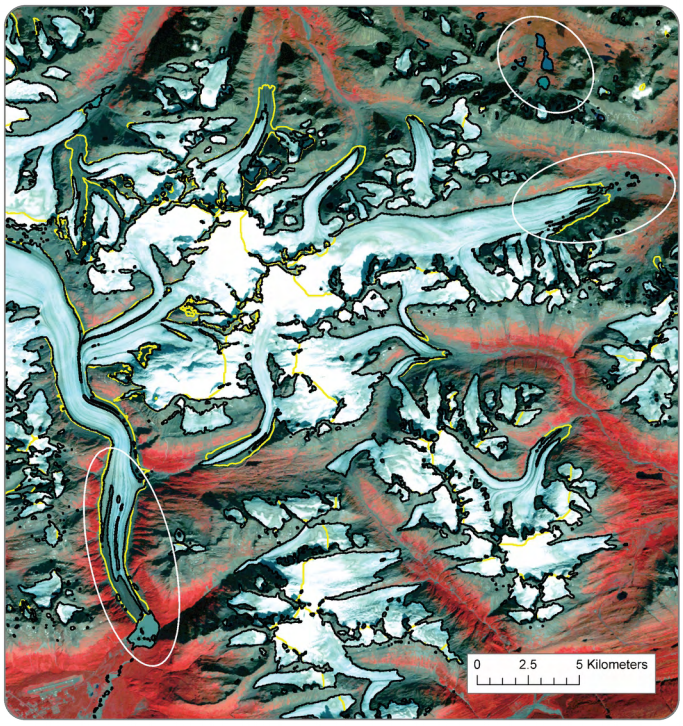

Figure 5.5*: Manual correction in the post-processing step. White ellipses show omission and commission errors (from Le Bris et al., 2011).*

5.2.2 Watershed analysis to derive drainage divides

Drainage divides are used to separate continuous ice masses into individual glaciers (e.g. Manley, 2008) by digital intersection with the glacier outlines created from the satellite scenes. They are derived from the NED DEM and the glacier outlines following a method described by Bolch *et al.* (2010). This approach is likely faster than a complete manual digitizing, but manual editing in a post-processing step is needed to improve the results (Le Bris *et al.*, 2011). All steps of this method were preformed within the ESRI™ ArcMap software and are detailed in the table below along with the specific commands applied (see also Appendix A4):

Step	ArcMap command	Description
Create a buffer zone around glaciers	Spatial Analysis Tools> Proximity>Buffer	A buffer zone (e.g. 1 km) is used to constrain hydrological calculations to glaciers rather than to the entire DEM extent.
Cut the DEM with the buffer zone	Spatial Analysis Tools> Extraction>Extract by mask	The hydrological calculations are applied only to a subsample of the DEM.
Correct anomalies of the DEM	Spatial Analysis Tools>Hydrology>Fill	This step allows to fill sinks and to erase small anomalies in the DEM.
Calculate flow direction grid	Spatial Analysis Tools>Hydrology>Flow Direction	This function models the natural flow from one cell to the neighbour cell according to their elevation until the edge of the DEM is reached.
Calculate basins	Spatial Analysis Tools>Hydrology>Basin	This command uses the flow direction grid to generate basins around each entity.
Convert basins into shapefile	Conversion Tools> From Raster>Raster to polygon	This function converts basins from raster to vector format for the later post-processing.
Post-processing	Toolbox> Merge, Reshape, Cut etc…	Manual corrections of basins.

Table 7: *Steps of the workflow to create drainage divides for all glaciers from a DEM.*

5.2.3 Zonal statistics and other methods to compute glacier parameters

Glacier parameters can be derived when digital outlines and a suitable DEM are available (Schiefer *et al.* 2008). Using the zonal statistic tools available in the ESRI™ ArcMap software, and following recommendations for compiling glacier-specific parameters (Paul *et al.* 2009), the topographic parameters for the new inventory were computed from the corrected outlines and the NED DEM. Basic parameters (e.g. area, elevations (max, min, mean, median), mean slope) are obtained automatically from inherent GIS commands while derivative information or parameters like hypsography, mean aspect and length require further modelling. The latter are detailed here:

- Hypsography:

To compute glacier hypsometry (area-elevation distribution), the DEM is reclassified into 100 m elevation bins with the ArcMap "Raster Calculator tool" using the "Int([DEM]/100)" syntax command. The "Tabulate Area tool" from the Spatial Analyst toolbox allows then, to generate an exportable database file which can be used in a

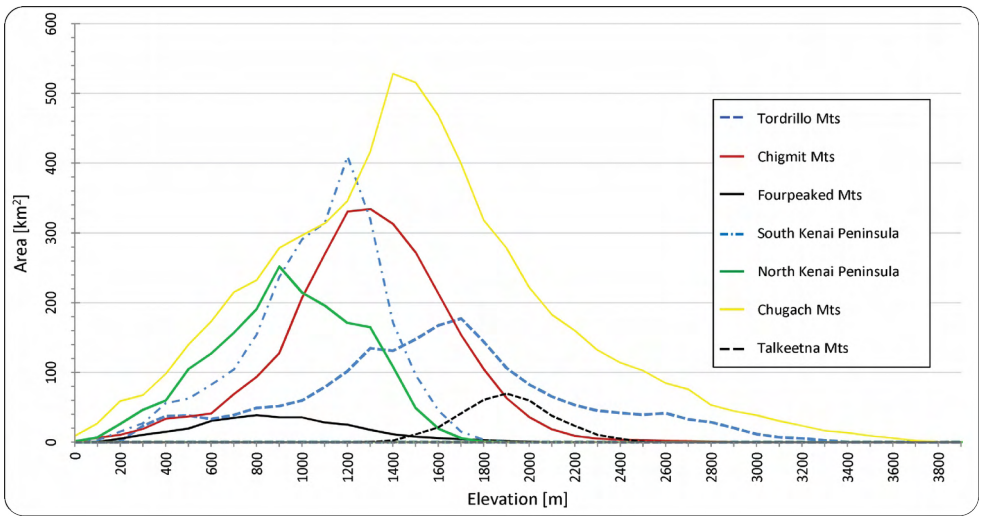

Figure 5.6: *Example of hypsographic curves for various sub-regions.*

spreadsheet software for creating the respective plots (Fig 5.3).

- Mean Aspect:

To obtain the eight aspect sectors, three steps are required: (i) sine and cosine grids are computed from the aspect grid derived from the DEM; (ii) glacier-specific mean sine and cosine values are then calculated using the "Zonal Statistics" tool, and finally (iii) successive syntax commands (e.g. ATAN2(a:a), DEGREES(a), MOD(a), INT((a/45)) +0.5), MOD(a;8)+1 where (a) represents the specific cells) are applied within a spreadsheet software. As an example, Fig. 5.4 illustrates area change (between DLG and the new inventory) per aspect sector for a subset of 347 glaciers.

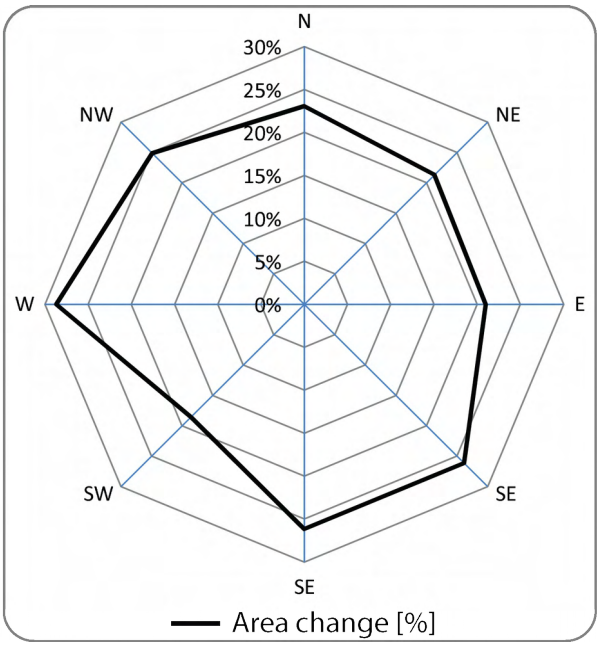

Figure 5.7: *Area change per aspect sector [%]*

- Specific reference year:

The reference year is an important parameter (especially for glacier change analysis) and is obtained from the data source (date of the satellite scene or topographic maps) and added to the database.

- Glacier length

Programming helps to automate processing of digital data within a GIS environment. Programming languages allows handling both the raster and the vector format. Currently, glacier length is still obtained manually usually using contour lines and a DEM hillshade in the background to aid in visual interpretation. This gives accurate vector lines, although it is very time consuming doing this for thousands of glaciers. Moreover, the manual digitizing is not repetitive and would result each time in slightly different length values and vectors. An automatic method would help to overcome these shortcomings

In paper II (Le Bris and Paul, 2012) such an automatic method is presented. It only requires glacier outlines and a suitable DEM as an input and should thus be widely applicable. The open source programming language Python along with additional libraries (the Geospatial Data Abstraction Library – Open source Geospatial Resources (GDAL/OGR)) are used to properly deal with the raster and vector formats. Successive operations implemented in the script lead to the generation of flow lines (with a length value) and the terminus positions for a complete dataset. The script has been successfully tested with the extents from the new inventory and the former DLG outlines. Figure 5.5 shows an example of glacier flow lines and terminus positions automatically derived with the script, further details are presented in paper II.

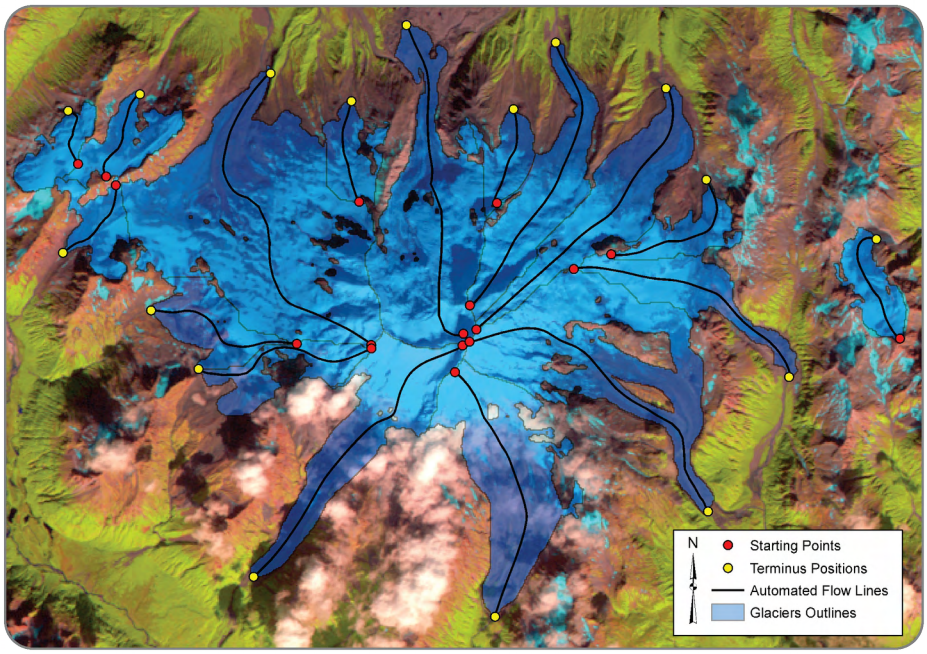

Figure 5.8: *Example of flow lines on the Redoubt Volcano generated by the flow line algorithm (FLA).*

5.2.4 Glacier change assessment

Glacier changes in three components (i.e. area, length and elevation) have been investigated for different subsets of the new inventory. An example of such changes for the two benchmark mass balance glaciers Gulkana and Wolverine is depicted in Figure 5.6. In terms of area changes, black arrows (Fig. 5.6A and Fig. 5.6D) highlight the grey areas that represent changes between the DLG and the extents in the new inventory. In Figure 5.6B and Figure 5.6E, length changes are shown with thick black lines. Automatically derived flow lines are also shown while elevation changes are illustrated by Figure. 5.6C and 5.6F. Red ellipses specify that the stronger changes occurred in the ablation regions. Basically, the calculations are performed in three ways:

- Area changes: estimated from a difference of the scalar values (rather than the rasters). All parts that belong to the former glacier in case of split (inside the same drainage divide) are considered (see Paper I for details).

- Length changes: the flowlines derived for the former extent (DLG) are digitally intersected with the new glacier extent. The flow line segment remaining at the terminus gives the length change (i.e. the front variation). Paper II provides further details.

- Elevation changes: from the $\Delta h/\Delta t$ raster maps three ways to exclude DEM artefacts are considered using raster based operations: all values > 0 are set to zero or no data and glaciers covered by more than 20% data voids are excluded. Also the calculation of mean changes per glacier (using zonal statistics) is a GIS based operation. Further details are provided in Paper III.

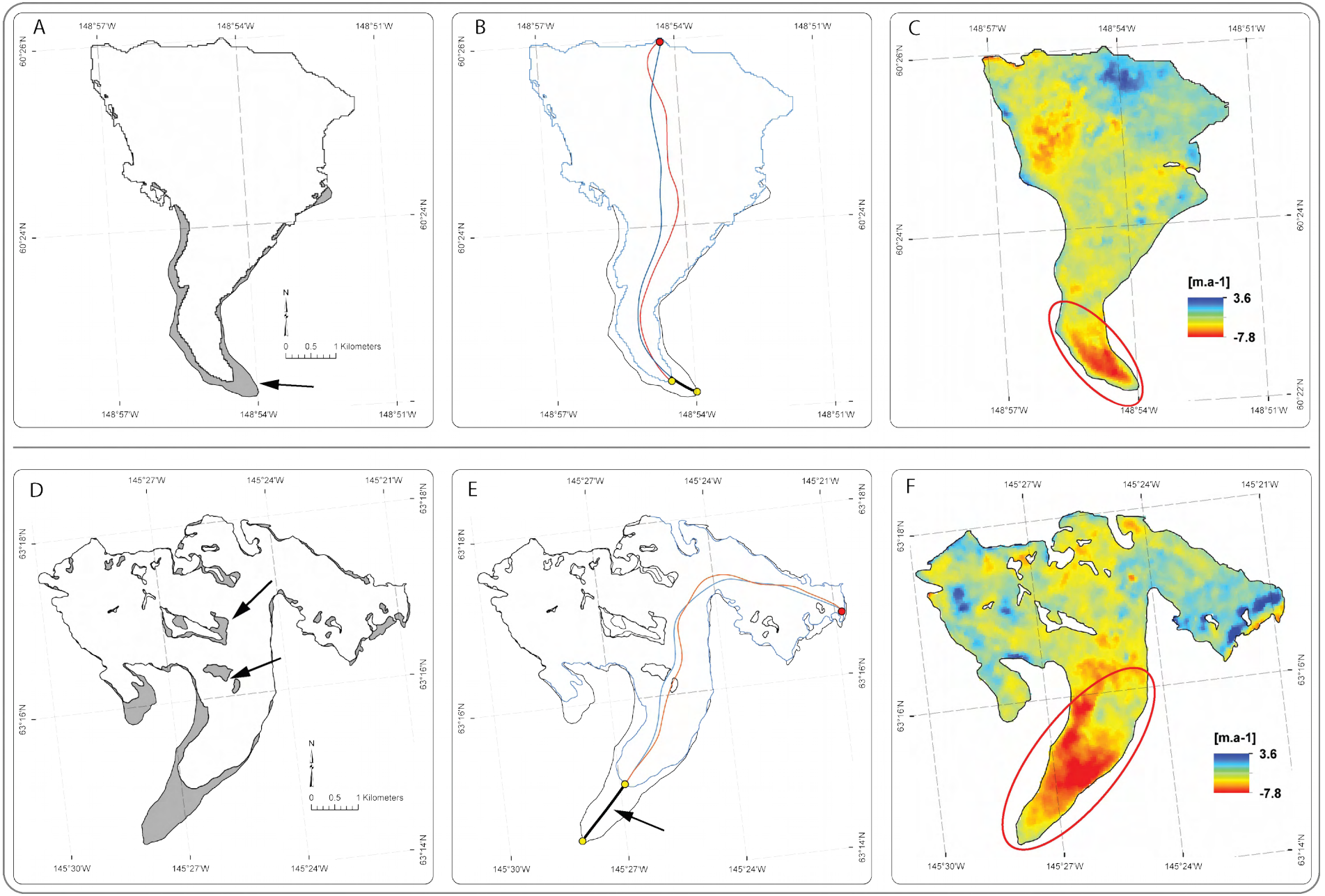

Figure 5.9: *Example of area, length and elevation changes for Gulkana and Wolverine Glaciers*

6

Summary of Research Papers

6.1 Paper I: A new glacier inventory for Western Alaska

Le Bris, R., Paul, F., Frey, H., Bolch, T., 2011. *A new satellite derived glacier inventory for Western Alaska.* Annals of Glaciology, 52(59), 135-143.

The main objective of this study was to create a detailed glacier inventory for a larger part of western Alaska. Alaskan glaciers represent a substantial part of all glaciers in the world and they contribute strongly to global sea-level rise, but are only poorly covered in glacier inventories. The region has thus been defined as a key region for the GlobGlacier project. With the opening of the USGS Landsat archive in 2008 and the free availability of DEMs from USGS (NED) and ASTER (GDEM), compilation of an inventory became possible. This new inventory also serves as a base for assessment of changes in glacier length, area and volume as well as being a key input to the now globally completed Randolph Glacier Inventory (RGI). The regions considered for the inventory are the Tordrillo and Chigmit Mts., the Kenai Peninsula and the northern part of the Chugach Mts. The climate regime in this region ranges from maritime at the southern coast to continental in the interior. Nearly all types of glaciers are found in the region and a wide range of mapping challenges is present (debris-cover, deep shadows, turbid lakes, smoke and fog from wild fires, seasonal snow and volcanic ash).

Glaciers were mapped with the well established semi-automated band-ratio method (TM3/TM5) and manual corrections for misclassified regions using nine Landsat TM scenes acquired between 2004 and 2009. Glacier complexes were separated into entities using drainage divides derived from the NED DEM. In comparison with other available DEMs (GDEM, SRTM) the NED was found to be the most appropriate in terms of coverage and artefacts. In total, c. 9000 glaciers (>0.02 km^2) with a total area of c. 16,250 km^2 were mapped and complemented with topographic data (e.g. minimum, maximum, median and mean elevation, mean slope and aspect) derived from the NED DEM (minimum elevation was derived from the GDEM). Further analysis revealed that large parts of the area (47%) are covered by only a few (31) but large (>100 km^2) glaciers. Glaciers <1 km^2 contribute only 7.5% to the total area, but 86% to the total number. However, these percentages vary with the specific mountain range analysed. The spatial analysis of mean glacier elevation (which can be seen as a proxy for the equilibrium line altitude) revealed a strong increase of values from glaciers located close to the coast towards the interior of the country (from about 100 to 2960 m a.s.l.), but this more regional trend has a high local variability. Glacier area change was assessed by selecting a subsample of 347 glaciers from all parts of the study region. In total, glaciers have lost 23% of their 1948-54 area. The entire inventory data is available in the GLIMS glacier database.

The major lessons learned from this study are:

- Highest preference has to be given to scenes without seasonal snow outside of glaciers, even if it requires remapping of an entire scene or the combination of two scenes where only the upper/lower parts of the glaciers can be mapped in each scene

- The visual comparison with high-resolution data that are sometimes available in Google Maps or Earth is often very helpful in identifying glacier outlines, in particular when they are debris covered and/or located in deep shadow

- A rather old DEM can still be used to derive drainage divides and key topographic parameters for each glacier (apart from minimum elevation) when other DEMs have too many artefacts

- Digital glacier outlines from other sources need to be carefully checked (location, reference year, interpretation) before they can be used for change assessment

- The accuracy of the derived outlines mostly depends on the quality of the mapping of debris-covered glaciers

6.2 Paper II: Flow lines for determination of glacier length

Le Bris, R. Paul, F., 2012. *An automatic method to create flow lines for determination of glacier length: A pilot study with Alaskan glaciers*. Computers & Geosciences.

Glacier length is an important, but largely missing parameter in digital glacier inventories as the vector line required to determine length has to be digitized by hand (with the related variability in the interpretation). Its vector representation (a central flow line) is also a most important input for modelling glacier evolution through time. Length changes of glaciers are key indicators of climate change, but are only measured in the field at a few hundred selected glaciers globally. Repeat satellite data provide an ideal tool to determine frontal changes for large glacier samples, but the reference points (e.g. at the centre of the terminus) need to be identified. Hence, to support the above purposes there is an urgent need to generate such flow lines from automated methods for a large number of glaciers.

This paper describes a new method to automatically create central flowlines of glaciers along with an application to automatically derive changes in glacier length. The algorithm is based on Python scripting and additional libraries (GDAL / OGR) and requires only a DEM and glacier outlines as an input. The core of the method is based on a glacier axis concept that is combined with geometry rules such as the k-d Tree, Nearest Neighbour and crossing test theory. We have applied the method to 400 glaciers located in western Alaska for both the new glacier inventory (described in paper I) and the former glacier outline dataset from USGS (i.e. Digital Line Graph).

Due to strong changes in glacier topography and/or geometry, many of the vector lines are not directly comparable, which implies that length changes cannot be derived from subtraction of the length values of the two lines. Instead, only the changes at the terminus (front variations) were considered. The cumulative length change over the entire period is -277.3 km or 700 m per glacier (or 15 m per year). This varies from about 0 to 6700 m with the total changes for the two benchmark glaciers Gulkana and Wolverine being -1329 ±101 m and -327 ±101 m, respectively.
The accuracy of the method to create the flow lines for length determination was assessed by a quantitative and qualitative (outline overlay) comparison with manually digitized vector lines for 20 glaciers. This comparison revealed for 17 out of the 20 glaciers a length value that is within the range of the variability of the manual digitizations. Other potential methods to determine glacier length performed less well. However, for some of the automatically derived lines manual corrections had to be applied as well. The new method will strongly facilitate the population of the GLIMS glacier database with length values and help to obtain a more complete picture of length changes over recent decades.

The major lessons learned from this study are:

- Differences in geolocation and interpretation of glacier extents in historic datasets need careful attention and correction in the pre-processing stage

- When glacier flow lines are manually digitized, standard deviations between 25 m and 452 m are found for the 20 glaciers

- Strong deviations between length changes derived from a simple Euclidian distance and the flow line based value hint to glaciers that require manual correction

- More sophisticated or follow-on approaches to the one proposed here might further reduce the post-processing work and give a more consistent way of determining the values (e.g. longest length vs. the here calculated length from max. to min. elevation)

- A graphical user interface (GUI) should be programmed to facilitate external application

6.3 Paper III: Elevation changes in western Alaska

Le Bris, R., Paul, F., 2013. *Glacier-specific elevation changes in western Alaska*. Annals of Glaciology *(submitted)*.

One of the largest challenges in correctly assessing the contribution of glaciers to sea-level rise is the extrapolation of the measured glacier mass balances to an entire mountain range. In general, the measured glaciers are small and cover a different elevation range than the large valley glaciers with low-lying tongues that contribute more to sea-level rise. The measured mass balances might thus be considered as being non-representative for a region and large errors would occur when regionally upscaling the values without applying corresponding correction factors. Such factors can be inferred from determination of glacier specific geodetic volume changes as derived from differencing two DEMs combined with digital glacier outlines. A particularly important point is to accurately co-register both DEMs prior to subtraction and to mark tidewater and calving glaciers in the attribute table of the dataset to later exclude them from the sample. This is also required to separate impacts of climate change on volume changes from those related to glacier dynamics. The latter is a particular problem in our test region, where one tidewater glacier (Columbia) dominates the mass loss for the entire region and needs to be excluded from the sample to obtain unbiased results.

To achieve this, we have digitally combined the elevation changes between the 1950s and 2007 as derived from two DEMs with glacier-specific extents and marked all calving and tidewater glaciers (36 in total). This allowed us to determine the representativeness of the long-term mass balance measurements at the two benchmark glaciers Wolverine and Gulkana for the entire region. As a reference DEM we used the NED from USGS (acquired around 1950), and the more recent DEMs were from SPOT5 (acquired in 2007 for the SPIRIT project), and the ASTER GDEM. Glacier outlines were taken from the Digital Line Graph (referring to c. 1950s) combined with the drainage divides created for the new inventory (see paper I). In total, elevation changes were calculated for about 3180 glaciers using two ways of statistical averaging: (a) as a mean for the entire region and (b) as the average of mean values per glacier. Positive elevation changes in the accumulation region over this time period might be a result of DEM artefacts and were excluded using three different approaches (e.g. setting them to zero or no data).

The derived rate of elevation change is of -0.6 m/year for calving and tide water glaciers together while it is only -0.25 m/year for the land-terminating glaciers. Considering only the latter, the rather similar mean elevation changes for Gulkana and Wolverine glacier (-0.6 and -0.7 m/year) are about 1.5 to 3 times more negative than the mean value derived with methods (a) and (b) described above, respectively. On the other hand, they resemble the mean value for the tidewater and calving glaciers (calculated with method b) as well as

the overall mean value very closely. In other words, although they are not representative for the glaciers of their own type, their values can be used to determine the mass loss for the entire region.

The major lessons learned from this study are:

- The ASTER GDEM is suitable to derive elevation changes when the changes are large
- Identification and handling of DEM artefacts is challenging
- The way of calculating mean changes for a region has a strong impact on the result
- Despite their different elevation, size and topographic setting, the measured glaciers can nevertheless be representative for a large region

7 Discussion

This chapter discusses the main findings of this thesis. First, glacier mapping challenges such as snow conditions and debris-cover mapping are addressed. Issues related to data quality of former datasets used for change detection is described afterwards. The research papers are integrated by discussing them under the glacier change topic (area, length and elevation changes) along with results, challenges and other considerations. A summary of further possible developments in modelling glacier length and potential related studies are given in the outlook section.

7.1 Glacier mapping challenges

7.1.1 Snow and cloud conditions on satellite images

The new Alaskan glaciers inventory is based on satellite images from 2005 to 2009. This 5 year period resulted from the difficulty to find suitable scenes (cloud free and acquired at the end of the ablation period without seasonal snow outside of glaciers) in the Landsat archive. Good snow conditions are a prerequisite to derive precise glacier outlines and to reduce the workload for manual corrections (e.g. Paul and Andreassen 2009a). The importance of good snow and also cloud conditions is illustrated in Figure 7.1. Starting with an already corrected Landsat scene from 2002 with adverse snow conditions, it was attempted to correct glacier outlines derived from scene B using scenes A and C from 2009 (see Table 1 in § 2.2.2). Figures 7.1A and 7.1C show the automatically derived glacier outlines with a false-colour composite in the background for 2002 and 2009. Glacier

outlines were inverted to highlight the influence of seasonal snow. The over interpretation of glacier extents on figure 7.1B is obvious and indicated with white arrows in figure 7.1D. After several days were spent on correcting the original data set, it was finally decided that it was more practical, accurate and faster to completely re-process the outlines from the scenes with the better snow conditions. This experience clearly revealed the importance of only using scenes with the best snow conditions in glacier classification.

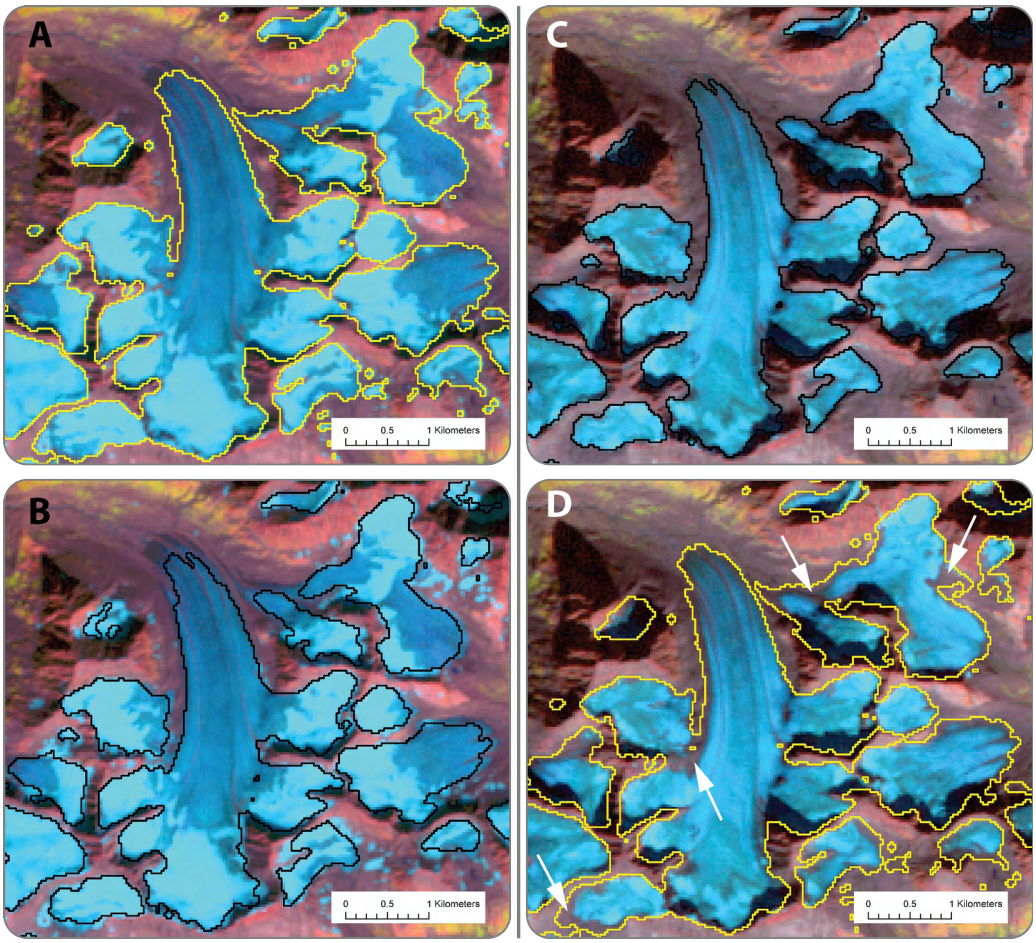

Figure 7.1: *Comparison of snow conditions for the 2002 and 2009 Landsat scenes*

7.1.2 Mapping of debris-covered areas

Automatic classification of debris-covered glaciers with band ratioing remains problematic as the debris has similar spectral properties as the surrounding terrain. In these cases, manual corrections are needed to delineate glacier extents accurately. When the contrast is low, this could introduce considerable uncertainties in the derived glacier area, especially for small glaciers. Radar remote sensing techniques (coherence images) represent an interesting potential to map debris-covered parts of glaciers, (e.g. Atwood *et al.* 2010; Frey *et al.* 2012) but they were not utilized in this thesis.

7.1.3 Quality of former datasets

Despite their usefulness and high quality, the USGS NED DEM and DLG outlines products should be used with some care especially when performing glacier change assessment. The most important issue is related to the date of the data sources. In case of the NED DEM, which was derived from topographic maps from the 1950s (Gesch *et al.* 2009), it is quite difficult to precisely determine the exact year for a specific area. In fact, vertical aerial photographs that served to create the maps (DRG) and in turn to build the DEM were acquired between 1948 and 1957.

This difficulty obviously also applies to the DLG, because these vector outlines were compiled from the same maps. To overcome this problem, we rely on years provided in a study by Berthier *et al.* (2010) or directly determine from the USGS 1:63 000 topographic maps the reference dates to the DLG glaciers. Furthermore, overlapping between DLG and DRG revealed mismatches of glacier extents for several cases. For the glacier elevation change assessment performed in Paper III, ca. 400 glaciers were manually corrected according to the DRG maps before calculation of glacier-specific mean elevation changes. The very high correlation of mean changes between corrected and uncorrected glacier outlines ($R^2 = 0.98$) reveals that overall volume changes could also be calculated with sufficient accuracy without further correction of the outlines. In the case of glacier area change assessment, only glaciers with a good agreement of the glacier extents visible on the DRG maps were selected. The complete correction of DLG outlines with the DRG extents would much reduce the uncertainties in glacier area determination and be extremely valuable for further change assessment.

7.2 Glacier area change

In total, glacier shrinkage represents -23% of to the initial area (1948-1957), with the observed changes mainly occurring in the ablation areas (glacier tongues). The size-class distribution reveals a large variability of the changes with an increase of relative loss towards the smallest glaciers. Glaciers smaller than 1 km^2 have lost -2% to -16% of their area whereas glaciers larger than 10 km^2 have lost -2% to -6% of their area. The scatter is even smaller for glaciers larger than 50 km^2 with values ranging from -0.5 to -2%. This reveals a clear size-class dependency of the changes.

7.2.1 Challenges for change assessment

Direct comparisons of glacier extents from two points in time are difficult. This results from the different nature of the source data used to create glacier inventories (photogrammetry, map digitizing, satellite data etc.). Snow conditions and/or solar illumination on both the air photographs and the satellite scenes can strongly influence the visual interpretation and lead to sometimes large deviations of glacier extents from one inventory to the other (Paul and Andreassen 2009a). Also, former drainage divides

could have been located at a different place (Andreassen *et al.* 2008). Furthermore, manual interpretation of debris-covered zones of glaciers introduces additional uncertainty which can slightly bias area change results. These aspects, as well as the inventory purposes (e.g. cartography, glaciology, and hydrology) should be taken into account when performing area change assessments. This implies that glacier extents should not be compared without manual checking and if possible, all data should be adjusted to the same base (divides, debris, rock outcrops) which can only be done using digitized and properly geocoded data sets.

Another challenge to assess glacier area changes is the case of disintegrated glaciers. Here, the use of drainage divides helps to sum up areas by assigning a common glacier ID to each entity in the same polygon (basin) and then to compare the value to the one from the (unsplit) DLG glacier extents. This is also how changes were calculated in Paper I.

Large deviations of glacier extents are illustrated in Figure 7.2 with three examples where (A) indicates glaciers that have disappeared or were not mapped in the former inventory, (B) shows glacier front retreat and mismatches between the DLG and the DRG extents, and (C) highlights different interpretations in the accumulation region.

Unlike mass-balance and length changes, the link to climate forcing using glacier area change is less straightforward. Nevertheless, glacier area changes are interesting as they can be derived from remote sensing data on a global scale (e.g. DeBeer and Sharp 2009; Paul and Andreassen 2009b) and because they reveal the large variability of glacier reactions. Glacier surface elevation changes can also be indirectly observed from area change with the emergence of rock outcrops. Thus, area changes of glaciers are a valuable source of information for global scale climate-change impacts.

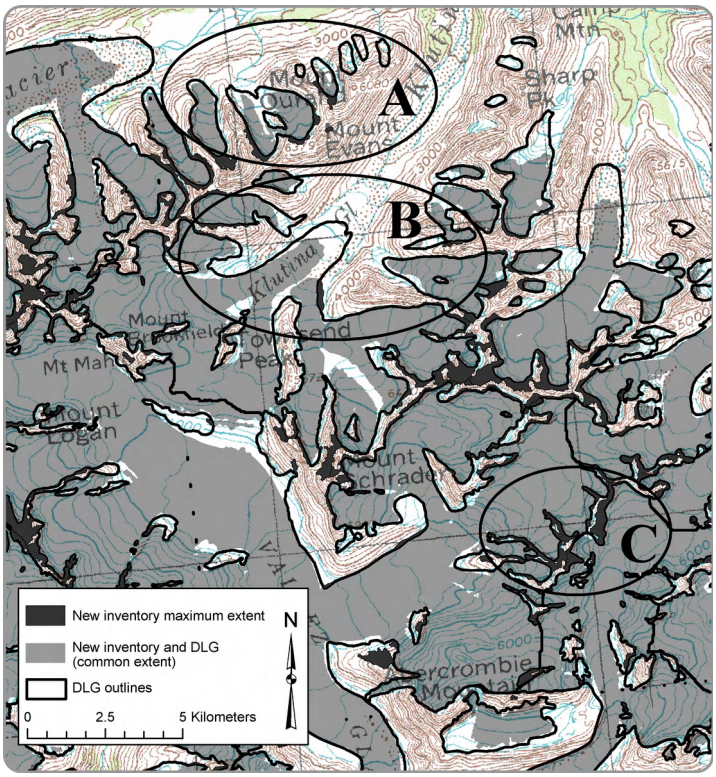

Figure 7.2: *Area change assessment*

7.3 Glacier length change

7.3.1 The flow line algorithm

The central flow line of a glacier has a special meaning in the modelling community by interpreting it as a trajectory of a particle. However, the term is not exclusively used by modellers. The term flow line has been used for decades by the glaciological community to describe and determine glacier length (Müller *et al.* 1977). Hence, introducing a new terminology (e.g. length vector lines or glacier medial lines) would be rather confusing. For example, flow lines that have been used for dynamical modelling (see Oerlemans 2001, p. 84, Fig. 8.1) are always located in the centre of the ablation region (along the medial moraine) and thus do not follow the principles of being a particle trajectory when starting in the accumulation area. Hence, the flow lines modelled by the algorithm presented here are very similar to those used by the modellers and their denomination should not be changed.

The Flow Line Algorithm (FLA) developed in this thesis (Le Bris and Paul, 2012) is based on a 2-D concept (glacier axis) using glacier outlines and a DEM. The algorithm generates flow lines automatically for a complete sample of glaciers once the required input data are prepared correctly (e.g. points within the glacier outline marking the highest elevation).

With these lines also created for the former extent (derived from the corrected DLG), assessment of length change was performed for about 400 glaciers in western Alaska over the 1950's-2007 period.

The automatic determination of length change is not straightforward and brings several challenges. A key point is the identification of corresponding glaciers between the two inventories investigated. Over the 50 year time period investigated here (i.e. between the DLG and the new Alaskan glacier inventory), glaciers have experienced large geometric changes (e.g. new rock outcrops emerged, tributary glaciers split). As consequence, a clear identification of corresponding glaciers is often challenging and manual selection of suitable glaciers is required. Figure 7.3 depicts an example of a glacier that split into several smaller glaciers. The separation of tributaries (shown with a black arrow) implies that only one of the new glaciers (from the new inventory) can be used for length change assessment.

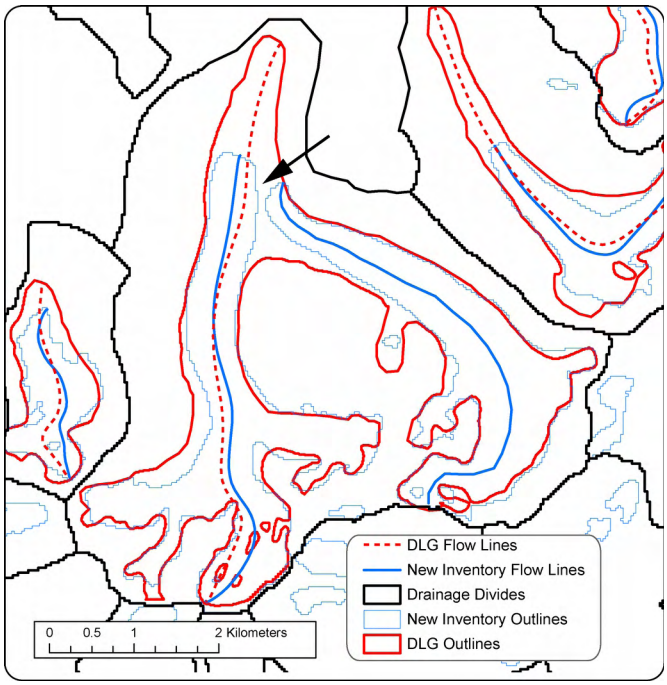

Figure 7.3: *Example of glacier split into two smaller glaciers*

Another challenge when performing an automatic length change assessment using the flow line algorithm is to get accurate starting positions. These points should refer to the same glacier in the two inventories. Their automated calculation is problematic as glacier outlines often not exactly match between two inventories (e.g. due to geolocation errors in steep mountain terrain, snow fields or visual interpretation). As the starting points must be located inside a common glacier extent of the two inventories, a manual shift might be required. An illustration of this issue is shown in Figure 7.4 where the upper part of this

glacier (yellow ellipse) is enlarged. The white arrow indicates the automatically derived highest point that has been manually slightly displaced to an overlapping area of the two inventories.

There are basically two possibilities to derive length changes: (i) difference of the total length from two points in time and (ii) front variation only. (i) does not work as changes occurring at the surface of glaciers (i.e. emergence of rock outcrops) impact the trajectory of the glacier flow and then its representative line. Length changes calculated for the Alaskan glaciers are obtained from a digital intersection between the flow lines derived from the DLG and the new inventory glacier outlines. They thus represent the glacier front variations (ii) rather than the change of the complete length. A visual selection of suitable flow lines to assess length changes remains necessary.

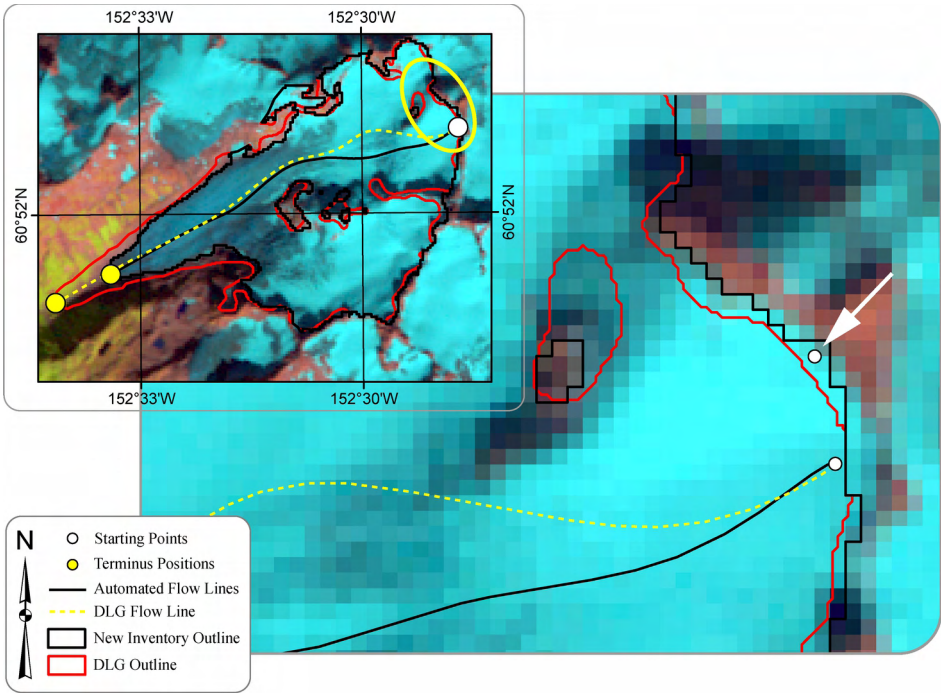

Figure 7.4: *Starting points from two inventories. The starting point for the FLA had to be shifted from its original position (arrow) to a new one that is located inside both outlines.*

7.3.2 Accuracy

The measurement of length changes from digital datasets comes with some uncertainties (e.g. geolocation, digitization) that can be assessed. To be significant, the changes must at least be larger than the pixel size of the used raster data. Hence, with an assumed glacier recession of about 5 to 10 m per year, a couple of years between the datasets are required to detect changes. So the efficiency of automated glacier length change determination depends on spatial resolution and the pace of glacier retreat. Uncertainty in the geolocation of the outlines also needs to be taken into account as well as co-registration

errors between the compared raster data sets (Hall *et al.* 2003). Following Williams et al. (1997), the uncertainty for a given spatial resolution is:

$$Uncertainty = E\sqrt{n}$$

where E is the error of measurement (pixel size) and n is the number of measurements (the two components of a pixel). Admitting a maximum manual precision of one pixel when digitizing outlines (Berthier *et al.,* 2010), this error is ±42 m for the new inventory and ±35 m in the case of the DRG. For the purpose of length change assessment we have to consider these two errors plus the co-registration error. As these errors are independent, they are quadratically added. The overall uncertainty for these datasets is thus:

$$Uncertainty = \sqrt{(\varepsilon_{TM})^2 + (\varepsilon_{DLG})^2 + (\varepsilon_{Registration})^2}$$

$$= \pm 101 \text{ m}$$

According to this uncertainty, only length changes larger than this value should be considered for change assessment. Length changes observed in the study region range from -3 m to -6736 m. 4.7% of them are too small to be considered significant and have to be disregarded.

7.4 Glacier elevation change

To better estimate the sea-level rise contribution of western Alaskan glaciers, an analysis of glacier-specific elevation changes was performed (see Paper III). Based on DEM differencing from two points in time and glacier outlines available for this region (as used by Berthier *et al.*, 2010), glacier-specific elevation changes were calculated for more than 3100 individual glaciers based on the drainage divides derived for the new glacier inventory (see Paper I). A differentiation of the ice volume loss by glacier type was achieved by marking them in the attribute table (i.e. land terminating, lake terminating and tide water glaciers). This differentiation also helps to assess the representativeness of the two benchmark glaciers with long-term mass balance measurements (Gulkana and Wolverine) for the land-terminating glaciers only and the entire region.

The mean changes (arithmetic mean of individual mean elevation change values) are -0.24 ±0.44 m yr^{-1} for the land terminating, -0.63 ±0.40 m yr^{-1} for lake terminating and -0.64 ±0.66 m yr^{-1} for tide-water glaciers. For Gulkana and Wolverine glaciers the rates are -0.68 and -0.60 m yr^{-1} respectively. Interestingly, these values reveal that both glaciers are more representative for the calving and tide water glaciers than for glaciers of their own type (Fig. 7.5). However, the mean change for the entire region (when considering the overall changes and including all types of glaciers in the statistical averaging) is -0.67 ±0.76 m yr^{-1} which is close to the Gulkana and Wolverine glacier mass budgets. Columbia Glacier (in the Chugach Mts.) exhibits the strongest mean thinning rate (-2.8 m yr^{-1}) and definitely

needs to be excluded when the impact of climate change for the region should be determined. The large spatial variability of mean elevation changes across the entire region has no correlation with glacier size, mean slope, exposition, or mean elevation.

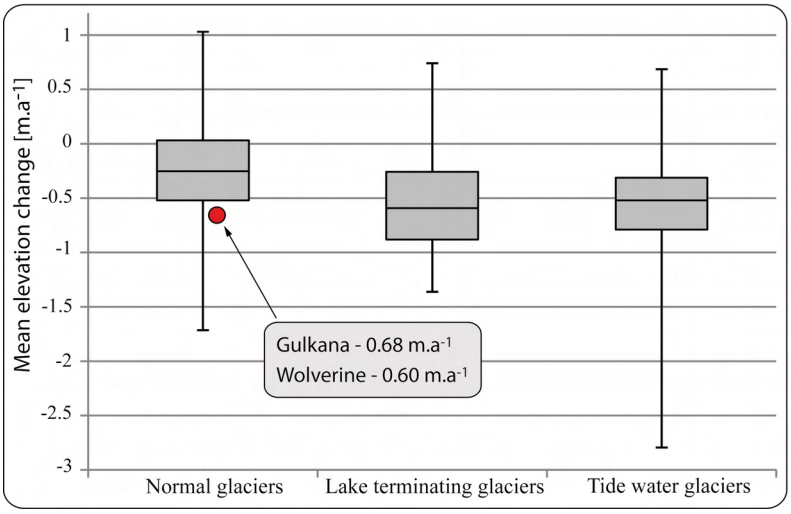

Figure 7.5: *Box plot of mean elevation changes*

7.4.1 Discussion

The representativeness of glaciers with long-term mass balance measurements for an entire region (e.g. Gulkana and Wolverine for Alaska) is a topic rarely discussed. This aspect should nevertheless be assessed before extrapolating their mass budgets to the considered region as these glaciers usually cover a different elevation range and are comparably smaller than the large valley glaciers that mainly contribute to sea-level rise (Fountain *et al.* 2009). Furthermore, this analysis demonstrates the importance of treating glaciers separately (according to their types) to remove bias by excluding calving and tide water glaciers from computations.

We have not compared the cumulative mass balance of Gulkana/Wolverine glaciers as measured in the field with the here-derived geodetic volume changes as the density required for converting volume into mass changes is not known. This can give huge differences for glaciers that also had some mass gain during the observed period (e.g (Haug *et al.* 2009). The geodetic method is based on a non-changing reference (i.e. the bedrock) when the glaciological method refers to the previous year's surface (Elsberg *et al.* 2001). Furthermore, the geodetic method also includes volume loss due to basal and internal melting which are not measured at the surface (Zemp *et al.* 2009; e.g. Fischer 2011). These elements can cause large deviations between the two methods. However, the analysis of volume changes for the corrected and uncorrected glacier extents revealed little influence on the total change.

An accurate co-registration between the DEMs used is mandatory before elevation changes are calculated (e.g. Nuth and Kääb 2011). In the case of Gulkana and Wolverine

glaciers the mean elevation changes were derived from differencing between the NED and the ASTER GDEM which is likely to be less accurate than the SPOT DEM used for the other regions. However, a comparison of those two DEMs in flat terrain off-glaciers (with slopes less than 5°) did not reveal any systematic difference. The mean elevation difference was 2.60 m (± 21.62 m), revealing that the ASTER GDEM is suitable to derive elevation change when the changes are large. Such a comparison is helpful to check for potential systematic errors and should always be done before differencing between two DEMs.

If glaciers with extreme behaviour are part of a sample, they should be excluded for climate change impact assessment. This requires using drainage divides from an inventory, calculating glacier specific changes from zone statistics and assigning markers to specific glacier types (e.g. all calving glaciers)

7.5 Outlook

7.5.1 Further possible developments of the FLA

Paper II describes a new algorithm that has been developed in this thesis. Even though the resulting flow lines represent well the glacier length in both the scalar and the vector formats, some steps could be improved with further developments. They mainly concern the location of the highest points (which is along with the lowest points the fundamental input for the axis concept), the densification of traverses, the influence of glacier tributaries and the smoothness of the vector lines. Furthermore, creation of a user interface is an important future development. Some more details on these specific aspects are described in the following:

Location of the starting point

The starting point is a required input for the FLA. This point can be defined as being the highest point (such as in paper II), or also as the farthest point. An approach to use the latter as the starting point could be to determine the farthest point from the end point (lowest). In this case the resulting central flow line will likely be the longest rather than reaching the highest glacier elevation. However, up to now there is no algorithm available to automatically derive the location of the farthest points, as the normally used upstream flow routing models have problems with convex surfaces (as found in the ablation region). A possibility could be to calculate straight distances from the lowest point to all summit points (vertices) found along the glacier outline and select the farthest one as a starting point. But this is computationally very expensive and could thus be a topic for further model development.

By setting the starting position to the highest point (which is easily computed with zonal statistic tools using the GIS), a longest flow line will be computed in the majority of

cases. However, this might not be the case for a more complex glacier shape (e.g. with several tributaries). In the end, it is important to be clear what the flow line should represent which, depending on the latter application, can be a subject of debate. Our implementation with the highest elevation has the advantages of being computationally very fast and that this point is likely the most stable in the context of future climate change (i.e. further temperature increase).

Densification of the traverses

Results of the FLA depend to some extent on the overall glacier shape. The algorithm performs well for a "normal" elongated valley glacier, but may fail to create the central flow line in the case of very complex glacier geometries (e.g. with many tributaries and/or rock outcrops). In order to overcome this shortcoming and increase the percentage of flow lines obtained automatically, denser traverses along the glacier axis can be created. This will in turn create more middle points (see Fig. 2E in Paper II) and then give extra possibilities for the algorithm to find a way downwards. On the other hand, this will result in increasing the computation time, as the number of internal points will proportionally grow. As a compromise, a conditional parameter depending, for example, on glacier size or slope can be introduced.

Smoothing parameter for glacier flow lines

For some large glaciers with complex geometry the modelled vector lines can follow a spurious sinusoidal way within the accumulation area. This is due to the influence of glacier tributaries. Depending on the glacier axis orientation, traverses can be larger than the "mean" glacier width in some specific parts. Middle traverse points are then located off the glacier centre. This effect tends to deflect the lines into the glacier tributary. To a large extent this problem is solved in a post-processing step by applying the Kernel (PAEK) algorithm (Bodansky *et al.* 2002) within the GIS software. However, this requires manual intervention and thus reduces computational efficiency. To treat these special cases and avoid case-by-case manual intervention, further developments allowing implementing a smoothing parameter in the FLA are necessary. Possibilities to automate smoothing would be (i) to implement a size-dependent parameter, so that larger glaciers would receive a higher smoothing factor (e.g. 3000 m) without affecting smaller glaciers, or (ii) to have a second iteration using scan lines orthogonal to the initial central flow lines (I. Evans, pers. com.).

Concave and convex surface of glaciers

The surface of a glacier depicted with digital elevation models usually has a concave (in the accumulation area) or convex (in the ablation area) cross-valley surface profile. Consequently, water-routing algorithms have problems in generating suitable vector flow lines reaching the terminus and are very dependent on DEM quality. Though water routing algorithms work well in accumulation areas, the lines are often deflected to the

lateral margin of glaciers in the ablation region which is mainly due to the convex surface. Thus, the resulting vector lines can not be used to determine glacier length as they do not reach the glacier front.

7.5.2 Geomorphologic analysis and glacier change index

The morphological changes of glaciers are strongly driven by climatic conditions as well as topographic properties and related climate forcing impacts on glaciers have already been analyzed (e.g. Burrough and McDonnell, 1998; Paul, 2007). However, geomorphologic analysis of glaciers are often based on either a limited number of glaciers or a reduced number of parameters. For example, Dyurgerov *et al.* (2009) computed a glacier index based on the difference between two states of the Accumulation Area Ratio (AAR) for 99 glaciers. In Haeberli and Hoelzle (1995), lengths of the ablation area were empirically set as $0.5L_0$ and $0.75L_0$ for glaciers shorter and longer than 2 km, respectively (according to Müller, 1988).

Thus, a relation of the observed changes in length, area and volume with climatic data would be interesting, but has not been performed here. The relation with geomorphometric properties would also be interesting, but revealed no correlations for individual parameters. Most promising might be to attempt it vice versa, derive climate parameters from the topographic parameters (e.g. annual precipitation from mean or median elevation) and to compare these to given (gridded) climatologies.

8

Conclusion

The main purposes of this thesis were (i) to create a glacier inventory for the western part of Alaska which contributes to fill the existing gap in both the World Glacier Inventory and the Global Land Ice Measurements from Space (GLIMS) databases, (ii) to develop an automatic method to create central flow lines of glaciers providing a length value, and (iii) to assess glacier changes. This chapter summarizes the main results obtained and the steps followed to achieve these goals.

8.1 Summary of results

The conclusions summarized here are explained in detail in Part II (Research papers). Main findings are linked to the research questions expressed in the introduction and are summarized here in a broader context:

What is the glacier area in Alaska?

- The new Alaskan glacier inventory compiled in this study encompasses 5 mountains ranges (Tordrillio, Chigmit, Fourpeaked, Talkeetna Chugach, North and South Kenai Peninsula) with 8827 glaciers larger than 0.02 km^2 being mapped. Their total area is 16,250 km^2 with glaciers larger than 100 km^2 representing 47% of the total area but only 0.4% of the total number. 7627 glaciers (86%) are smaller than 1 km^2 and they represent only 7.5% of the area.

- Topographic parameters were calculated for each glacier entity by a digital intersection between the glacier outlines and the drainage divides following Paul *et al.* (2009).

- The glaciers' mean size is rather similar for five regions but slightly larger in Chugach and South Kenai Peninsula (2.6 and 2.3 km^2).

- A spatial analysis reveals a strong increase of glacier mean elevation from 100 m at the coast to 3000 ma.s.l. towards the interior of Alaska. This increase hints at strongly decreasing precipitation sums and might thus even be used as a proxy to derive the precipitation. The variation of mean elevation with aspect for each sub-region shows only a small dependence on this factor which indicates that precipitation, rather than radiation, is the main factor explaining this trend.

- A glacier area change analysis for a subsample of 347 glaciers shows a total loss of 23% of the initial area (1948–1957). All glaciers in this subsample lost area and the relative area loss increases towards the smallest glaciers.

- The new Alaskan glacier inventory is available through the GLIMS website and part of the new Randolph Glacier Inventory (RGI) that was heavily used to improve glacier-related calculations for the forthcoming 5th Assessment Report (AR5) of the IPCC.

Can glacier specific drainage divides be derived from the USGS National Elevation Dataset?

- We performed a cross-comparison between the DEMs available for Alaska to find the most suitable DEM for calculating the drainage divides. This comparison revealed that the drainage divides are similar in all DEMs and that horizontal deviations are less than 100 m for distinct mountain ridges.

- Large shifts of the location (>1000 m) however, are observed in the flat terrain of accumulation areas. Those shifts likely result from more uncertain elevations in these regions that are due to the low contrast in optical imagery (e.g. Svoboda and Paul, 2009; Bolch *et al.* 2010).

- As the NED DEM performed slightly better than the GDEM (showing less unnatural peaks and sinks) and because it covers the entire study region (contrary to the SRTM), we decided to use this elevation dataset to derive drainage divides.

Can Digital Line Graph (DLG) be used for area change assessment?

- An overlay of the DLG and DRG clearly revealed mismatches of extents for several glaciers which indicate that the DLG outlines have been partly updated. Thus, the DLG outlines require adjustment.

- For the 347 glaciers selected for area change assessment a good agreement with the glacier extents visible on the DRG maps was manually checked.

- About 400 glaciers were manually corrected according to the DRG maps to use them for determination of glacier elevation changes.

- A very valuable dataset for change assessment can be created from the DLG when the remainder of the outlines are also corrected.

Why and how to create central flow lines of glaciers automatically?

- Glacier length represents a key parameter in global glacier inventories. The scalar value itself is key for numerous applications (e.g. deriving glacier mean thickness) and the vector representation of a glacier flow line is an important input for modelling past and future climatic fluctuations (Oerlemans 2005; Leclercq *et al.* 2011) or changes in sea level (Oerlemans *et al.* 2007).

- To create glacier central flow lines automatically, a new algorithm (FLA) was developed and written in an open source programming language (Python) using the GDAL-OGR (Geospatial Data Abstraction Library – Open source Geospatial Resources) library. The algorithm is thus cross-platform compatible and/or software independent. It only requires glacier outlines (vector format) and a suitable DEM (raster format) as input data.

- The FLA algorithm was applied to 400 glaciers of the new inventory and to the DLG to also derive length changes. Length values range from 1.1 km to 44.5 km (for the new inventory) and the maximum length change value is -6.7 km (Hayes glacier).

- Results of the FLA have been validated by comparison with results from manual and multiple (three times) digitizing of flow lines for 20 selected glaciers. For 17 out of 20 glaciers, the length values of the FLA were close to the mean (±5%) of the manual digitizations.

How to derive glacier length changes automatically?

- Although vector lines are correctly computed according to the glacier shapes and DEMs, the 'correct' length change values cannot be calculated as a difference of their length values. This is mainly due to strong glacier geometry changes (e.g. emergence of rock outcrops, separation of glacier tributaries) that occurred in the time passed (ca. 50 years). Thus, length changes have to refer to the front variation rather than changes in total length. This value is calculated by digital intersection of the flow lines obtained for the earlier glacier extents (DLG) with the outlines from the new inventory.

- A comparison between length changes computed and based on the FLA (ΔL) and the Euclidian distance between the glacier terminus points (δL) allows the identification of glaciers that have to be checked before consideration. In fact, when δL is larger than ΔL it means that something has strongly changed for one of the line.

- A correlation of the length change values with other topographic parameters (e.g. mean slope or mean elevation) has not been found.

How to upscale mass balance measurements from Gulkana and Wolverine glaciers to the entire region and how to eliminate Columbia glacier from the calculation?

- Before extrapolation of the available mass balance measurements to the entire region can be made, an evaluation of the representativeness of these two glaciers for the region is required. This evaluation was achieved by differencing two digital elevation models (DEMs) that are temporally separated (by a few decades), and masking them with glacier extents (e.g. Berthier *et al.* 2010). The resulting $\Delta h/\Delta t$ raster maps were used to perform a glacier-specific elevation change assessment for a sample of 3180 glaciers in western Alaska.

- A proper determination of the representativeness of Gulkana and Wolverine glaciers requires that glacier types are treated separately (i.e. land-terminating, lake-terminating and tide-water glaciers) using the outlines of the new inventory and manually assigning a type in the attribute table. The changes of the individual glaciers according to their type are then assessed.

- Comparison of the mean elevation changes of Gulkana and Wolverine glaciers (-0.7 and -0.6 m yr^{-1}) to the mean values of the three glacier types clearly reveals that only the tide-water and lake terminating glaciers have similarly negative values. In other words, these glaciers are not representative

for their own type, but provide a correct mean value when all glaciers are considered.

- Extrapolation of the mean elevation changes from Gulkana and Wolverine glaciers would overestimate the loss of other land-terminating glaciers by factors of 2.5 (for Wolverine) and 2.9 (for Gulkana).

8.2 Main contributions and conclusion

Changes of glaciers and ice caps are among the best indicators for ongoing climate change. Additionally, their presence itself is related to specific climatic conditions that can be determined from glacier inventory data. Glaciers located in Alaska constitute a substantial fraction of the total area covered by glaciers on Earth and they have already contributed significantly to the observed global sea-level rise (e.g. Arendt *et al.* 2006; VanLooy *et al.* 2006). However, a more precise estimation of their past changes in length, area and volume would help to better understand their response to climate forcing. The here derived datasets (inventory and changes) thus fill a key gap in the related recent calculations (e.g. Radić and Hock 2010). Combined with the here developed new method to derive glacier length and length changes more or less automatically (input data have to be prepared beforehand), the datasets and methods presented in this thesis provide an important step forward towards a much better understanding of ongoing and calculation of past and future glacier changes.

In this regard, the ESA GlobGlacier project (Paul and others, 2009) has made a significant contribution to the international effort to globally map glaciers and ice caps according to Tier 5 of the Global Terrestrial Network for Glaciers (GTN-G). A special emphasis was on selected key regions with poor coverage and/or even with large gaps in the glacier databases, for instance the World Glacier Inventory (WGI; WGMS, 1989) and the Global Land Ice Measurements from Space (GLIMS; Raup *et al.* 2007) database. With these gaps being closed recently also on a global scale thanks to a special effort by the community (Arendt *et al.* 2012), a globally complete glacier inventory could be prepared in time for the IPCC report.

Although methodologies and techniques to automatically map glaciers and ice caps have already existed for at least a decade (Paul *et al.* 2002), it is surprising to see the large number of studies still using manual digitization. For large glacier samples and entire mountain ranges glacier mapping as well as change assessment should be based on automatic processing with manual editing (e.g lakes, debris-cover and shadow) to be applied only in the post-processing stage. In this regard, automatic tools remain an urgent objective facilitating production of accurate glacier extent information over large regions and their changes through time.

References

Albert TH (2002) Evaluation of remote sensing techniques for ice-area classification applied to the tropical Quelccaya ice cap, Peru. *Polar Geography* **26**(3), 210–226.

Andreassen LM, Elvehoy H, Kjollmoen B, Engeset RV, Haakensen N (2005) Glacier mass-balance and length variation in Norway. Annals of Glaciology **42**(1), 317-325.

Andreassen LM, Paul F, Kääb A, Hausberg JE (2008) Landsat-derived glacier inventory for Jotunheimen, Norway, and deduced glacier changes since the 1930s. *The Cryosphere* **2**(15), 131-145.

Andreassen LM, Kjollmoen B, Rasmussen A, Melvold K, Nordli O (2012) Langfjordjokelen, a rapidly shrinking glacier in northern Norway. Journal of Glaciology **58**(209), 581–593.

Arendt A, Bolch T, Cogley J, Gardner A, Hagen J, Hock R, Kaser G, Pfeffer W, Moholdt G, Paul F, others (2012) Randolph Glacier Inventory [v1. 0]: A Dataset of Global Glacier Outlines. Global Land Ice Measurements from Space, Boulder Colorado, USA. *Digital Media*.

Arendt A, Echelmeyer K, Harrison W, Lingle C, Zirnheld S, Valentine V, Ritchie B, Druckenmiller M (2006) Updated estimates of glacier volume changes in the western Chugach Mountains, Alaska, and a comparison of regional extrapolation methods. *Journal of Geophysical Research* **111**.

Arrighi P, Soille P (1999) From scanned topographic maps to digital elevation models. *Proceedings of Geovision* **99**, 1–4.

ASTER G (2009) 'Validation Team. ASTER Global DEM Validation Summary Report.'

Atwood DK, Meyer F, Arendt A (2010) Using L-band SAR coherence to delineate glacier extent. *Canadian Journal of Remote Sensing* **36**(S1), S186–S195. doi:10.5589/m10-014.

Bahr DB, Peckham SD (1996) Observations and analysis of self-similar branching topology in glacier networks. *Journal of Geophysical Research* **101**(B11), 25511–25521. doi:10.1029/96JB02536.

Bamber JL, Rivera A (2007) A review of remote sensing methods for glacier mass balance determination. *Global and Planetary Change* **59**(1–4), 138–148. doi:10.1016/j.gloplacha.2006.11.031.

Bamler R (1997) Digital terrain models from radar interferometry.

Bayr KJ, Hall DK, Kovalick WM (1994) Observations on glaciers in the eastern Austrian Alps using satellite data. *International Journal of Remote Sensing* **15**(9), 1733–1742. doi:10.1080/01431169408954205.

Berry Pam, Garlick JD, Smith RG (2007) Near-global validation of the SRTM DEM using satellite radar altimetry. *Remote Sensing of Environment* **106**(1), 17–27.

Berthier E, Le Bris R, Mabileau L, Testut L, Rémy F (2009) Ice wastage on the Kerguelen Islands (49° S, 69° E) between 1963 and 2006. *Journal of Geophysical Research* **114**, F03005.

Berthier E, Schiefer E, Clarke GKC, Menounos B, Rémy F (2010) Contribution of Alaskan glaciers to sea-level rise derived from satellite imagery. *Nature Geoscience* **3**(2), 92–95.

Berthier E, Toutin T (2008) SPOT5-HRS digital elevation models and the monitoring of glacier elevation changes in North-West Canada and South-East Alaska. *Remote Sensing of Environment* **112**(5), 2443–2454.

Bodansky E, Gribov A, Pilouk M (2002) Smoothing and compression of lines obtained by raster-to-vector conversion. *Graphics Recognition Algorithms and Applications* 256–265.

Bolch T, Menounos B, Wheate R (2010) Landsat-based inventory of glaciers in western Canada, 1985-2005. *Remote Sensing of Environment* **114**(1), 127–137.

Bonham-Carter G (1994) 'Geographic information systems for geoscientists: modelling with GIS.' (Pergamon press).

Bouillon A, Bernard M, Gigord P, Orsoni A, Rudowski V, Baudoin A (2006) SPOT 5 HRS geometric performances: Using block adjustment as a key issue to improve quality of DEM generation. *ISPRS Journal of Photogrammetry and Remote Sensing* **60**(3), 134–146.

Braithwaite RJ (2009) After six decades of monitoring glacier mass balance we still need data but it should be richer data. *Annals of Glaciology* **50**(50), 191–197.

Brown DG, Bara TJ (1994) Recognition and reduction of systematic error in elevation and derivative surfaces from 7 1/2-minute DEMs. *Photogrammetric Engineering and Remote Sensing* **60**(2), 195–202.

Burrough PA, McDonnell R (1998) 'Principles of geographical information systems.' (Oxford university press Oxford).

C.J. Van der Veen (1999) 'Fundamentals of glacier dynamics.' (Balkema).

Cogley JG (2009) Geodetic and direct mass-balance measurements: comparison and joint analysis. *Annals of Glaciology* **50**(50), 96–100.

Cogley J, Hock R, Rasmussen L, Arendt A, Bauder A, Braithwaite R, Jansson P, Kaser G, Möller M, Nicholson L, others (2011) Glossary of glacier mass balance and related terms. *IHP-VII Technical Documents in Hydrology* **86**.

Colvocoresses AP (1982) 'Automated satellite mapping system (MAPSAT).'

Crosetto M, Pérez Aragues F (2000) Radargrammetry and SAR Interferometry for DEM Generation: Validation and Data Fusion. In 'SAR workshop: CEOS Committee on Earth Observation Satellites', P 367.

DeBeer CM, Sharp MJ (2009) Topographic influences on recent changes of very small glaciers in the Monashee Mountains, British Columbia, Canada. *Journal of Glaciology* **55**, 691–700.

Denton GH, Field WO (1975) Glaciers of the Alaska Range. *Mountain Glaciers of the Northern Hemisphere US Army Corps of Engineers* **2**, 573–620.

Dozier J (1989) Spectral signature of alpine snow cover from the landsat thematic mapper. *Remote Sensing of Environment* **28**(0), 9–22. doi:10.1016/0034-4257(89)90101-6.

Dozier J, Painter TH (2004) Multispectral and hyperspectral remote sensing of alpine snow properties. *Annual Review of Earth and Planetary Sciences* **32**, 465–494.

Dyurgerov M (2003) Mountain and subpolar glaciers show an increase in sensitivity to climate warming and intensification of the water cycle. *Journal of Hydrology* **282**(1–4), 164–176. doi:10.1016/S0022-1694(03)00254-3.

Dyurgerov M, Meier MF, Bahr DB (2009) A new index of glacier area change: a tool for glacier monitoring. *Journal of Glaciology* **55**(192), 710–716. doi:10.3189/002214309789471030.

Egenhofer MJ (1994) Spatial SQL: A query and presentation language. *Knowledge and Data Engineering, IEEE Transactions on* **6**(1), 86–95.

Ehlers M, Welch R (1987) Stereocorrelation of Landsat TM images. *Photogrammetric Engineering and Remote Sensing* **53**, 1231–1237.

Elsberg D, Harrison W, Echelmeyer K, Krimmel R (2001) Quantifying the effects of climate and surface change on glacier mass balance. *Journal of Glaciology* **47**(159), 649–658.

Escher-Vetter H, Kuhn M, Weber M (2009) Four decades of winter mass balance of Vernagtferner and Hintereisferner, Austria: methodology and results. *Annals of Glaciology* **50**(50), 87–95. doi:10.3189/172756409787769672.

Farr TG, Rosen PA, Caro E, Crippen R, Duren R, Hensley S, Kobrick M, Paller M, Rodriguez E, Roth L (2007) The shuttle radar topography mission. *Reviews of Geophysics* **45**(2).

Fischer A (2011) Comparison of direct and geodetic mass balances on a multi-annual time scale. *The Cryosphere* **5**(1), 107–124.

Fountain AG, Hoffman MJ, Granshaw F, Riedel J (2009) The 'benchmark glacier' concept does it work? Lessons from the North Cascade Range, USA. *Annals of Glaciology* **50**(50), 163–168.

Fountain AG, Walder JS (1998) Water flow through temperate glaciers. *Reviews of Geophysics* **36**(3), 299–328.

Fowler RJ, Little JJ (1979) Automatic extraction of Irregular Network digital terrain models. In 'Proceedings of the 6th annual conference on Computer graphics and interactive techniques', Chicago, Illinois, United States. Pp 199–207. (ACM: Chicago, Illinois, United States)

Frey H, Paul F (2012) On the suitability of the SRTM DEM and ASTER GDEM for the compilation of topographic parameters in glacier inventories. *International Journal of Applied Earth Observation and Geoinformation* **18**(0), 480–490. doi:10.1016/j.jag.2011.09.020.

Frey H, Paul F, Strozzi T (2012) Compilation of a glacier inventory for the western Himalayas from satellite data: methods, challenges, and results. *Remote Sensing of Environment* **124**(0), 832–843. doi:10.1016/j.rse.2012.06.020.

Fujisada H, Ono A (1994) Observational performance of ASTER instrument on EOS-

AM1 spacecraft. *Advances in Space Research* **14**(3), 147–150. doi:10.1016/0273-1177(94)90207-0.

Gao F, Masek J, Wolfe RE (2009) Automated registration and orthorectification package for Landsat and Landsat-like data processing. *Journal of Applied Remote Sensing* **3**(1), 033515–033515.

Gardelle, J, Berthier, E, & Arnaud, Y (2012) Slight mass gain of Karakoram glaciers in the early twenty-first century. *Nature geoscience*, *5*(5), 322-325.

Gens R, van Genderen JL (1996) Analysis of the Geometric Parameters of SAR Interferometry for Spaceborn Systems. *International Archives of Photogrammetry and Remote Sensing* **31**, 107–110.

Gesch D, Evans G, Mauck J, Hutchinson J, Carswell Jr WJ (2009) The National Map–Elevation. *US geological survey fact sheet* **3053**(4), .

Guth PL (1999) Contour Line‘ Ghosts’ in USGS Level 2 DEMs. *Photogrammetric engineering and remote sensing* **65**, 289–296.

Haeberli W (1995) Glacier fluctuations and climate change detection. *Geogr Fis Dinam Quat* **18**, 191-199.

Haeberli W, Frauenfelder R, Hoelzle M, Zemp M (2003) Glacier mass balance bulletin no. 7 (2000-2001). *IAHS (ICSI), Zürich*.

Haeberli W, Hoelzle M (1995) Application of inventory data for estimating characteristics of and regional climate-change effects on mountain glaciers: a pilot study with the European Alps. *Annals of Glaciology* **21**, 206–212.

Haeberli W, Hoelzle M, Paul F, Zemp M (2007) Integrated monitoring of mountain glaciers as key indicators of global climate change: the European Alps. *Annals of Glaciology* **46**(1), 150–160.

Hall DK, Bayr KJ, Schöner W, Bindschadler RA, Chien JYL (2003) Consideration of the errors inherent in mapping historical glacier positions in Austria from the ground and space (1893–2001). *Remote Sensing of Environment* **86**(4), 566–577. doi:10.1016/S0034-4257(03)00134-2.

Hall DK, Williams RS, Barton JS, Sigurdsson O, Smith LC, Garvin JB (2000) Evaluation of remote-sensing techniques to measure decadal-scale changes of Hofsjokull ice cap, Iceland. *Journal of Glaciology* **46**(154), 375–388. doi:10.3189/172756500781833061.

Haug T, Rolstad C, Elvehøy H, Jackson M, Maalen-Johansen I (2009) Geodetic mass balance of the western Svartisen ice cap, Norway, in the periods 19681985 and

19852002. *Annals of Glaciology* **50**(50), 119–125. doi:10.3189/172756409787769528.

Hayakawa YS, Oguchi T, Lin Z (2008) Comparison of new and existing global digital elevation models: ASTER G-DEM and SRTM-3. *Geophysical Research Letters* **35**(17), L17404.

Hirano A, Welch R, Lang H (2003) Mapping from ASTER stereo image data: DEM validation and accuracy assessment. *ISPRS Journal of Photogrammetry and Remote Sensing* **57**(5–6), 356–370. doi:10.1016/S0924-2716(02)00164-8.

Hoelzle M, Haeberli W, Dischl M, Peschke W (2003) Secular glacier mass balances derived from cumulative glacier length changes. *Global and Planetary Change* **36**(4), 295–306 http://www.sciencedirect.com/science/article/B6VF0–47TFG5D–1/2/6f2aad8a953c863a354d0bf4f2453d84.

Huggel C, Haeberli W, Kääb A, Bieri D, Richardson S (2004) An assessment procedure for glacial hazards in the Swiss Alps. *Canadian Geotechnical Journal* **41**(6), 1068–1083.

Huss M, Farinotti D (2012) Distributed ice thickness and volume of all glaciers around the globe. *Journal of Geophysical Research* **117**(F4), F04010. doi:10.1029/2012JF002523.

IPCC: Parry M.L., O.F. Canziani, J.P. Palutikof, P.J. van der Linden and C.E. Hanson, Eds., 2007, *Climate Change 2007: Impacts, Adaptation and Vulnerability. Contribution of Working Group II to the Fourth Assessment Report of the Intergovernmental Panel on Climate Change,* Cambridge University Press, Cambridge, UK, 982pp.

Jordan RL, Caro ER, Kim Y, Kobrick M, Shen Y, Stuhr FV, Werner MU (1996) Shuttle radar topography mapper (SRTM). In 'Satellite Remote Sensing III', Pp 412–422.

Kääb A (2005) 'Remote sensing of mountain glaciers and permafrost creep.' (Geographisches Institut der Universität Zürich).

Kääb A, Huggel C, Paul F, Wessels R, Raup B, Kieffer H, Kargel J (2002) 'Glacier monitoring from ASTER imagery: accuracy and applications.' Proceedings of E ARSeL-LISSIG-Workshop Observing our Cryosphere from Space, Bern, March 11 – 13, 2 002.

Kargel JS, Abrams MJ, Bishop MP, Bush A, Hamilton G, Jiskoot H, Kääb A, Kieffer HH, Lee EM, Paul F, Rau F, Raup B, Shroder JF, Soltesz D, Stainforth D, Stearns L, Wessels R (2005) Multispectral imaging contributions to global land ice measurements from space. *Remote Sensing of Environment* **99**(1-2), 187–219 %U http://www.sciencedirect.com/science/article/B6V6V–4HBSH2R–1/2/4516e432b73d11bd08e2ba2f94c7c074.

Kaser G, Cogley JG, Dyurgerov MB, Meier MF, Ohmura A (2006) Mass balance of

glaciers and ice caps: consensus estimates for 1961-2004. *Geophysical Research Letters* **33**, 19.

Kaser G, Fountain A, Jansson P, others (2003) 'A manual for monitoring the mass balance of mountain glaciers.' (UNESCO).

Kaser G, Juen I, Georges C, Gomez J, Tamayo W (2003) The impact of glaciers on the runoff and the reconstruction of mass balance history from hydrological data in the tropical Cordillera Blanca, Perù. *Journal of Hydrology* **282**(1-4), 130–144.

Korona J, Berthier E, Bernard M, Rémy F, Thouvenot E (2009) SPIRIT. SPOT 5 stereoscopic survey of Polar Ice: reference images and topographies during the fourth International Polar Year (2007-2009). *ISPRS Journal of Photogrammetry and Remote Sensing* **64**(2), 204–212.

Kuhn M, Abermann J, Bacher M, Olefs M (2009) The transfer of mass-balance profiles to unmeasured glaciers. *Annals of Glaciology* **50**(50), 185–190. doi:10.3189/172756409787769618.

Larsen CF, Motyka RJ, Arendt AA, Echelmeyer KA, Geissler PE (2007) Glacier changes in southeast Alaska and northwest British Columbia and contribution to sea level rise. *J Geophys Res* **112**(F01007), F01007.

Le Bris R, Paul F, Frey H, Bolch T (2011) A new satellite-derived glacier inventory for western Alaska. *Annals of Glaciology* 52(59), 135–143.

Le Bris R, and Paul, F, (2012) An automatic method to create flow lines for determination of glacier length: A pilot study with Alaskan glaciers. *Computer & Geosciences Journal.*

Le Bris R, and Paul, F, 2013 (submitted). Glacier-specific elevation changes in western Alaska. Annals of Glaciology.

Leclercq PW, Oerlemans J (2012) Global and hemispheric temperature reconstruction from glacier length fluctuations. *Climate dynamics* **38**(5), 1065–1079.

Leclercq P, Oerlemans J, Cogley J (2011) Estimating the Glacier Contribution to Sea-Level Rise for the Period 1800-2005. *Surveys in Geophysics* **32**(4), 519–535.

Manley WF (2008) Geospatial inventory and analysis of glaciers: A case study for the eastern Alaska Range. *Satellite image atlas of glaciers of the world Denver, CO, United States Geological Survey, K* **424**, .

Marble DF (1990) Geographic information systems: an overview. *Introductory readings in geographic information systems* 8–17.

Markham BL, Storey JC, Williams DL, Irons JR (2004) Landsat sensor performance: history and current status. *Geoscience and Remote Sensing, IEEE Transactions on* **42**(12),

2691–2694.

Molnia BF (2009) Glaciers of North America–Glaciers of Alaska, by Bruce F. Molnia. *Arctic* **62**(4), 482–483.

Moore RD, Fleming SW, Menounos B, Wheate R, Fountain A, Stahl K, Holm K, Jakob M (2009) Glacier change in western North America: influences on hydrology, geomorphic hazards and water quality. *Hydrological Processes* **23**(1), 42–61.

Müller F, Caflisch T, Müller G, Müller F, Müller F (1977) 'Instructions for compilation and assemblage of data for a World Glacier Inventory.' (Department of Geography, Swiss Federal Institute of Technology (ETH)).

Müller, P. (1988) Paramet risierung der Gletscher- Klima-Bezichung für die Praxis Grundlagen und Beispiele. *Eidg. Tech. Horhschule. Zürich.Versuchsanst. Wasserbau, Hydrol. Glaziol. Mill. 95*.

Nuth C, Kääb A (2011) Co-registration and bias corrections of satellite elevation data sets for quantifying glacier thickness change. *The Cryosphere, Volume 5, Issue 1, 2011, pp 271-290* **5**, 271–290.

Oerlemans J (2001) 'Glaciers and climate change.' (Taylor & Francis).

Oerlemans J (2005) Extracting a Climate Signal from 169 Glacier Records. *Science* **308**(5722), 675–677 http://www.sciencemag.org/cgi/content/abstract/308/5722/675.

Oerlemans J, Dyurgerov M, Van de Wal R, others (2007) Reconstructing the glacier contribution to sea-level rise back to 1850. *The Cryosphere Discussions* **1**(1), 77–97.

Ohmura A, Kasser P, Funk M (1992) Climate at the equilibrium line of glaciers. *Journal of Glaciology* **38**(130), 397–411.

Parry ML, Canziani OF, Palutikof JP, van der Linden PJ, Hanson CE (2007) 'IPCC, 2007: climate change 2007: impacts, adaptation and vulnerability. Contribution of working group II to the fourth assessment report of the intergovernmental panel on climate change.' (Cambridge University Press, Cambridge).

Paterson WSB (1994) 'The physics of glaciers, 480 pp.' (Pergamon, New York).

Paul F (2002) Changes in glacier area in Tyrol, Austria, between 1969 and 1992 derived from Landsat 5 Thematic Mapper and Austrian Glacier Inventory data. *International Journal of Remote Sensing* **23**(4), 787–799.

Paul F (2007) The New Swiss Glacier Inventory 2000 - Application of Remote Sensing and GIS. Schriftenreihe Physische Geographie, Universität Zürich, 52, 210 pp.

Paul, F., N. Barrand, E. Berthier, T. Bolch, K. Casey, H. Frey, S.P. Joshi, V. Konovalov, R. Le Bris, N. Mölg, G. Nosenko, C. Nuth, A. Pope, A. Racoviteanu, P. Rastner, B. Raup, K. Scharrer, S. Steffen and S. Winsvold (2013): On the accuracy of glacier outlines derived from remote sensing data. *Annals of Glaciology,* **54**(63), 171-182.

Paul F, Andreassen LM (2009) A new glacier inventory for the Svartisen region, Norway, from Landsat ETM+ data: challenges and change assessment. *Journal of Glaciology* **55**(192), 607–618.

Paul F, Barry RG, Cogley JG, Frey H, Haeberli W, Ohmura A, Ommanney CSL, Raup B, Rivera A, Zemp M (2009) Recommendations for the compilation of glacier inventory data from digital sources. *Annals of Glaciology* **50**(53), 119–126.

Paul F, Frey H, Le Bris R (2011) A new glacier inventory for the European Alps from Landsat TM scenes of 2003: challenges and results. *Annals of Glaciology* **52**(59), 144–152. doi:10.3189/172756411799096295.

Paul F, Haeberli W (2008) Spatial variability of glacier elevation changes in the Swiss Alps obtained from two digital elevation models. *Geophysical Research Letters* **35**(21), L21502.

Paul F, Huggel C, Kääb A, Kellenberger T, Maisch M (2002) 'Comparison of TM-derived glacier areas with higher resolution data sets.'

Paul F, Kääb A (2005) Perspectives on the production of a glacier inventory from multispectral satellite data in Arctic Canada: Cumberland Peninsula, Baffin Island. *Annals of Glaciology* **42**(1), 59–66.

Paul F, Kääb A, Haeberli W (2007) Recent glacier changes in the Alps observed by satellite: consequences for future monitoring strategies. *Global and Planetary Change* **56**(1-2), 111–122.

Paul F, Kaab A, Maisch M, Kellenberger T, Haeberli W (2002) The new remote-sensing-derived Swiss glacier inventory: I. Methods. *Annals of Glaciology* **34**(1), 355–361.

Paul F, Kääb A, Rott H, Shepherd A, Strozzi T, Volden E (2009) GlobGlacier: a new ESA project to map the world's glaciers and ice caps from space. *EARSeL eProceedings* **8**(1), 11.

Paul F, Strozzi T, Kaab A (2010) Mapping clean and debris-covered glaciers from Palsar coherence images. In 'EGU General Assembly Conference Abstracts', P 13091

Pellikka P, Rees W (2010) 'Remote Sensing of Glaciers.' (London, UK: Taylor & Francis).

Peuquet DJ (1979) Raster processing: An alternative approach to automated cartographic data handling. *Cartography and Geographic Information Science* **6**(2), 129–139.

Post A, Mayo LR (1971) Glacier dammed lakes and outburst floods in Alaska. *United States Geological Survey, Hydrologic Investigations Atlas HA-455*.

Rabus B, Eineder M, Roth A, Bamler R (2003) The shuttle radar topography mission—a new class of digital elevation models acquired by spaceborne radar. *ISPRS Journal of Photogrammetry and Remote Sensing* **57**(4), 241–262. doi:10.1016/S0924-2716(02)00124-7.

Racoviteanu AE, Paul F, Raup B, Khalsa SJS, Armstrong R (2009) Challenges and recommendations in mapping of glacier parameters from space: results of the 2008 Global Land Ice Measurements from Space (GLIMS) workshop, Boulder, Colorado, USA. *Annals of Glaciology* **50**, 53–69.

Radić V, Hock R (2010) Regional and global volumes of glaciers derived from statistical upscaling of glacier inventory data. *Journal of Geophysical Research* **115**(F1), F01010 http://dx.doi.org/10.1029/2009JF001373.

Raup B, Kääb A, Kargel JS, Bishop MP, Hamilton G, Lee E, Paul F, Rau F, Soltesz D, Khalsa SJS (2007) Remote sensing and GIS technology in the Global Land Ice Measurements from Space (GLIMS) project. *Computers & geosciences* **33**(1), 104–125.

Reid HF (1901) The Variations of Glaciers. VI. *The Journal of Geology* 250–254.

Rodriguez E, Morris CS, Belz JE (2006) A global assessment of the SRTM performance. *Photogrammetric Engineering and Remote Sensing* **72**(3), 249–260.

Rott H (1994) Thematic studies in alpine areas by means of polarimetric SAR and optical imagery. *Advances in Space Research* **14**(3), 217–226. doi:10.1016/0273-1177(94)90218-6.

Schiefer E, Menounos B, Wheate R (2008) An inventory and morphometric analysis of British Columbia glaciers, Canada. *Journal of Glaciology* **54**(186), 551–560.

Schowengerdt RA (1983) 'Techniques for image processing and classification in remote sensing.' (Academic Press Orlando).

Schowengerdt RA (2006) 'Remote sensing: models and methods for image processing.' (Academic press)

Sidjak RW (1999) Glacier mapping of the Illecillewaet icefield, British Columbia, Canada, using Landsat TM and digital elevation data. *International Journal of Remote Sensing* **20**(2), 273–284. doi:10.1080/014311699213442.

Snyder JP (1987) 'Map projections–A working manual.' (USGPO).

Star J, Estes J (1990) 'Geographic information systems.' (Prentice-Hall).

Svoboda F, Paul F (2009) A new glacier inventory on southern Baffin Island, Canada, from ASTER data: I. Applied methods, challenges and solutions. *Annals of Glaciology* **50**(53), 11–21.

Toutin T (1995) Generating DEM from stereo images with a photogrammetric approach: examples with VIR and SAR data. *EARSeL Advances in Remote Sensing* **4**(2), 110–117.

Toutin T (2004) Comparison of stereo-extracted DTM from different high-resolution sensors: SPOT-5, EROS-A, IKONOS-II, and QuickBird. *Geoscience and Remote Sensing, IEEE Transactions on* **42**(10), 2121–2129.

Toutin T (2008) ASTER DEMs for geomatic and geoscientific applications: a review. *International Journal of Remote Sensing* **29**(7), 1855–1875.

UNEP (2007) 'Global outlook for ice and snow.' (UNEP/GRID-Arendal, Norway).

UNESCO (1970) 'Perennial ice and snow masses: a guide for compilation and assemblage of data for a world inventory.' (UNESCO/IASH).

UNFCCC, 2004 Guidelines for the preparation of national communications by Parties included in Annex I to the Convention, Part I: UNFCCC reporting guidelines on annual inventories (following incorporation of the provisions of decision 13/CP.9). FCCC/SBSTA/2004/8, United Nations Framework Convention on Climate Change.

U.S. Geological Survey, (1997) Part 1: General—Standards for digital elevation models, 11 p., URL: http://rockyweb.cr.usgs.gov/nmpstds/acrodocs/dem/1DEM0897.PDF (last date accessed: 20 January 2006).

VanLooy J, Forster R, Ford A (2006) Accelerating thinning of Kenai Peninsula glaciers, Alaska. *Geophysical Research Letters* **33**(21), L21307.

WGMS (1989) World glacierinventory: status 1988, ed. Haeberli, W., H. Bösch, K. Scherler, G. Østrem and C. Wallen. IAHS (ICSI)/UNEP/UNESCO, World Glacier Monitoring Service, Zürich.

WGMS (2008): Fluctuations of Glaciers 2000–2005, Volume IX. Haeberli, W., Zemp, M., Kääb, A., Paul, F. and Hoelzle, M. (eds.), ICSU (FAGS)/IUGG(IACS)/UNEP/UNESCO/WMO, World Glacier Monitoring Service, Zurich, Switzerland. *Fluctuations of Glaciers 2000–2005* **Volume IX**.

Williams R, Hall DK, Sigurosson O, Chien JYL (1997) Comparison of satellite-derived with ground-based measurements of the fluctuations of the margins of Vatnajökull, Iceland, 1973-92. *Annals of Glaciology* **24**: 72–80.

Wood FB (1988) Global alpine glacier trends, 1960s to 1980s. *Arctic and Alpine Research*

404–413.

Wulder MA, Masek JG, Cohen WB, Loveland TR, Woodcock CE (2012) Opening the archive: How free data has enabled the science and monitoring promise of Landsat. *Remote Sensing of Environment* **122**(0), 2–10.

Zemp M, Hoelzle M, Haeberli W (2009) Six decades of glacier mass-balance observations: a review of the worldwide monitoring network. *Annals of Glaciology* **50**(50), 101–111. doi:10.3189/172756409787769591.

Part II

Paper I

Le Bris, R., Paul, F., Frey, H., Bolch, T., 2011. *A new satellite derived glacier inventory for Western Alaska.* Annals of Glaciology, 52(59), 135-143.

A new satellite-derived glacier inventory for western Alaska

R. LE BRIS, F. PAUL, H. FREY, T. BOLCH

Department of Geography, Glaciology, Geomorphodynamics and Geochronology, University of Zürich-Irchel, Winterthurerstrasse 190, CH-8057 Zürich, Switzerland
E-mail: rlebris@geo.uzh.ch

ABSTRACT. Glacier inventories provide the baseline data to perform climate-change impact assessment on a regional scale in a consistent and spatially representative manner. In particular, a more accurate calculation of the current and future contribution to global sea-level rise from heavily glacierized regions such as Alaska is much needed. We present a new glacier inventory for a large part of western Alaska (including Kenai Peninsula and the Tordrillo, Chigmit and Chugach mountains), derived from nine Landsat Thematic Mapper scenes acquired between 2005 and 2009 using well-established automated glacier-mapping techniques (band ratio). Because many glaciers are covered by optically thick debris or volcanic ash and partly calve into water, outlines were manually edited in these wrongly classified regions during post-processing. In total we mapped ~8830 glaciers (>0.02 km^2) with a total area of ~16 250 km^2. Large parts of the area (47%) are covered by a few (31) large (>100 km^2) glaciers, while glaciers less than 1 km^2 constitute only 7.5% of the total area but 86% of the total number. We found a strong dependence of mean glacier elevation on distance from the ocean and only a weak one on aspect. Glacier area changes were calculated for a subset of 347 selected glaciers by comparison with the Digital Line Graph outlines from the US Geological Survey. The overall shrinkage was ~23% between 1948–57 and 2005–09.

1. INTRODUCTION

In response to global temperature increase, glaciers located in Alaska, as in almost every region of the world, have shown a strong retreat since their Little Ice Age maximum extent, with a more pronounced acceleration during the last decades of the 20th century (Molnia, 2007; WGMS, 2008). To better understand and model the response of glaciers to climate change, global inventories in a digital format are required (e.g. Beedle and others, 2008; Radić and Hock, 2010). In the case of Alaska, the main purpose of an inventory is better quantification of the glacier melt contribution to global sea-level rise (e.g. Kaser and others, 2006; Berthier and others, 2010), as well as the modeling of future changes in water resources (Zhang and others, 2007).

As a contribution to the European Space Agency (ESA) GlobGlacier project (Paul and others, 2009), this study focuses on the generation of accurate glacier inventory data from nine Landsat Thematic Mapper (TM) scenes acquired between 2005 and 2009 for a region with previously poor coverage (from the Chugach to the Chigmit Mountains) in both the World Glacier Inventory (WGI; WGMS, 1989) and the Global Land Ice Measurements from Space (GLIMS) glacier database (Raup and others, 2007). In a previous study, Manley (2008) stressed the importance of putting effort into creating a glacier inventory from already available data compiled by the US Geological Survey (USGS) in the 1950s for the eastern part of the Alaska Range. We have thus decided to use the digitally available version of this earlier glacier survey to assess mean decadal changes in glacier size for a subset of selected glaciers. The new dataset is available through the GLIMS website (www.glims.org).

2. STUDY REGION AND INPUT DATA

2.1. Study region

The study region is situated around the Gulf of Alaska (Fig. 1), with glaciers ranging in altitude from sea level up to 4000 m a.s.l. To provide a more regionalized assessment of glacier inventory data, the region was divided into seven subregions: (1) Tordrillo Mountains, (2) Chigmit Mountains, (3) Fourpeaked Mountain, (4 and 5) south and north Kenai Mountains, (6) Chugach Mountains and (7) Talkeetna Mountains. While the Tordrillo Mountains are situated in the southern part of the Alaska Range, the Chigmit Mountains and Fourpeaked Mountain are also considered to belong to the Aleutian Range and extend south of the Tordrillo Mountains to Kamishak Bay. There are several thousand glaciers in these mountain ranges, representing a large variety of glacier types from small cirques to large valley glaciers with multiple basins (Denton and Field, 1975). Several of the glaciers are classified as surge-type (e.g. Hayes and Harpoon Glaciers) and some of them cover volcanoes (e.g. Crater Glacier on Mount Spurr (3374 m a.s.l.)).

The Kenai Mountains are located on the Kenai Peninsula between Cook Inlet and the Gulf of Alaska. The maximum elevation of glaciers here is ~2000 m a.s.l., and the three main ice masses are the Sargent and Harding ice fields and an unnamed ice cap. The part of the Chugach Mountains considered here is bounded on the east by the Copper River and on the west by the Knik Arm. Together, these mountain ranges contain about one-third of the glacierized area of Alaska (Post and Meier, 1980). Many large glaciers (e.g. Harvard, Yale, Columbia, Shoup and Valdez glaciers) are of tidewater type and drain into northern Prince William Sound. In the west, until 1966, Knik Glacier dammed the outflow from Lake George, resulting in nearly annual glacier-outburst floods (Post and Mayo, 1971). The Talkeetna Mountains are the final region surveyed in this study. They are located north of the Matanuska River and north of the Chugach Mountains. Many peaks are higher than 2000 m a.s.l., with a maximum elevation of 2550 m a.s.l. As the entire study region includes glaciers of all types, with highly variable elevation ranges and locations (from the coast to the interior), different climatic regimes and responses to climate change can be expected.

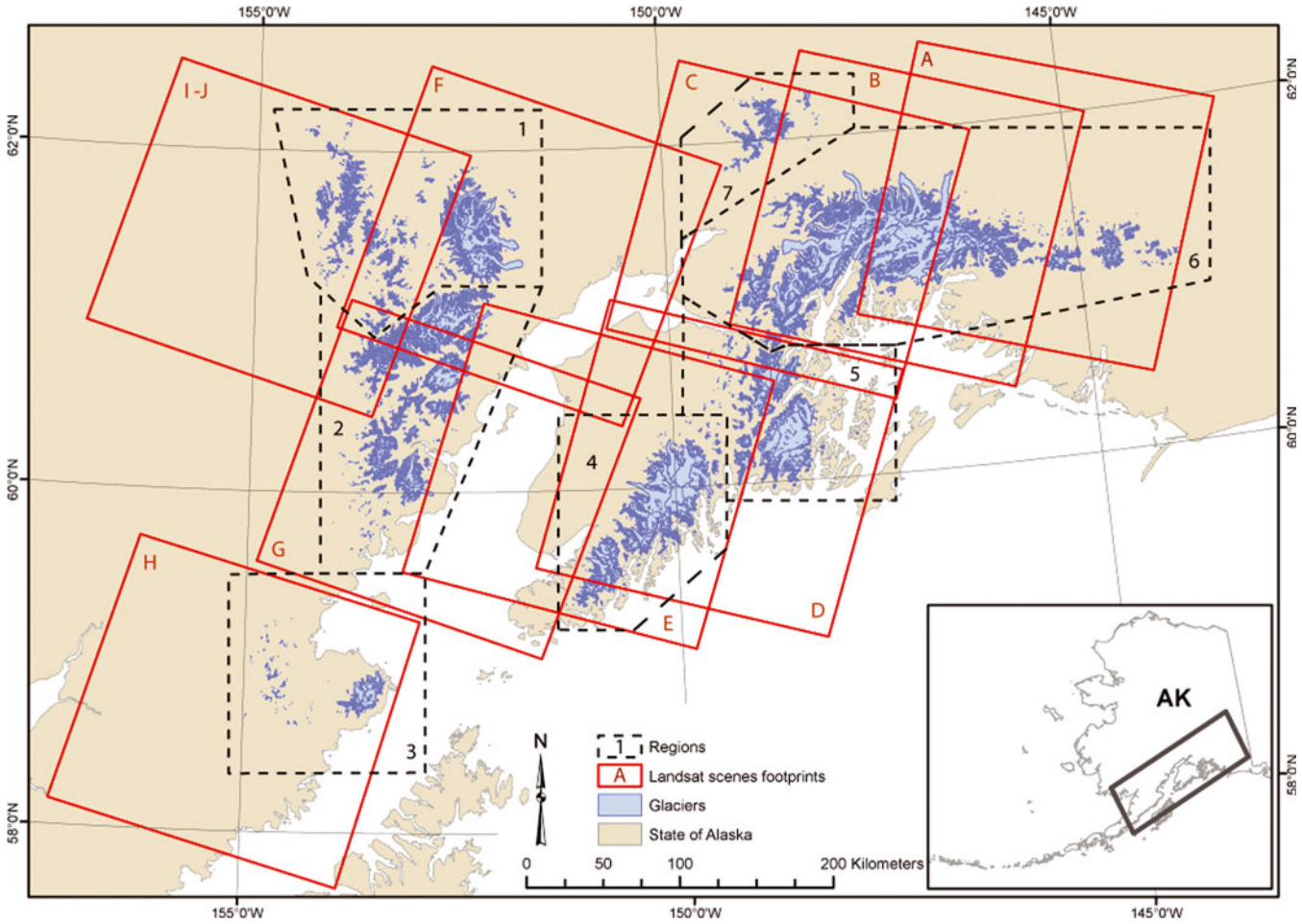

Fig. 1. Location map showing the footprint of the ten Landsat scenes originally analyzed in this study (red squares, where the red letters refer to the scene IDs). The sub-regions are delimited by dashed polygons, with the numbers referring to the IDs (see Tables 1 and 3), and glaciers are in light blue. The location of the study region in Alaska, USA, is shown in the inset.

In general, the study region experiences a predominantly maritime climate near the coast and a more continental climate further inland (e.g. http://climate.gi.alaska.edu). In the maritime region, mountain ranges act as a barrier for the westerlies, resulting in high amounts of annual precipitation along the coast of the Gulf of Alaska and frequent cloud cover. Clouds and frequent seasonal snowfields considerably decrease the number of useful satellite scenes in this region, so the inventory data refer to a 5 year period.

Table 1. List of the Landsat scenes used in the glacier inventory of western Alaska (source: http://glovis.usgs.gov). See Figure 1 for location of footprints; scene B was finally not used

ID	Type	Path	Row	Date
A	Landsat 5 TM	66	17	6 Sep 2009
B	Landsat 7 ETM+	67	17	1 Aug 2002
C	Landsat 5 TM	68	17	3 Aug 2009
D	Landsat 5 TM	68	18	12 Sep 2006
E	Landsat 5 TM	69	18	9 Jul 2009
F	Landsat 5 TM	70	17	28 Aug 2007
G	Landsat 5 TM	70	18	28 Aug 2007
H	Landsat 5 TM	71	19	14 Sep 2005
I	Landsat 5 TM	72	17	20 Aug 2005
J	Landsat 5 TM	72	17	26 Aug 2007

2.2. Input data

We analyzed all Landsat scenes from 1999 to 2009 that are freely available in the glovis.usgs.gov archive and processed to the standard terrain correction (level 1T). We selected ten of them covering our study region (Fig. 1; Table 1).

Scene B (Enhanced TM Plus (ETM+) from 2002) was processed at the beginning of the study, though it had considerable amounts of seasonal snow hiding several glacier boundaries. When two scenes from 2009 (A and C) with much better snow conditions became available we decided to use these for the Chugach Mountains inventory.

For the western Alaska Range (scenes 72-17), we combined two scenes. The scene from 2005 (I) had much better snow conditions (particularly in the accumulation region), but the lower part of most low-lying glacier tongues was barely visible due to a dense layer of fog and/or smog from fire. The lower glacier parts were hence derived from the 2007 scene (J), in large part by manual digitization of the debris-covered tongues.

A digital elevation model (DEM) is required to calculate topographic glacier parameters (e.g. minimum, mean and maximum elevation, mean slope and mean aspect) and to perform hydrological analysis (watersheds) for determination of drainage divides to separate contiguous ice masses into individual glaciers (e.g. Schiefer and others, 2008; Bolch and others, 2010b). For the study region, we used the Advanced Spaceborne Thermal Emission and Reflection

Radiometer (ASTER) global DEM (GDEM) and the USGS National Elevation Dataset (NED), both with a spatial resolution of 30 m, and for part of the region (south of 60° N) the Shuttle Radar Topography Mission (SRTM) C-band DEM with resolutions of 1″ (~30 m, SRTM-1) and 3″ (~90 m, SRTM-3). The SRTM DEM is known for its accuracy, with a mean deviation from a reference dataset of $\sim 3 \pm 15$ m (Berry and others, 2007). However, it is less accurate in the rough terrain of high mountains, with typical problems of synthetic aperture radar (SAR)-derived DEMs (radar shadow, layover, foreshortening) causing data voids. We thus use the seamless SRTM DEM from the Consultative Group for International Agriculture Research (CGIAR), version 4, where these voids were filled with additional elevation information (http://srtm.csi.cgiar.org). A study comparing SRTM-1 data with NED data in the USA revealed slightly higher accuracy of the SRTM-1 DEM in both the horizontal and vertical directions (Smith and Sandwell, 2003).

The GDEM can be of good accuracy (Hayakawa and others, 2008) but has inaccuracies mainly in regions of steep slopes and snow, due to missing contrast (Frey and Paul, unpublished information), and contains artifacts like local bumps and pits (depressions) which are typical for ASTER-derived DEMs (Kääb and others, 2003; Toutin, 2008). However, these artifacts were not a problem for this study. Due to its northern limitation (60° N), the SRTM DEM was available only for the southern part of the Kenai Peninsula, while the NED and the GDEM cover the entire region. Several tiles of both DEMs were downloaded, mosaicked and reprojected to Universal Transverse Mercator (UTM) zone 5 and bilinearly interpolated to 30 m cell size. Hillshades were created for all three DEMs to better recognize artifacts. While the NED refers to the contour lines of the related topographic maps from the 1950s, the GDEM was created from all available scenes in the ASTER archive acquired between 1999 and 2007. Hence, the topography in the GDEM fits much better to the acquisition period of the Landsat data (Table 1) and was therefore used to calculate minimum glacier elevation.

The Digital Line Graph (DLG) dataset was utilized to calculate changes in glacier size (see section 3.3). This earlier glacier mapping was compiled by the USGS from the 1 : 63 360-scale 15″ topographic quadrangle maps. Because the DLG has been partly updated compared to the Digital Raster Graph (DRG), we only selected glaciers with a good coincidence of the outlines. The DRGs are a scan of the topographic maps that were created from vertical aerial photographs (1948–57) by stereophotogrammetric techniques. For glacier identification we used this DRG dataset from the USGS, the Geographic Names Information Service (GNIS) which is also available in a digital format (http://geonames.usgs.gov/), the *Alaska atlas and gazetteer* (DeLorme, 2004) and the recently published Alaska volume of the *Satellite image atlas of glaciers of the world* (Williams and Ferrigno, 2008).

3. METHODS

3.1. Glacier mapping

We use automated mapping as the basic method and only edit regions with wrong classification. The glacier-mapping technique is the well-established semi-automated band ratio method (TM3/TM5) with manual threshold selection (e.g. Paul and Kääb, 2005). This method is based on the specific spectral reflectance properties of snow and ice compared with other terrain. While reflectance of glacier ice and snow in band TM3 (red) is comparably high (with possible sensor saturation over fresh snow), it is very low in band TM5 (shortwave infrared (SWIR)). These spectral differences make the TM3/TM5 ratio very efficient at discriminating glaciers from other terrain. Further advantages of the technique are its reproducibility and consistency for an entire region, and its accuracy for clean to slightly dirty glacier ice (e.g. Albert, 2002; Paul and others, 2003; Andreassen and others, 2008; Bolch and others, 2010a). However, manual corrections are still needed, in particular for debris-covered ice, calving glacier termini and water surfaces. Applying an additional threshold in band TM1 (blue) improves the classification in cast shadow (Paul and Kääb, 2005). Before outlines are edited, a noise filter (low pass 3×3 median filter) is applied to remove isolated snowpatches and to close local gaps. The classified map is then converted to vector format and imported by Geographic Information System (GIS) software. In a post-processing step, the necessary corrections for clouds, shadow, debris cover and water bodies are applied. To facilitate the interpretation, false-color composite images (e.g. with bands 5, 4 and 3 as red, green and blue) are used in the background. Higher spatial resolution data (e.g. aerial photographs, high-resolution imagery such as from QuickBird and IKONOS in Google Earth™) are also utilized for interpretation of selected glaciers when available. In Figure 2, we show the automatically derived and the corrected glacier outlines for a subset of the Chugach Mountains region. Some critical regions (e.g. debris-cover or water surfaces) are highlighted by circles.

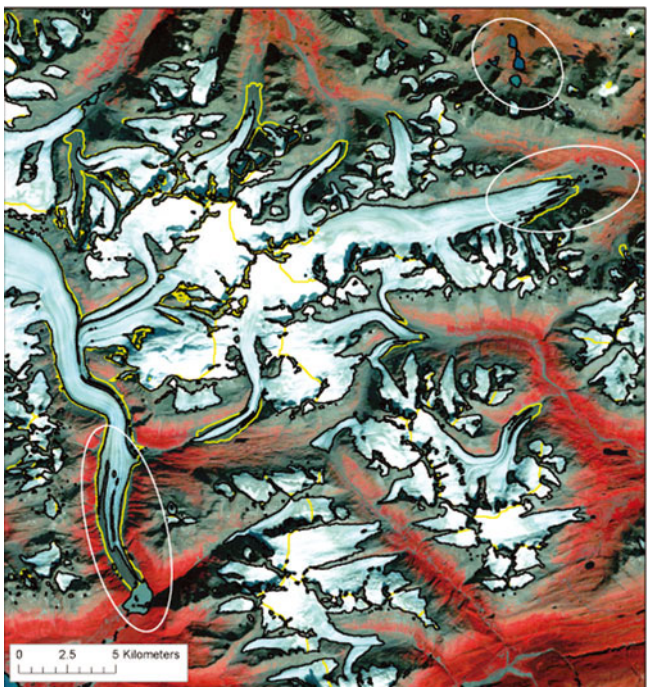

Fig. 2. Raw classification result from the algorithm (black) and manually corrected outlines (yellow) for a small region in the Chugach Mountains (scene A). Circles denote examples of misclassification of water bodies and non-classification of the debris-covered glaciers. A false-color composite (bands 432 as RGB) of the respective Landsat scene is displayed in the background.

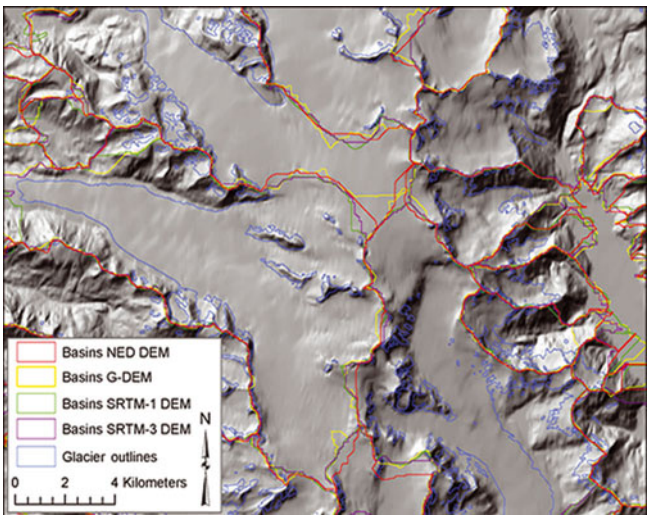

Fig. 3. Comparison of drainage divides derived from the four different DEMs where the background is a shaded relief of the USGS NED.

In the case of the eastern part of the Chugach Mountains, we first processed the Landsat ETM+ scene from 2002, but later two scenes from 2009 with much better snow conditions became available. As a simple update of the previously mapped extent by digital combination of the 2002 and 2009 outlines was not practical, we completely reprocessed the outlines for this region with the latest imagery.

3.2. Drainage divides

One of the main outcomes of a glacier inventory is a comprehensive set of topographic parameters for each glacier entity (Paul and others, 2009). A DEM allows us to create the drainage divides required to clip the contiguous ice masses into individual glaciers (e.g. Manley, 2008; Schiefer and others, 2008; Bolch and others, 2010b).

To find the most suitable DEM for calculating the divides, we compared the performance of all four DEMs with each other. In all DEMs the sinks were removed and they were smoothed with a 3×3 median filter to minimize the effect of possible outliers. Then we applied the approach of Bolch and others (2010b) to calculate the divides from the DEMs. For this purpose, a 1 km buffer is created around all glaciers to constrain the hydrological calculations to this buffer. As this method can generate many artificial and very small polygons in the ablation area, these were selected with a spatial query tool and removed. The resulting drainage divides are similar in all DEMs for distinct mountain ridges (deviation <100 m), although the coarser resolution of the SRTM-3 DEM is recognizable (Fig. 3). Large shifts of the location (>1000 m) are observed in the flat terrain of the accumulation areas where low contrast in the optical imagery can introduce errors in the DEM (e.g. Svoboda and Paul, 2009; Bolch and others, 2010a). Divides derived by SRTM-1 and SRTM-3 DEMs seemed to be most realistic when visually compared with the satellite data. Larger deviations of the basins as calculated from the GDEM could be attributed to unnatural peaks and sinks which commonly occur in the GDEM (Fig. 3) and which can show a deviation of $>\pm 25$ m compared to the SRTM DEMs (Frey and Paul, unpublished information). In most cases, the ice divides varied by <500 m in the accumulation regions. We finally selected the NED DEM because it covered the entire study region and performed slightly better than the GDEM.

Visual inspection was used to further improve the resulting divides, especially in the accumulation area where anomalies in the NED DEM also occur. A hillshade raster, a flow direction grid, topographic maps and false-color composites are used additionally for this purpose. After intersection of the drainage divides with the glacier outlines, topographic glacier inventory parameters were calculated for each glacier entity from the NED DEM following Paul and others (2009). As mentioned above, minimum elevation was derived from the ASTER GDEM.

Table 2. Summary of glacier count and area value per size class for the entire dataset

Size class km^2	Count	% by number	Area km^2	% by area
<0.1	4701	53.3	211.1	1.3
0.1–0.5	2240	25.4	520.1	3.2
0.5–1	686	7.8	487.7	3.0
1–5	856	9.7	1874	11.5
5–10	132	1.5	876	5.4
10–50	160	1.8	3236	19.9
50–100	21	0.2	1444	8.9
>100	31	0.4	7601.1	46.8
Total	**8827**	**100.0**	**16 250**	**100.0**

3.3. Change assessment

To use the glacier outlines from the DLG for calculation of size changes, we first adjusted the drainage divides created for the glacier inventory to the DLG outlines and then used them to separate the contiguous ice masses. We then manually selected a subset of 347 glaciers in the seven subregions that are suitable to assess area changes. To be suitable, the glaciers in both datasets must be clearly identifiable, which is often not the case (see section 5.2). Because the large glaciers are often calving (in lakes) or are of tidewater type, the resulting selection contains relatively 'smaller' glaciers, the largest one being 68 km^2. For most of the glaciers, the dates to which the DLG outlines refer were obtained from Berthier and others (2010) or directly from the USGS 1 : 63 000 topographic maps. Because the available DLG outlines have been partly updated, we visually controlled that the selected glaciers were in good agreement with the extents visible on the map (DRG). We are aware that the DLG outlines come with some (maybe systematic) uncertainty, but we think it is worth using them in this study as also recommended by Manley (2008).

4. RESULTS

The glacier inventory of western Alaska includes 8827 glaciers larger than 0.02 km^2 and covers a total area of ~16 250 km^2 (Table 2). The 31 (0.4%) glaciers larger than 100 km^2 account for 47% of the total area, while the 7627 glaciers (86%) smaller than 1 km^2 account for only 7.5% of the area. These percentages vary with the specific mountain range analyzed, but the general picture is similar in all

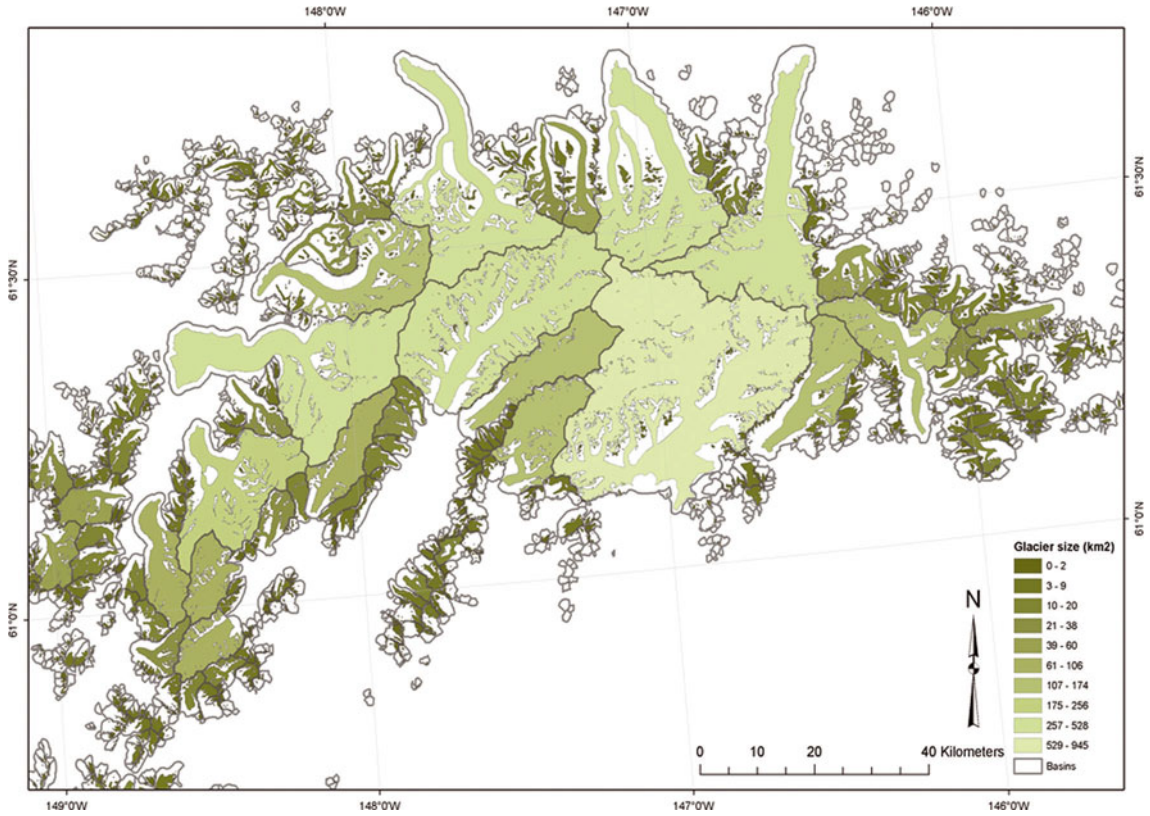

Fig. 4. Color-coded illustration of the glacier size distribution in the Chugach Mountains. Thick lines represent the basins.

regions. The strong contrast in the number and size contribution is visualized for the Chugach Mountains in Figure 4. The largest glaciers are also located in this region, but some are also found in the Kenai Peninsula and the Tordrillo Mountains (Table 3). This table also provides selected parameters from the inventory for the ten largest glaciers. Three of these huge glaciers are land-terminating, while seven are calving into lakes or the ocean. In Table 4 the number and area covered for the seven sub-regions is listed along with the mean glacier size in each region. While four regions have an ice cover between 1900 and 2700 km^2, that in the Chugach Mountains region is nearly 6500 km^2, while in the two smallest regions (Fourpeaked Mountain and Talkeetna Mountains) it is ~340 km^2. On the other hand, the mean size of the glaciers in each region is similar for five regions (1.1–1.8 km^2) and only slightly larger for the south Kenai Peninsula and the Chugach Mountains (2.3 and 2.6 km^2). This indicates that a region with comparably large glaciers is always accompanied by a proportionally higher number of small glaciers.

Figure 5 shows the area–elevation distribution for the seven sub-regions with 100 m binning. While most (84%) of the ice is located between 600 and 2000 m a.s.l., the glaciers in the Chugach Mountains have an elevation range from sea level to almost 4000 m. The much higher mean elevation of the glaciers in the more continental regions, Tordrillo and Talkeetna, is clearly visible. The different curves thus reflect the differences in the topoclimatic conditions.

Mean elevation of a glacier can be seen as a proxy for the equilibrium-line altitude (ELA) that represents balanced-budget conditions (e.g. Braithwaite and Raper, 2009). It is also a proxy for the climatic conditions in a region,

Table 3. The ten largest glaciers in the study region (sorted by size) with some topographic parameters

No.	Glacier name	Sub-region	Area km^2	Year	Mean elevation m	Mean slope °	Mean aspect ° east of north
1	Columbia	Chugach Mtns	945.4	2009	1426	10.4	279.8
2	Harvard	Chugach Mtns	528.2	2009	1821	18.9	290.3
3	Knik	Chugach Mtns	441.5	2009	1599	8.8	1.5
4	Chenega	North Kenai Peninsula	392.2	2006	1005	7.4	94.1
5	Tazlina	Chugach Mtns	384.7	2009	1510	6.3	23.8
6	Nelchina	Chugach Mtns	337.6	2009	1781	9.7	30.5
7	Tustumena	South Kenai Peninsula	336.5	2006	1202	5.3	10.4
8	Triumvirate	Tordrillo Mtns	333.2	2007	1533	11.2	147.6
9	Matanuska	Chugach Mtns	319.1	2009	1961	12.0	29.4
10	Blockade	Chugach Mtns	256.0	2007	1291	8.2	86.4

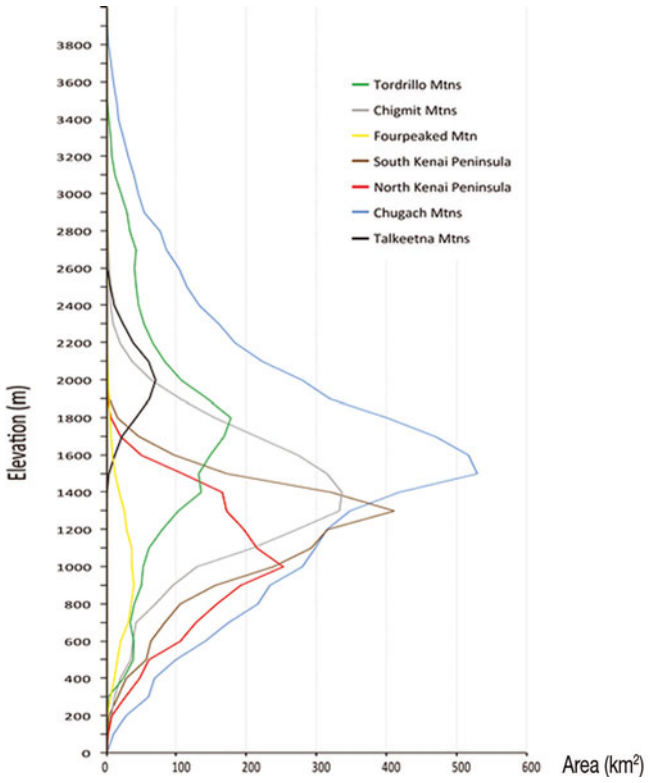

Fig. 5. Glacier area–elevation distribution (hypsography) for the seven sub-regions (see Fig. 1 for location) with 100 m binning.

especially precipitation amounts. The spatial analysis of this parameter reveals a strong increase from ~100 m at the coast to 3000 m a.s.l. in the interior (Fig. 6). To give this visual interpretation more weight, we defined an arbitrary point in the Gulf of Alaska that is located at the end of two sector lines enclosing the region (753200, 655100; World Geodetic System 1984 (WGS84) UTM zone 5N), and calculated the distance from each glacier to this point. A linear regression yields a high correlation ($R^2 = 0.91$; significance level (p value) 0.003) between this distance (100-500 km) and the mean elevation (1000 to nearly 2000 m). This regional trend has of course a high local variability, indicating that changes in temperature and/or precipitation will affect each glacier differently. We have also analyzed the variation of mean elevation with aspect sector for each sub-region (Fig. 7). Apart from the already described increase of mean elevation with distance from the coast, the graph reveals only a small variability with aspect sector (in the mean) in each region, indicating little dependency on this factor. This suggests that the precipitation regime has a much stronger influence on mean elevation in this region than received radiation, at least for the overall trend. On a more regional scale, glacier aspect can also have a more dominant influence on mean elevation (Evans, 2006).

In Figure 8 the relative change in glacier area per decade versus glacier size is illustrated for the subsample of

Table 4. Summary of glacier value per sub-region. Region names are from DeLorme (2004)

Region ID	Region name	Count	Area km²	Mean size km²
1	Tordrillo Mtns	1672	1998.4	1.2
2	Chigmit Mtns	1971	2778.0	1.4
3	Fourpeaked Mtn	280	329.4	1.2
4	South Kenai Peninsula	1051	2408.3	2.3
5	North Kenai Peninsula	1079	1900.9	1.8
6	Chugach Mtns	2466	6491.8	2.6
7	Talkeetna Mtns	308	343.1	1.1

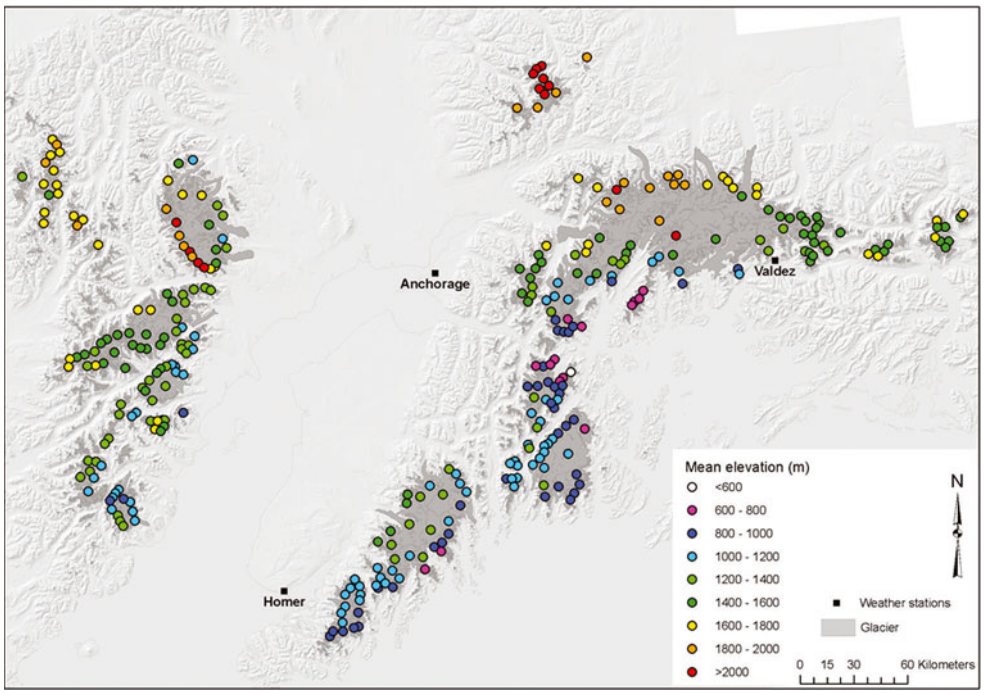

Fig. 6. Spatial variability of mean elevation with size for glaciers larger than 5 km² over the entire study region. Glaciers are in light grey, and in the background is a shaded relief from the USGS NED. Weather stations are located with black square dots.

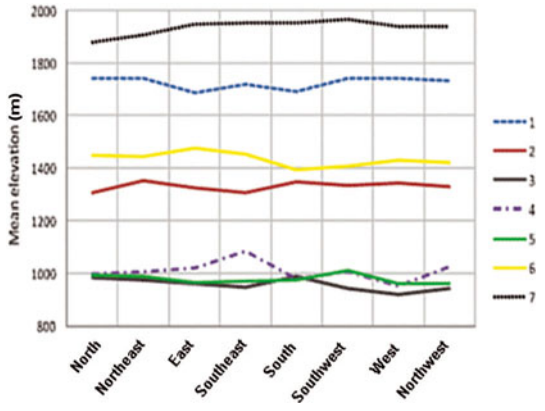

Fig. 7. Mean elevation as a function of aspect for each sub-region. (See Table 4 for region.)

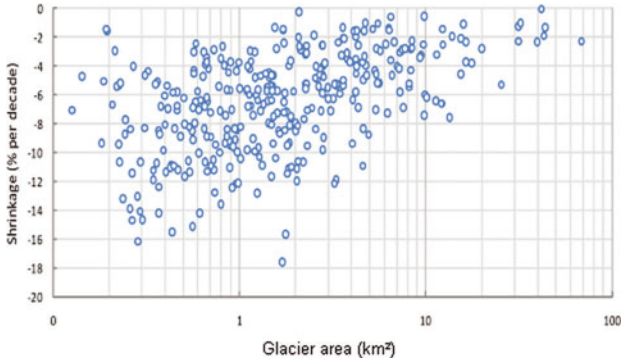

Fig. 8. Glacier shrinkage as a function of initial glacier area (1951–57) for a subset of 347 glaciers.

347 selected glaciers. As for several other regions where such analysis has been performed (e.g. for the western Canadian glaciers by Bolch and others, 2010b), a large variability of the changes is found, with an increase in scatter and an increasing relative area loss towards the smallest glaciers. All glaciers in this subsample lost area; the calculated total loss represents ~23% of the initial area (1948–57). (See section 5.2 for discussion of potential uncertainties.) This area loss is in good agreement with the changes found by Barrand and Sharp (2010) for Yukon (Canada) glaciers. However, it must be noted that the size-class distribution might be different in our sample, making the two samples less comparable.

5. DISCUSSION

5.1. Glacier inventory data

Because of the importance of Alaskan glaciers for global sea-level rise (e.g. Kaser and others, 2006; Radić and Hock, 2010), most of the recent studies on glacier change in Alaska focus on changes in glacier volume, either for selected glaciers (e.g. Arendt and others, 2006; Muskett and others, 2009) or entire mountain ranges (e.g. VanLooy and others, 2006; Berthier and others, 2010). Several of these studies could not exclude certain types of glaciers (e.g. calving or surging) from the analysis to better assess the impact of climate change on mass balance, as outlines of individual glaciers in this region have not been available so far. Moreover, Kaser and others (2006) highlighted the difficulties of determining the mass balance for an entire mountain range from direct measurements of a few selected and often comparably small glaciers. This is only possible when the representativeness of the measurements for the entire region is clear (e.g. Paul and Haeberli, 2008; Fountain and others, 2009). With the outlines now available, we hope that these glacier-specific changes can be calculated.

Though we would have preferred to have all satellite scenes used for the inventory acquired within 1 year (at best) or a few years, we decided to use only the scenes with the best snow conditions (Table 1), in order to minimize the workload and error for manual corrections due to seasonal snow (e.g. Paul and Andreassen, 2009). In the resulting 5 year period, some glaciers (e.g. Columbia Glacier) have shown considerable changes in extent. However, for each glacier outline, the acquisition date is given in the attribute table, so a proper reference for change assessment can be made. This is of particular importance when dates for the comparison dataset also vary strongly (e.g. Andreassen and others, 2008).

Apart from debris-covered small glaciers or those with an unclear transition to creeping permafrost bodies, the manual correction of the outlines was generally straightforward. This is due to the comparably good contrast of the debris-covered parts with surrounding terrain that results from the low solar elevation at high latitudes. We are aware that the manually corrected outlines of individual (in particular, small) glaciers might have larger errors, but based on previous studies that have determined the accuracy of the outlines (e.g. Paul and others, 2003; Andreassen and others, 2008) we are confident that for most glaciers the accuracy of the derived area is better than ±5%. This does not, however, include differences due to a different interpretation of a glacier entity as a whole (e.g. position of drainage divides, tributaries, attached snowfields). For example, in several cases we may have included perennial snowfields in the inventory, as no bare ice was visible on the satellite images. This is a common problem in all inventories (e.g. DeBeer and Sharp, 2009; Paul and Andreassen, 2009), but these elements can be marked in the attribute table (Paul and others, 2009).

Considering the workload involved in editing the automatically derived outlines, we strongly recommend using automated methods for the initial mapping. This also helps to cover the entire sample of glaciers in a region and to create a consistent and reproducible dataset (Svoboda and Paul, 2009). During manual editing, an inconsistent interpretation and certain degree of generalization is applied, i.e. the same spectral properties of a pixel are always interpreted differently. Though this might not have a large influence on the total area of a glacier, overlays of multiple manual digitizations of the same glacier by the same person revealed a considerable variability (±1 pixel) of the outline position. Comparing outline overlays from several analysts reveals an even higher variability (±2 pixels or more), i.e. the digitized extent is not reproducible (GlobGlacier, http://www.globglacier.ch/docs/globgl_deliv7.pdf).

The strong dependence of glacier mean elevation on distance from an arbitrarily chosen point in the ocean is very promising for establishing simple parameterization of either ELA or precipitation in high mountain regions. There is virtually no influence of mean glacier aspect sector on mean elevation within a mountain range (Fig. 7), so compared

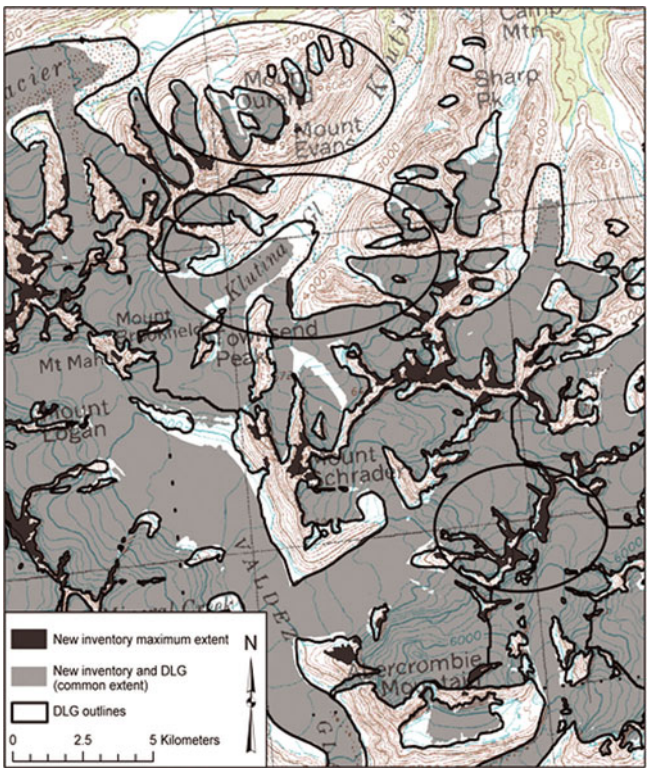

Fig. 9. Illustration of glacier recession in the Valdez district, southern Chugach Mountains. Thick black lines show the DLG glacier outlines, and light grey shading represents the new glacier inventory within the DLG extent, while the dark grey shading depicts the new glacier inventory outside the DLG extent. An example of the DRG (Valdez B-6) is displayed in the background. Black ellipses highlight examples of differences between the two datasets.

with other regions of the world the influence of reduced global radiation receipts for northerly-exposed glaciers is strongly reduced here (Evans, 2006). We assume that this observation can be explained by the influence of the high annual precipitation amounts on the glacier location as well as by the multi-basin origin of many glaciers which often causes differences in the mean aspect of the entire glacier compared to the ablation region.

5.2. Area change assessment

To calculate area changes, we manually selected a sample of 347 glaciers, as we found several ambiguities between the DLG outlines and our new inventory (Fig. 9). The example in Figure 9 shows that the DLG outlines do not always match the glacier-covered area on the topographic maps, which implies that they must have been updated somehow. Apart from normal retreat with separation of tributaries, we see glaciers that have been mapped in the DLG but not in our inventory (and vice versa in other regions). This could mean that (1) the glacier has disappeared, (2) we failed to map the glacier because of complete debris cover, or (3) in the DLG, seasonal snow was mapped. Hence, despite changes being clearly visible, the outlines of the DLG can rarely be used for automated change assessment. Also for the manual selection performed here, the error bounds are likely large, as cartographers and glaciologists can have different perceptions of what a glacier is, and the 'truth' can be a matter of debate, even in the field. For the manual selection used here, these cases can be largely excluded so that our estimate of the relative area loss is probably a lower bound.

Though the link between glacier area change and climate change is less straightforward than for mass-balance or length changes, there are also a number of benefits in assessing the former. Area changes can best be derived from satellite sensors and have thus been determined for many regions of the world. This provides interesting insights into the highly variable behavior of glaciers in different regions (e.g. DeBeer and Sharp, 2009; Paul and Andreassen, 2009). They also provide evidence for changes in surface elevation, for example when area is shrinking along the entire perimeter or new rock outcrops appear (e.g. Paul and others, 2007). When this occurs in the accumulation region, the glacier will likely disappear (Pelto, 2010). Area changes of glaciers are thus a valuable proxy for climate-change impact assessment on a global scale.

6. CONCLUSIONS

We have presented a new satellite-derived glacier inventory of western Alaska based on nine scenes from Landsat TM acquired between 2005 and 2009. This 5 year period is required because of frequent clouds and seasonal snow on most scenes in the USGS archive. The mapped 8827 glaciers larger than 0.02 km^2 cover an area of 16 250 km^2, a few of them (31) being >100 km^2 and most (86% by number) being <1 km^2. We found a strong relationship between glacier mean elevation and the distance from the ocean, which is related to the decreasing amount of precipitation inland.

We used the band ratio method (TM3/TM5) with a threshold to automatically map all glaciers in the region. Misclassified lakes or water bodies and the omitted debris-covered parts of glaciers were manually corrected. Drainage divides derived from the NED DEM allowed us to derive watersheds and obtain individual glacier entities and topographic inventory parameters. Because of large changes in the ablation zones, the parameter minimum elevation was calculated from the more recent ASTER GDEM. For a selection of 347 glaciers we found an overall recession of ~23% (by area) between the 1948–57 (DLG) and 2005–09 (Landsat) epochs. Due to several omission and commission errors between the two datasets, a more detailed analysis of the DLG is required before it can be used for further change analyses. In forthcoming studies, we will use the glacier inventory dataset derived here to assess glacier-specific changes. All inventory data are made available in the GLIMS glacier database to enable their use in the required additional studies and assessments.

ACKNOWLEDGEMENTS

This study was funded by the ESA GlobGlacier project (21088/07/I-EC). Landsat scenes, DLG outlines, DRG maps and the DEM NED were obtained from the USGS (http://glovis.usgs.gov and http://seamless.usgs.gov). The ASTER GDEM is a product of Japan's Ministry of Economy, Trade and Industry (METI) and NASA and was downloaded from http://www.gdem.aster.ersdac.or.jp and the also used seamless SRTM DEM was downloaded from http://srtm.csi.cgiar.org. We thank E. Berthier for providing data and useful comments on the paper. The comments of the editor, B. Raup, and an anonymous reviewer helped to improve the clarity of the paper.

REFERENCES

Albert, T.H. 2002. Evaluation of remote sensing techniques for ice-area classification applied to the tropical Quelccaya ice cap, Peru. *Polar Geogr.,* **26**(3), 210–226.

Andreassen, L.M., F. Paul, A. Kääb and J.E. Hausberg. 2008. Landsat-derived glacier inventory for Jotunheimen, Norway, and deduced glacier changes since the 1930s. *Cryosphere,* **2**(2), 131–145.

Arendt, A. *and 7 others*. 2006. Updated estimates of glacier volume changes in the western Chugach Mountains, Alaska, and a comparison of regional extrapolation methods. *J. Geophys. Res.,* **111**(F3), F03019. (10.1029/2005JF000436.)

Barrand, N.E. and M.J. Sharp. 2010. Sustained rapid shrinkage of Yukon glaciers since the 1957–1958 International Geophysical Year. *Geophys. Res. Lett.,* **37**(7), L07051. (10.1029/2009GL042030.)

Beedle, M.J. *and 7 others*. 2008. Improving estimation of glacier volume change: a GLIMS case study of Bering Glacier System, Alaska. *Cryosphere,* **2**(1), 33–51.

Berry, P.A.M., J.D. Garlick and R.G. Smith. 2007. Near-global validation of the SRTM DEM using satellite radar altimetry. *Remote Sens. Environ.,* **106**(1), 17–27.

Berthier, E., E. Schiefer, G.K.C. Clarke, B. Menounos and F. Rémy. 2010. Contribution of Alaskan glaciers to sea-level rise derived from satellite imagery. *Nature Geosci.,* **3**(2), 92–95.

Bolch, T. *and 7 others*. 2010a. A glacier inventory for the western Nyainqentanglha Range and Nam Co Basin, Tibet, and glacier changes 1976–2009. *Cryosphere,* **4**(2), 429–467.

Bolch, T., B. Menounos and R. Wheate. 2010b. Landsat-based inventory of glaciers in western Canada, 1985–2005. *Remote Sens. Environ.,* **114**(1), 127–137.

Braithwaite, R.J. and S.C.B. Raper. 2009. Estimating equilibrium-line altitude (ELA) from glacier inventory data. *Ann. Glaciol.,* **50**(53), 127–132.

DeBeer, C.M. and M.J. Sharp. 2009. Topographic influences on recent changes of very small glaciers in the Monashee Mountains, British Columbia, Canada. *J. Glaciol.,* **55**(192), 691–700.

DeLorme. 2004. *Alaska atlas and gazetteer. Sixth edition*. Yarmouth, ME, DeLorme Publishing.

Denton, G.H. and W.O. Field. 1975. Glaciers of the Alaska Range. *In* Field, W.O., *ed. Mountain glaciers of the Northern Hemisphere. Volume 2*. Hanover, NH, US Army Corps of Engineers. Cold Regions Research and Engineering Laboratory, 573–620.

Evans, I.S. 2006. Local aspect asymmetry of mountain glaciation: a global survey of consistency of favoured directions for glacier numbers and altitudes. *Geomorphology,* **73**(1–2), 166–184.

Fountain, A.G., M.J. Hoffman, F. Granshaw and J. Riedel. 2009. The 'benchmark glacier' concept – does it work? Lessons from the North Cascade Range, USA. *Ann. Glaciol.,* **50**(50), 163–168.

Hayakawa, Y.S., T. Oguchi and Z. Lin. 2008. Comparison of new and existing global digital elevation models: ASTER G-DEM and SRTM-3. *Geophys. Res. Lett.,* **35**(17), L17404. (10.1029/2008GL035036.)

Kääb, A. *and others*. 2003. Glacier monitoring from ASTER imagery: accuracy and applications. *EARSeL eProc.,* **2**(1), 43–53.

Kaser, G., J.G. Cogley, M.B. Dyurgerov, M.F. Meier and A. Ohmura. 2006. Mass balance of glaciers and ice caps: consensus estimates for 1961–2004. *Geophys. Res. Lett.,* **33**(19), L19501. (10.1029/2006GL027511.)

Manley, W.F. 2008. Geospatial inventory and analysis of glaciers: a case study for the eastern Alaska Range. *In* Williams, R.S., Jr and J.G. Ferrigno, *eds. Satellite image atlas of glaciers of the world*. Denver, CO, United States Geological Survey, K424–K439. (USGS Professional Paper 1386-K.)

Molnia, B.F. 2007. Late nineteenth to early twenty-first century behavior of Alaskan glaciers as indicators of changing regional climate. *Global Planet. Change,* **56**(1–2), 23–56.

Muskett, R.R. *and 6 others*. 2009. Airborne and spaceborne DEM- and laser altimetry-derived surface elevation and volume changes of the Bering Glacier system, Alaska, USA, and Yukon, Canada, 1972–2006. *J. Glaciol.,* **55**(190), 316–326.

Paul, F. and L.M. Andreassen. 2009. A new glacier inventory for the Svartisen region, Norway, from Landsat ETM+ data: challenges and change assessment. *J. Glaciol.,* **55**(192), 607–618.

Paul, F. and W. Haeberli. 2008. Spatial variability of glacier elevation changes in the Swiss Alps obtained from two digital elevation models. *Geophys. Res. Lett.,* **35**(21), L21502. (10.1029/2008GL034718.)

Paul, F. and A. Kääb. 2005. Perspectives on the production of a glacier inventory from multispectral satellite data in Arctic Canada: Cumberland Peninsula, Baffin Island. *Ann. Glaciol.,* **42**, 59–66.

Paul, F., C. Huggel, A. Kääb, T. Kellenberger and M. Maisch. 2003. Comparison of TM-derived glacier areas with higher resolution data sets. *EARSeL eProc.,* **2**(1), 15–21.

Paul, F., A. Kääb and W. Haeberli. 2007. Recent glacier changes in the Alps observed from satellite: consequences for future monitoring strategies. *Global Planet. Change,* **56**(1–2), 111–122.

Paul, F., A. Kääb, H. Rott, A. Shepherd, T. Strozzi and E. Volden. 2009a. GlobGlacier: a new ESA project to map the world's glaciers and ice caps from space. *EARSeL eProc.,* **8**(1), 11–25.

Paul, F. *and 9 others*. 2009b. Recommendations for the compilation of glacier inventory data from digital sources. *Ann. Glaciol.,* **50**(53), 119–126.

Pelto, M.S. 2010. Forecasting temperate alpine glacier survival from accumulation zone observations. *Cryosphere,* **4**(1), 67–75.

Post, A. and L.R. Mayo. 1971. Glacier dammed lakes and outburst floods in Alaska. *USGS Hydrol. Invest. Atlas* HA-455.

Post, A. and M.F. Meier. 1980. A preliminary inventory of Alaskan glaciers. *IAHS Publ.* 126 (Riederalp Workshop 1978 — *World Glacier Inventory*), 45–47.

Radić, V. and R. Hock. 2010. Regional and global volumes of glaciers derived from statistical upscaling of glacier inventory data. *J. Geophys. Res.,* **115**(F1), F01010. (10.1029/2009JF001373.)

Raup, B. *and 11 others*. 2007. Remote sensing and GIS technology in the Global Land Ice Measurements from Space (GLIMS) Project. *Comput. Geosci.,* **33**(1), 104–125.

Schiefer, E., B. Menounos and R. Wheate. 2008. An inventory of morphometric analysis of British Columbia glaciers, Canada. *J. Glaciol.,* **54**(186), 551–560.

Smith, B. and D. Sandwell. 2003. Accuracy and resolution of shuttle radar topography mission data. *Geophys. Res. Lett.,* **30**(9), 1467. (10.1029/2002GL016643.)

Svoboda, F. and F. Paul. 2009. A new glacier inventory on southern Baffin Island, Canada, from ASTER data: I. Applied methods, challenges and solutions. *Ann. Glaciol.,* **50**(53), 11–21.

Toutin, T. 2008. ASTER DEMs for geomatic and geoscientific applications: a review. *Int. J. Remote Sens.,* **29**(7), 1855–1875.

VanLooy, J., R. Forster and A. Ford. 2006. Accelerating thinning of Kenai Peninsula glaciers, Alaska. *Geophys. Res. Lett.,* **33**(21), L21307. (10.1029/2006GL028060.)

Williams, R.S., Jr and J.G. Ferrigno, *eds*. 2008. S*atellite image atlas of glaciers of the world.* Denver, CO, United States Geological Survey. (USGS Professional Paper 1386-K.)

World Glacier Monitoring Service (WGMS). 1989. *World glacier inventory: status 1988, ed.* Haeberli, W., H. Bösch, K. Scherler, G. Østrem and C. Wallén. IAHS (ICSI)/UNEP/UNESCO, World Glacier Monitoring Service, Zürich.

WGMS. 2008. *Global glacier changes: facts and figures, ed.* Zemp, M., I. Roer, A. Kääb, M. Hoelzle, F. Paul and W. Haeberli. United Nations Environment Programme/World Glacier Monitoring Service, Zürich.

Zhang, J., U.S. Bhatt, W.V. Tangborn and C.S. Lingle. 2007. Climate downscaling for estimating glacier mass balances in northwestern North America: validation with a USGS benchmark

Paper II

Le Bris, R. Paul, F., 2012. *An automatic method to create flow lines for determination of glacier length: A pilot study with Alaskan glaciers*. Computers & Geosciences Journal.

Computers & Geosciences ▮ (▮▮▮▮) ▮▮▮–▮▮▮

Contents lists available at SciVerse ScienceDirect

Computers & Geosciences

journal homepage: www.elsevier.com/locate/cageo

An automatic method to create flow lines for determination of glacier length: A pilot study with Alaskan glaciers

Raymond Le Bris *, Frank Paul

Department of Geography, University of Zurich, Winterthurerstrasse 190, CH-8057 Zurich, Switzerland

ARTICLE INFO

Article history:
Received 6 February 2012
Received in revised form
18 October 2012
Accepted 19 October 2012

Keywords:
Glacier
Remote sensing
Flow lines
Algorithm

ABSTRACT

Glacier length is a key parameter in global glacier inventories, but difficult to determine in a consistent way and subject to frequent change. Its vector representation (a flow line) is a most important input for modeling future glacier evolution, but only seldom available from digital databases. Hence, there is an urgent need to generate such flow lines for a large number of glaciers from automated methods. We here present a new algorithm that is based on Python scripting and additional libraries (GDAL and OGR) and requires only a DEM and glacier outlines as an input. The core of the method is based on a glacier axis concept that is combined with geometry rules such as the *k*-d Tree, Nearest Neighbor and crossing test theory. We have applied the method to 400 glaciers located in Western Alaska, where a new glacier inventory was recently created. The accuracy of the method was assessed by a quantitative and qualitative (outline overlay) comparison with a manually digitized dataset for 20 glaciers. This comparison revealed for 17 out of the 20 glaciers a length value within the range of the manual digitizations. Other potential methods performed less well. Combined with previous glacier outlines from the same region (Digital Line Graph) we automatically determined length changes for 390 glaciers over a c. 50 year period.

1. Introduction

Glaciers are regarded as natural elements documenting climate change most clearly to a wide public (Lemke et al., 2007). For this and further reasons (e.g. their high sensitivity to climate change) glaciers were considered as one of the terrestrial essential climate variables (ECVs) by the Global Climate Observing System (GCOS, 2003). In the last century, glaciers worldwide experienced a strong decline (retreat and mass loss) with only a few local exceptions (WGMS, 2008). Whereas mass changes of a glacier are a direct and undelayed response to the atmospheric conditions in the respective year, changes in glacier length (or terminus fluctuations) are a delayed, filtered and enhanced response to atmospheric conditions over a climatically relevant period of a few decades. Though the link of glacier terminus fluctuations to climatic forcing is difficult to establish, it can be made nevertheless (Hoelzle et al., 2003; Klok and Oerlemans, 2004). The special advantages of terminus fluctuations are: (1) their long historical record, partly back to the 16th century (Nussbaumer and Zumbühl, 2011), and (2) their widespread availability from numerous mountain ranges. Length changes are thus a key element for the reconstruction of past climatic fluctuations (Oerlemans, 2005; Leclercq and Oerlemans, 2011) or changes in sea level (Oerlemans et al., 2007, updated by Leclercq et al., 2011).

However, the sample of glaciers that can be used in such assessments is small compared to the estimated total number of glaciers on Earth (about 200,000: Arendt et al., 2012) and might be considered as being biased (e.g. in regard to their size or location). This sample can be extended by using multitemporal satellite data (e.g. Paul et al., 2011) that document glacier changes over recent decades in all parts of the world. The satellite data can also be used to map the Little Ice Age (LIA) extent from trimlines and thus largely extend the time series (Lopez et al., 2010; Citterio et al., 2009; Glasser et al., 2011). As the length changes since that time are often measured in kilometers, the low spatial resolution of sensors such as Landsat has only a small effect on the quality of the results (Hall et al., 2003). One bottleneck for a wider application of such satellite-based length change measurements is the work load involved: as yet, the points for measuring changes have to be defined and digitized manually. To largely extend this application, there is a demand to find an appropriate reference point at the glacier terminus automatically. Though the lowest elevation of a glacier can be determined automatically within a Geographic Information System (GIS) from glacier outlines and a digital elevation model (DEM), this is only meaningful for glaciers with a sharp tongue and/or in steep terrain. For glaciers with a flat or wide tongue such a point can be at

* Corresponding author. Tel.: +41 44 6355208; fax: +41 44 6356841.
E-mail address: raymond.lebris@geo.uzh.ch (R. Le Bris).

0098-3004/$ - see front matter © 2012 Elsevier Ltd. All rights reserved.
http://dx.doi.org/10.1016/j.cageo.2012.10.014

almost any location on the glacier front and it would be beneficial to define such a point near the center of the terminus. This can be achieved by digitally intersecting a flow line that is located in the center of a glacier tongue (in the ablation region) with the glacier outline at the terminus (Paul et al., 2009). Hence the problem of automatically calculating terminus fluctuations also implies the need for automated creation of a flow line.

As mentioned above, glacier length has a key role in glacier inventories: As a scalar value length is a major input for several modeling approaches (Haeberli and Hoelzle, 1995; Bahr, 1997; Lüthi et al., 2010); in its vector form the flow line is a mandatory input for flow models that assess future glacier changes (e.g. Oerlemans, 2008). So both are needed, the scalar value and the vector line itself. They are, however, currently not part of most glacier data stored in the GLIMS database (Raup et al., 2007). As manual digitizing does not provide reproducible or consistent results, an automated determination would be highly preferable. This is particular true in times of strong geometric glacier changes (Paul et al., 2007), as in such cases the entire flow line needs to be digitized again for a new inventory. An automated determination will reduce the amount of work (and hence increase the number of glaciers for which a flow line will be available) and give reproducible results. With flow line we refer here to the terminology introduced for glacier inventories decades ago to describe glacier length (e.g. Müller et al., 1977). We thus do not refer to a particle trajectory in a strict physical sense, but are compliant with the flow lines practically used for glacier modeling, i.e. being located in the center of a glacier tongue in the ablation region (cf. Oerlemans, 2001). The method of calculation does not result in a longest flow line or a line providing the mean glacier length from several branches as defined in Müller et al. (1977). It is just seen as a line providing a reasonable and reproducible scalar value and vector segment for glacier length.

Besides the flow line, the automatic algorithm presented here creates points on the glacier terminus using only glacier outlines and a DEM as an input. The algorithm is thus widely applicable and avoids the shortcomings of approaches that require strong intervention by the analyst. The method is applied to a test region in Alaska, where glaciers have a large variety of shapes and a new glacier inventory was recently created from satellite data (Le Bris et al., 2011). For validation we performed a comparison of the algorithm results with manually created flow lines. The quality of the generated dataset is further demonstrated by a comparison of its results with two other approaches that are also applicable to large datasets. The flow lines are finally used to determine length changes for a sample of about 400 glaciers by digital intersection with earlier outlines that are available for this region from the US Geological Survey (USGS).

2. Input data and test region

2.1. Study region

While the outline dataset from the new glacier inventory (Le Bris et al., 2011) covers a large proportion of all Alaskan glaciers, we focus in this study on the western part of it. The study region is located in the southern part of the Alaska Range and includes the Tordrillo and the Chigmit Mountains (Fig. 1) with glaciers covering ca. 2000 and 2800 km^2, respectively. The Gulkana and Wolverine glaciers are located close to the study region (at 63°16'N, 145°25'E and 60°24'N, 148°54'E, respectively) and are separately analyzed as they are benchmark glaciers in terms of long-term mass balance observations (WGMS, 2009). Glaciers can be found in the study region at all altitudes ranging from sea level up to 4000 m a.s.l. Several glacier types are present with large valley glaciers of complex shape (like the 213 km^2 Trimble glacier), but also small cirque glaciers and glaciers on volcanoes (Denton and Field, 1975). The climate regime is predominantly of maritime type close to the coast, but gets more continental further inland (e.g. http://climate.gi.alaska.edu).

2.2. Datasets

Two kinds of input data are needed to apply the flow line algorithm: A DEM with sufficient quality (e.g. not too many artefacts, local sinks and data voids) and glacier outlines in a vector format. If the geomorphometric representation of the glacier surface is poor in the DEM, some filtering and editing is required beforehand. In this study we used the first release of the ASTER GDEM rather than the Shuttle Radar Topography Mission (SRTM) DEM because most of the study region (apart from South Kenai Peninsula) is located north of the 60° North limit of that DEM. The ASTER GDEM was compiled from all available scenes in the ASTER archive acquired between 2000 and 2007. For change assessment, we additionally used a subset of glacier outlines from the new Alaskan glacier inventory referring to the year 2007 (± 2 years), the USGS National Elevation Dataset (NED) (Gesch, 2007), the Digital Line Graph (DLG) and the Digital Raster Graph (DRG), which all refer to a former glacier surface topography and extent. The USGS 1:63,360-scale 15-min topographic quadrangle maps were created from vertical aerial photographs (acquired between 1948 and1957) by stereophotogrammetric techniques. These maps were scanned (http://topomaps.usgs.gov/drg) and used to both create the NED DEM by extracting contour lines and to compile the DLG glacier outlines (http://eros.usgs.gov/#/Guides/dlg). All datasets are re-projected to UTM zone 5 with WGS84 datum and 30 m cell size.

2.3. Pre-processing of the raw data

The satellite-derived glacier outlines were manually corrected for classification errors during post-processing. This concerns in particular debris-covered glacier parts, shadow regions and attached seasonal snow fields (e.g. Racoviteanu et al., 2009). For most glaciers these outlines and related terminus positions are assumed to be accurate to about ± 1 pixel (30 m) or ± 2 pixels in the case of debris cover on the glacier and poor contrast to the glacier forefield.

The drainage divides that are required to clip the contiguous ice masses into individual glaciers were derived from hydrological calculations within a GIS using the NED DEM and following a method described by Bolch et al. (2010). These drainage divides were also applied to the DLG outlines to refer to the same glacier entities in both datasets. Hillshades were also created from the DEM to aid in visual interpretation during the manual digitizing experiment.

As the glacier outlines in the DLG dataset were partly updated, the DLG extents were adjusted to the DRG maps to have a clear reference date for each glacier extent. Unfortunately, the DRG maps showed a systematic planimetric shift compared to the DLG that might have resulted from different parameters and/or software used during the georeferencing process. Hence, we first have corrected this displacement by applying a correction to the coordinates of each raster file (60–90 m in x and 90–150 m in y). This helped to achieve a very good match of the USGS vector dataset to the raster maps. The differences between the DLG and the DRG were mainly found in the ablation areas and were manually corrected (using the shifted DRG in the background) for a subset of 400 glaciers larger than 1 km^2. This dataset was later used for change assessment and covers a larger region than

Please cite this article as: Le Bris, R., Paul, F., An automatic method to create flow lines for determination of glacier length: A pilot study with Alaskan glaciers. Computers & Geosciences (2012), http://dx.doi.org/10.1016/j.cageo.2012.10.014

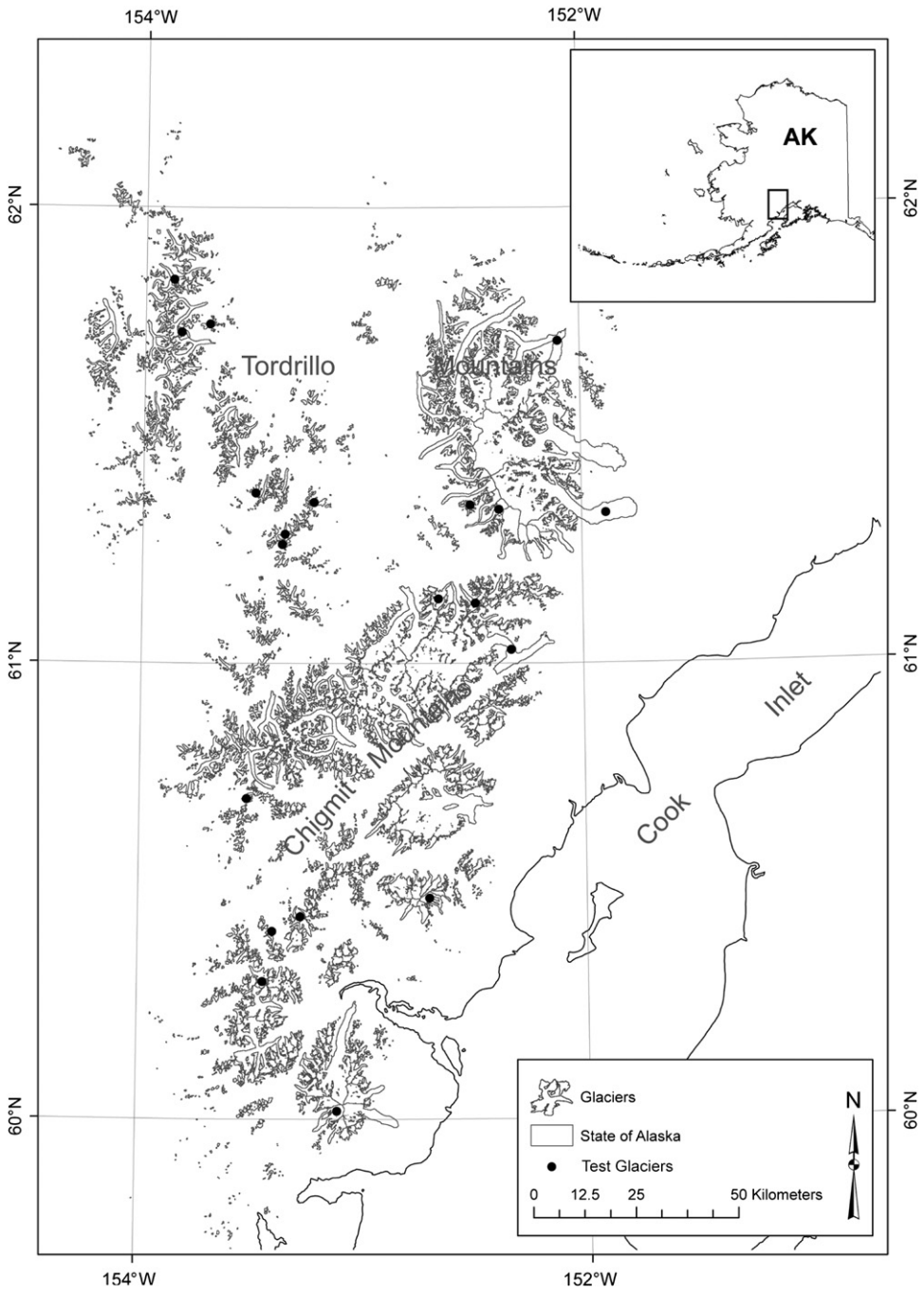

Fig. 1. Overview of the study region in Alaska. The thick lines mark glacier extents in the Tordrillo and Chigmit Mountains. Black dots indicate the twenty glaciers used for comparison with manual digitizing (see text for explanation). The inset shows the location of the study region in Alaska.

the study area selected for the methodological development (see Fig. 1).

3. Methods

3.1. Background

Glaciers originate from the accumulation of snow that is slowly transformed into ice by metamorphism and finally flows downward under its own weight. The resulting size and shape of a glacier does strongly depend on the climatic conditions and the topographic characteristics of the respective region. A glacier can thus have any geometry, ranging from a very simple elongated valley glacier (e.g. North Twin Glacier) to a more complex topology with many large multi-tributary branches (e.g. Triumvirate Glacier). In this regard, a suitable approach should be sufficiently flexible to create a flow line for any glacier form. On the other hand, glacier length as a parameter is highly ill-defined for complex shapes. Even when length is more precisely defined as the longest flow line or the line connecting the highest with the lowest point of a glacier, this does not necessarily result in a unique assignment for all glaciers as the path in-between is still subject to different interpretations. There is thus in any case some

Please cite this article as: Le Bris, R., Paul, F., An automatic method to create flow lines for determination of glacier length: A pilot study with Alaskan glaciers. Computers & Geosciences (2012), http://dx.doi.org/10.1016/j.cageo.2012.10.014

variability in this parameter that has to be considered when comparing a modeled value to a 'ground truth' (i.e. a manually digitized line).

The flow lines created here have to fulfill several rules to provide glacier length: The line must be located inside a glacier outline; basically stretch from the highest to the lowest point, should not cross rock outcrops, and should always be in the center of a glacier, in particular in the ablation region. However, considering that emerging rock outcrops are not part of the glacier, the line from the algorithm will correctly curves around them. Also in this case the line has to not be exactly located in the center of a glacier. Whereas the human brain is able to consider all these points during manual digitization (though not quite reproducible), this is much more difficult for an automated algorithm that can only consider a certain number of rules (one after another). And 'curving around a rock outcrop' is actually a highly complex concept, even in robotics using artificial intelligence. Hence, to get the method performing in a reasonable amount of time, we apply simple rules that are flexible enough to get a large number of glacier shapes correctly processed. Indeed, the algorithm will not work correctly for all cases and we can expect some post-processing work to correct misplaced flow lines. For the two glacier inventories (DLG and satellite-derived), distinct polyline (flow lines) and point (terminus position) shapefiles were generated by the algorithm which took about 2 h of processing time. This time depends on the computer system used to perform the algorithm and could be either faster or slower with an up-to-date or old system. The individual steps of the algorithm are described in Section 4.3.

3.2. Manual digitizing experiment

To assess the performance of the automated flow line delineation, a manual digitization experiment was performed. It is based on the repeat digitization of flow lines from 20 glaciers (covering sizes from 1 km^2 to ca. 250 km^2) by three persons, three times each. Each digitization was done with at least one day in-between to avoid recognition of the previous positioning of the line. False color composite images, the DEM hillshade and 50 m contour lines derived from the DEM were used to aid in the visual interpretation. The start and end points were given, but neither the automatically derived flow lines nor the results of the other participants were available. This procedure guarantees at least a certain independence of the individual digitizations. The dataset allows three comparisons to be performed: (a) variability of the manual digitization in absolute terms, (b) determination of the difference to the automatically derived length values, and (c) overlay of all lines to identify the problematic regions.

3.3. Other options to determine glacier length

Previous to the development of this algorithm, we performed tests with other approaches, for example using a water routing algorithm starting from seed points (e.g. Quinn et al., 1991). Although these tests gave good results in the accumulation region (with its concave shape), this method fails in the ablation area due to the convex shape of glacier tongues: they leave the glacier and can thus not stop at the terminus. Also in the accumulation region they are not really located in the center but follow the steepest downward gradient in the DEM, making them highly susceptible for DEM artefacts. Hence, they neither provide a suitable length value nor can they be used for assessment of length changes.

There are further possibilities to derive at least a scalar value for glacier length from easily available input data. Though this has clear shortcomings compared to direct determination from a flow line, they can be computed very fast for a large number of glaciers and we find a comparison interesting in regard to the potential error bounds of the automated method. One method is based on the high correlation between glacier area and length that is obviously based on a self-correlation (width multiplied with length estimates area). We have calculated a corresponding regression between the modeled length values and the area from the glacier inventory and applied this relation to the 20 selected test glaciers. The second method used for comparison is based on an inversion of the calculation of mean slope from the arctangent of glacier elevation range and length. We here use mean slope and elevation range as calculated per glacier from the DEM and outlines (using the ArcGIS zonal statistic tools) and calculate glacier length L from: L=elevation range/tan (slope).

This should work pretty well for constantly sloped (mountain) glaciers, but will underestimate real glacier length for long valley glaciers with a curved profile.

3.4. Calculating length changes

Using the adjusted glacier extents from the DLG, the outlines from the satellite-derived glacier inventory, and the flow lines derived here, we calculated length changes by digital intersection of the flow line for the DLG extent with the more recent outlines. Strictly speaking, this is only the change of the terminus position (or front variation) rather than the change of the entire length, as the latter can also result from a new path a flow line has to take due to changes in geometry (e.g. emerging rock outcrops). From a glacier dynamical and modeling point of view, only the frontal variation is of interest. We also computed the Euclidian distance between terminus positions of each glacier from the two inventories to assess the efficiency of this method. In total, 400 glaciers larger than 1 km^2 in both datasets served as a test sample.

4. Implementation

4.1. GDAL-OGR library and Python language

In order to create a cross-platform and/or software independent tool, the algorithm is written in Python. Python is an open source programming language with an efficient high-level data structure that uses functions and data types implemented in C or C++ (http://www.python.org). As we have to handle different sorts of data, we have implemented an additional library in the Python environment that allows us to properly work with glacier outlines and a DEM. In this regard, the GDAL-OGR (Geospatial Data Abstraction Library-Open source Geospatial Resources) library is used as a translator between raster and vector geospatial data formats (http://www.gdal.org).

4.2. Finding the highest glacier point

As described in the next section, the algorithm derives flow lines by joining the highest elevation point of any given glacier to its respective terminus position through several other middle points. The first task is thus to identify the highest point for each glacier, at best automatically. We have tested two different approaches to get these points called hereafter 'starting points'. The first one (A) determines the starting point as the highest elevation inside each glacier outline. The main advantage of this approach is that those points are derived automatically for all glaciers using GIS tools. The disadvantage is that the lines obtained starting at these points will not necessarily be the longest. Indeed, when the purpose is also to assess length changes, one has to keep in mind that the points could be outside

Please cite this article as: Le Bris, R., Paul, F., An automatic method to create flow lines for determination of glacier length: A pilot study with Alaskan glaciers. Computers & Geosciences (2012), http://dx.doi.org/10.1016/j.cageo.2012.10.014

the outline of the second glacier (from a newer or older date) with the consequence of reducing the number of comparable glaciers. The second approach (B) is to manually create the starting points with two possibilities: (1) first, automatically compute the highest points and then manually move them to a slightly displaced location to get them common to both datasets, or (2) directly place the points in what appears to be the longest branch. Choosing between (1) and (2) will mainly depend on the number of glacier in the dataset. In the case of a small dataset we recommend manual creation of the points (2), otherwise option (1) is the more practical.

4.3. Work flow of the algorithm

The algorithm described here creates a flow line for a given glacier and applies the individual steps depicted in Fig. 2 in a loop to an entire set of glaciers. Considering that a flow line is simply a line, it can be seen by definition as a succession of points that are linked to each other. The core principle of the algorithm is thus to find middle points inside any given glacier outline at all altitude bands and link them together. Though it is straightforward to find these points for a simple polygon geometry, this is different for glaciers that could have any shape. To solve this problem, we have developed the algorithm based on what we call the glacier axis concept. The individual steps of the work flow are explained in the following (cf. Fig. 2):

(a) Compute the starting and end points: Using glacier outlines, a DEM and the zonal statistics approach, the highest and lowest points for each glacier are calculated and stored in its attribute table. Assuming that a given glacier can have multiple points with the same elevation, only the first point in the resulting list is selected. Manual corrections are applied where necessary.

(b) Create the glacier axis: As the base for the axis concept we assume that the main direction of any given glacier can be defined as a straight line from its highest to its lowest elevation. In a first approach, this is assumed to give the general direction of flow and is further used to derive traverses across each glacier (c). In some specific cases (i.e. the glacier axis does not characterize the maximum elongation of the glacier geometry) the glacier axis needs to be extended. This is achieved by extending the line by 25% at both ends for all glaciers.

(c) Create perpendicular traverses: The algorithm then computes traverses at regular horizontal intervals along the axis (in 100 m steps). These traverses are used to slice the glacier by intersecting the glacier outline. In order to entirely cover the glacier, all traverses are set by default to 50 km width (25 km on each side) as no glacier in the new Alaskan glacier inventory is wider than 49 km (Columbia Glacier). For this step it has to be noted that the elevation intervals between traverses will affect the number of middle points and thus the smoothness of the resulting flow line. For a higher number of middle points there are more possibilities for the algorithm to find the way towards the end point of the given glacier.

(d) Intersect traverses with glacier outline: Using OGR library tools (see Section 4.1), the algorithm intersects traverses and glacier outlines. All traverses and glaciers are linked by a common ID.

(e) Compute the middle point of each segment: Because a traverse can be split into many segments from the glacier shape, the middle point of every segment is computed.

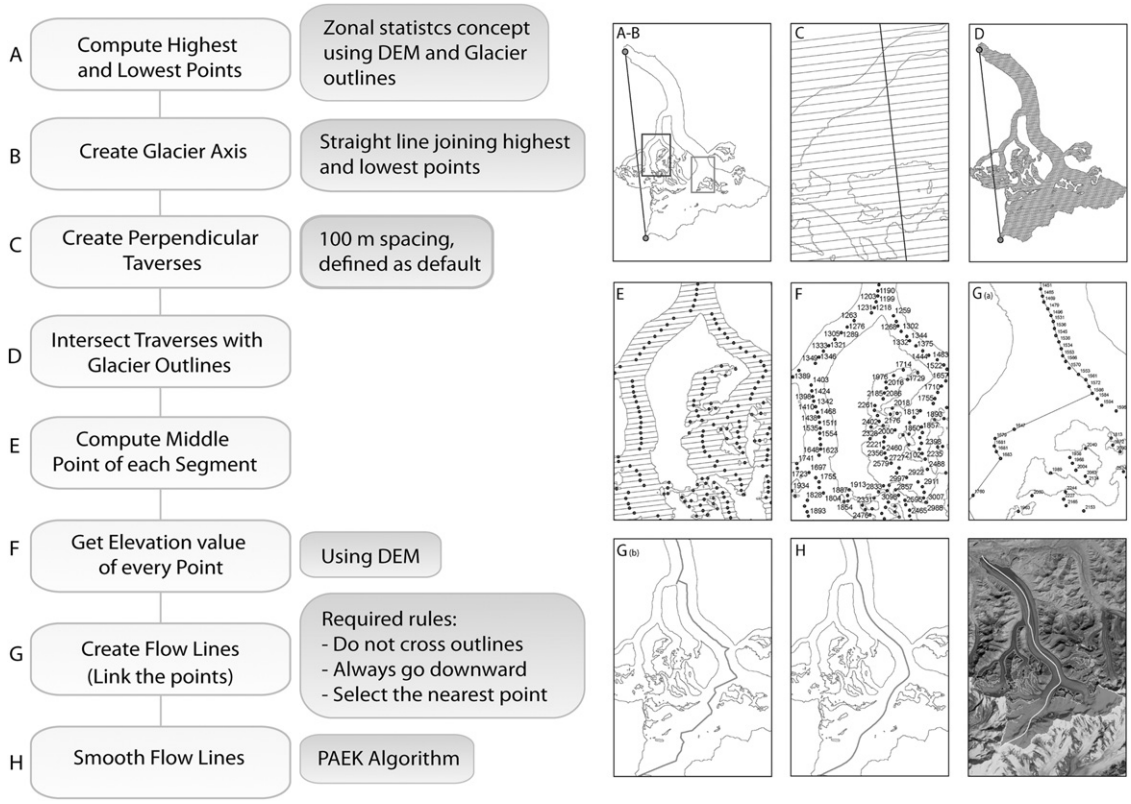

Fig. 2. Illustration of the principle work flow of the algorithm describing its major steps. Letters on the left top corner of each illustration refer to the respective step described on the flow chart. Squares in A and B represent enlargements showed in E and F and in G.

Please cite this article as: Le Bris, R., Paul, F., An automatic method to create flow lines for determination of glacier length: A pilot study with Alaskan glaciers. Computers & Geosciences (2012), http://dx.doi.org/10.1016/j.cageo.2012.10.014

(f) Get the elevation value for each middle point: Elevations of middle points derived in step e) are extracted from the DEM. Then, the algorithm will link all points following the rules in (g).

(g) Create the flow line: After middle points have been computed (step e), the Flow Line Algorithm (hereafter called FLA) will link them to create the flow line following the rules listed below. This is accomplished by implementing some computing science concepts in the script such as: (1) the *k*-Dimensional Tree (*k*d-tree), (2) Nearest Neighbor (NN), and (3) crossing test theories. A *k*d-tree is a data structure for storing a finite set of points from a *k*-dimensional space (Moore, 1991). This space-partitioning technique efficiently increases the processing speed in searching for the nearest neighbor point to a given position by answering a query for a large set of points (Manolopoulos et al., 2005; Tsaparas, 1999). Concept (3) refers to a line segment intersection theory used in the FLA to test whether or not the nearest point will be selected as being a part of the flow line (De Berg et al., 2008). Rules that have to be followed here are:
  (i) Go downward from the starting to the end points,
  (ii) Do not cross glacier outlines (including internal rock outcrops),
  (iii) Go from each point to its nearest neighbor.

  While (i) implies that in most cases the flow lines are not the longest ones (i.e. for a glacier with several tributaries), (iii) constrains the algorithm to link the current point with a lower nearest neighbor point in order to approximate the natural glacier flow. This constrain also prevents possible altitude inversions in DEMs especially in the ablation regions. It has to be noted here, that DEM accuracy will also affect the automated creation of flow lines. For that reason, we suggest smoothing the DEM with a low-pass filter (e.g. 3×3 median filter) to remove outliers and to fill local sinks.

(h) Smooth the flow line: This last step is given as a suggestion for the user and is not performed by the algorithm. Its intention is to smooth the lines to give them a more realistic shape. In this study we applied the Kernel (PAEK) algorithm (Bodansky et al., 2002) using ArcGIS software for this purpose. Users can apply different parameters to this polynomial approximation depending on the glacier shape and the required smoothing of the automatically generated flow lines.

5. Results

5.1. Glacier length

With the FLA we have computed glacier length values for a total of 788 entities from the DLG and the new glacier inventory. Vector lines are obtained for 98% of the processed glaciers (393) for the DLG and 98.7% (395) for the new inventory subset. In some cases the algorithm failed to create flow lines because of a particular glacier shape, resulting in 388 common lines (98.4%). However, due to strong changes in glacier topography and/or geometry, many lines are not directly comparable (see Section 5.2). This implies that length changes (i.e. front variations) cannot be obtained by direct subtraction of the length values of both lines.

5.2. Visual comparison of the flow lines

Fig. 3 shows an overlay of the flow lines obtained with the FLA from (a) the outlines of the new glacier inventory combined with the ASTER GDEM and (b) the DLG outlines with the NED DEM for the two glaciers Wolverine and Gulkana. In the case of Gulkana glacier, the two flow lines differ in shape due to the emerging rock outcrops at the confluence with the tributary, which results in a deflection of the flow direction. As there are only minor changes in the outline of Wolverine glacier but strong changes in surface elevation between the two DEMs, the differences in position are here due to the change of the DEM.

The overlay of the flow lines from the digitizing experiment (for glaciers ♯9 and ♯17) revealed only small overall differences in the positions from one session or operator to another (Fig. 4). However for some glaciers and more locally, also larger variations occurred, emphasizing the difficulty in digitizing all parts of the line consistently. Overall, the line derived with the FLA is more or less in the center of the manual digitizations pointing to its usefulness for other applications. However, the highest and lowest elevation points have to be provided to the analyst otherwise the digitizations could differ significantly (mainly due to a different consideration of tributaries). In any case, the line from the FLA has the clear benefit of being a consistent and reproducible product which is particularly useful for a glacier inventory.

5.3. Validation

A scatter plot of length values for all manually digitized flow lines compared to the FLA result is depicted in Fig. 5. For 17 out of 20 lines, the lengths of the FLA lines are within the variability of the lines that had been manually digitized. In three cases (♯8, ♯15 and ♯16, Fig. 6) the automated lines are outside this variability. Glacier ♯8 (Blockade glacier) is a large glacier (256 km^2) with a complex shape encompassing many tributaries and rock outcrops (mainly in the accumulation area) with a tongue flowing down in two opposite sides of a flat valley (Fig. 6A). These glacier characteristics can explain the spurious shape of the automated line which obviously needs to be corrected. For glaciers ♯15 and ♯16 the interpretation of the difference is less straightforward since the glacier shapes are rather usual (Fig. 6B and C). We speculate that DEM artefacts might explain these outliers and conclude that a visual control of the results and potential correction is required in the post-processing step.

The FLA length values as obtained for the new inventory were at first correlated with glacier area to investigate whether area can be used as a predictor for length. Fig. 7a shows the related log–log plot of length vs. area yielding a correlation coefficient of $R^2=0.88$. This seems to be a good correlation at first glance, but when plotting the relative differences versus glacier length (Fig. 7b), in particular shorter glaciers show large deviations of 50% or more compared to the length [L] computed from the algorithm. This might result from the much larger variability in width compared to the length for such small glaciers (Fig. 7). The comparison of glacier length as derived from mean glacier slope [α] and elevation range [Dh], ($L_{slope}=\Delta h/\tan\alpha$) is depicted in Fig. 8a. The correlation coefficient $R^2=0.83$ is somewhat lower here and compared to the identity the length is systematically underestimated. This is expected, as a curved line between two points is always longer than the direct connection. When plotting the relative difference of [L_{slope}] and [L] vs. [L] (Fig. 8b) a similar strong scatter as seen in Fig. 7b is obvious for small glaciers, but the range of the differences is smaller and the differences increase towards longer glaciers. This is in contrast using area to derive length, where differences are getting smaller for larger glaciers (though with a larger scatter). However, despite these interesting differences neither area nor slope are sufficiently accurate predictors for glacier length when calculated from a regression.

Lengths as computed from area and slope for the 20 selected glaciers are shown in Fig. 5 along with the results from the manual digitization experiment and the flow line algorithm. Apart

Please cite this article as: Le Bris, R., Paul, F., An automatic method to create flow lines for determination of glacier length: A pilot study with Alaskan glaciers. Computers & Geosciences (2012), http://dx.doi.org/10.1016/j.cageo.2012.10.014

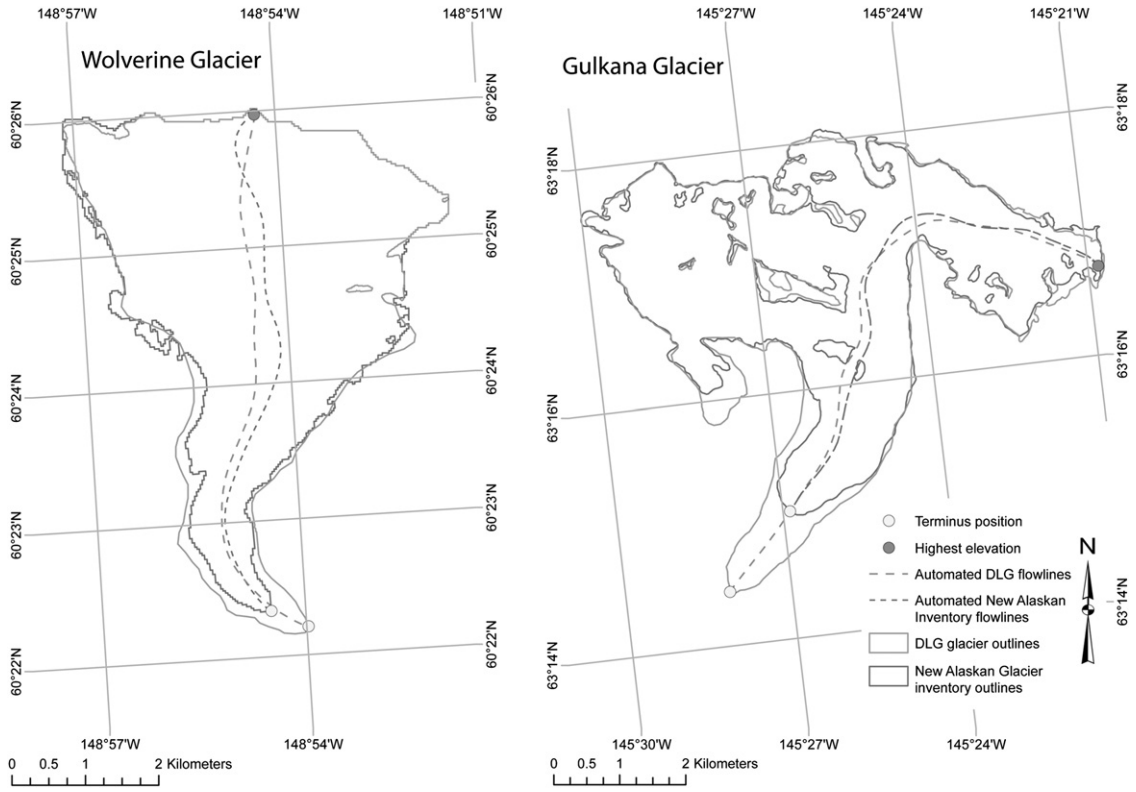

Fig. 3. Flow lines (dashed) as computed with the FLA for the two outlines of the DLG extent and the new inventory for Wolverine and Gulkana glaciers. The dots are the starting and terminus points.

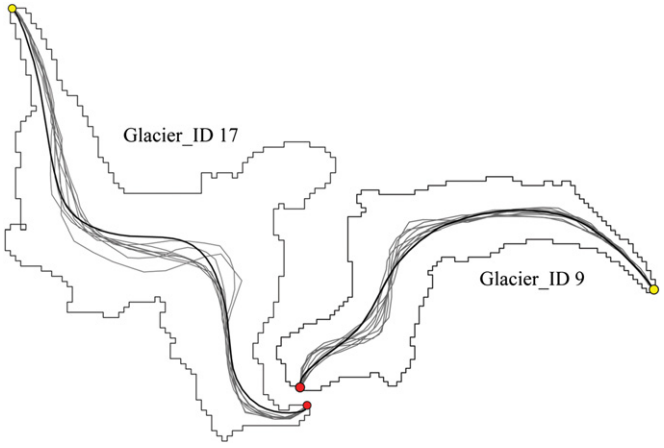

Fig. 4. Comparison of the manually digitized flow lines (thin, grey) and the automatically derived lines (thick, black) after smoothing. Rasterized lines are the glacier outlines. Dark and light dots are the starting and terminus points, respectively.

from a few cases (glaciers ♯6 & ♯14), $\text{length}_{(\text{area})}$ shows unsystematic variability around the mean value, while $\text{length}_{(\text{slope})}$ is systematically lower than the mean (apart from glacier ♯15). Overall, the length values from the FLA are in most cases much closer ($\pm 5\%$) to the mean of the manual digitizations, confirming that it is worth the effort to apply it.

5.4. Length changes

Fig. 9 shows examples of the length change assessment with the automatically created flow lines. Although in all cases the algorithm computed correct lines in regard to the glacier shapes and DEMs, the 'correct' length change values are a matter of debate. As changes in the shape of the terminus can have a strong impact on where terminus fluctuations can be measured, different methods of determination can lead to rather different results. For example, when the length change obtained from the flow lines (ΔL) is compared to the Euclidian distance between two terminus positions (δL), we get (a good agreement) for the glacier in Fig. 9a $\Delta L = 1430 \pm 101$ m and $\delta L = 1390 \pm 101$ m, but for the glacier in Fig. 9f a difference $>100\%$ ($\Delta L = 516 \pm 101$ m and $\delta L = 1100 \pm 101$ m). Though the difference is obvious here, such a complete relocation of the flow line due to strong geometric changes of a glacier cannot easily be overcome and requires careful analysis. In principle, length changes of glaciers are terminus fluctuations rather than changes in the length of the flow line, so only the distance between the two terminus positions should be measured. This requires clearly defining where the terminus is, which is not an easy task when considering the multilobate glaciers in Fig. 9e and f. The same applies to the Blockade Glacier depicted in Fig. 6a. The decision which of the lobes should be used as the terminus can only be decided manually.

A strong correlation ($R^2 = 0.88$) between length change from the flow lines ΔL and Euclidian distance between the glacier terminus points δL is found. A more detailed analysis of this correlation was performed by plotting the differences of the two methods vs. length change ΔL (Fig. 10). For a retreat along a line that is curved rather than straight, δL should be smaller than ΔL. However, Fig. 10 shows that there are several exceptions from this rule (δL is larger than ΔL) which can only occur when something is wrong with at least one of the methods (e.g. a strong geometric change has moved the terminus point to a different location). In that sense the scatter plot presented in Fig. 10 allows the identification of glaciers that have to be checked before consideration. We found no correlation of the length change values with other topographic parameters (e.g. mean slope or mean elevation).

Please cite this article as: Le Bris, R., Paul, F., An automatic method to create flow lines for determination of glacier length: A pilot study with Alaskan glaciers. Computers & Geosciences (2012), http://dx.doi.org/10.1016/j.cageo.2012.10.014

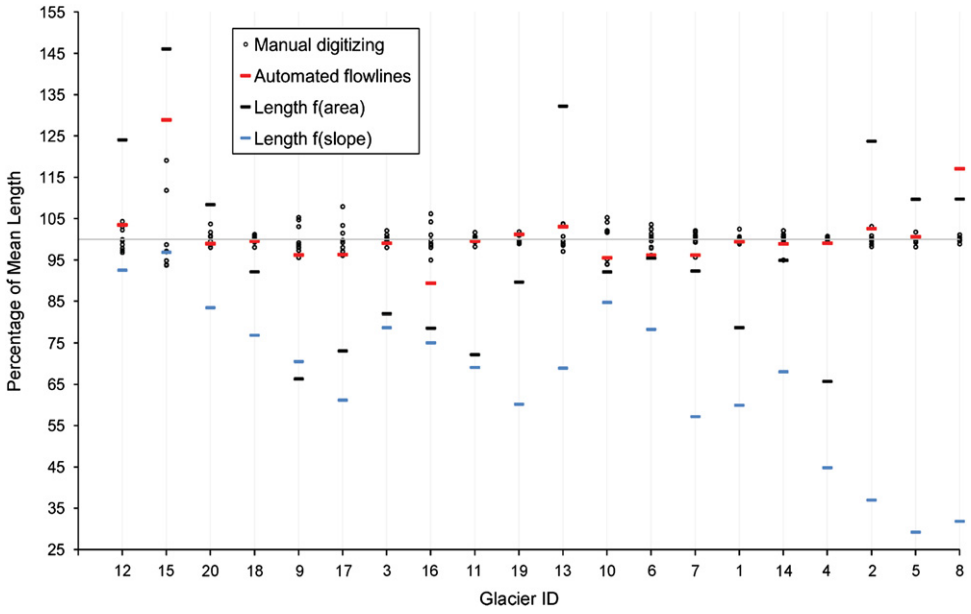

Fig. 5. Relative length differences of the manually digitized (grey) and automatically created flow lines for 20 selected glaciers. *Y*-axis represents the relative mean difference of the automated lengths compared to the manual values. Horizontal red bars show the length of each glacier computed with the FLA, while black and blue bars show the length estimated from area and slope, respectively. Glaciers (ID) are ordered according to the glacier length (as derived from the algorithm).

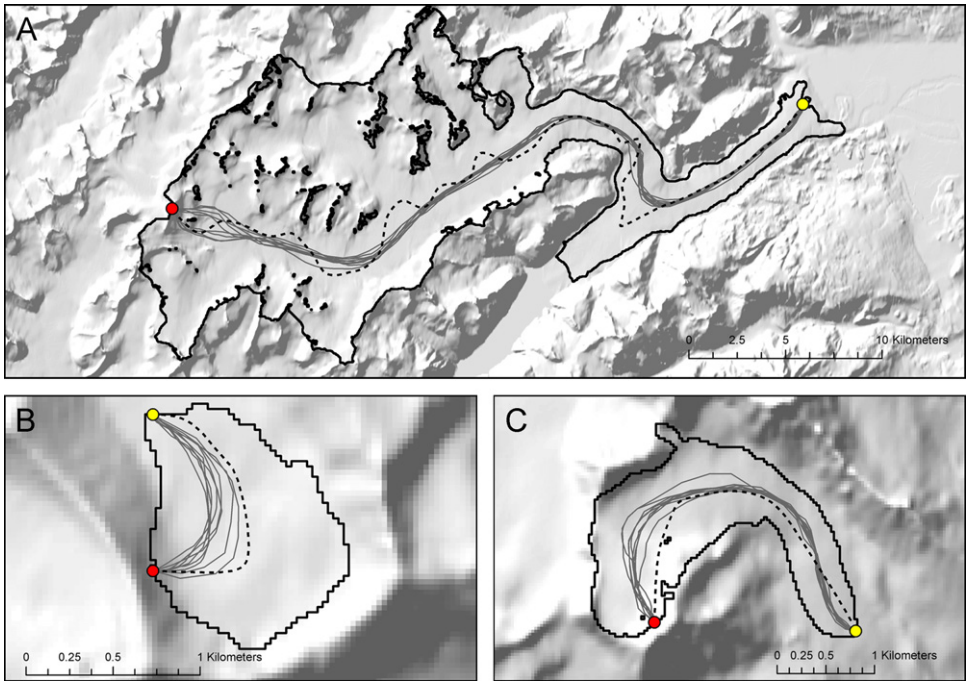

Fig. 6. Illustration of poor results obtained by the algorithm. A, B and C correspond to glaciers ♯8 (Blockade Glacier), ♯15 and ♯16 (two unnamed glaciers), respectively.

6. Discussion

6.1. Performance of the method

The FLA presented here creates a flow line and computes its length for several hundred glaciers in a fully automated way given that the two input datasets (glacier outline, DEM) are available. The main advantages compared to manual digitization come with the consistent, reproducible and fast computation. The computing time required to create the flow lines for an entire region depends on the number of large glaciers in the dataset. For small glaciers ($<5\ km^2$), lines are created within a second, while it may take 5 min or more for large glaciers ($>200\ km^2$). The examples in Fig. 9 illustrate that the performance of the FLA is in general very good (Fig. 9a–d), but can be quite different for the same glacier when a geometry change took place (Fig. 9e–f). Hence, visual inspection and manual corrections are still necessary to adjust poor line shapes or to select the most appropriate one. For the sample tested, 8% of the lines had to be manually corrected to give glacier front changes, but to provide acceptable flow lines 17% needed correction. When the algorithm did not create a line, it is possible to adjust the distance between traverses (see Section 4.3(c)). Due to the conceptual idea behind the algorithm, flow lines can be deflected by a glacier tributary as the points are

Please cite this article as: Le Bris, R., Paul, F., An automatic method to create flow lines for determination of glacier length: A pilot study with Alaskan glaciers. Computers & Geosciences (2012), http://dx.doi.org/10.1016/j.cageo.2012.10.014

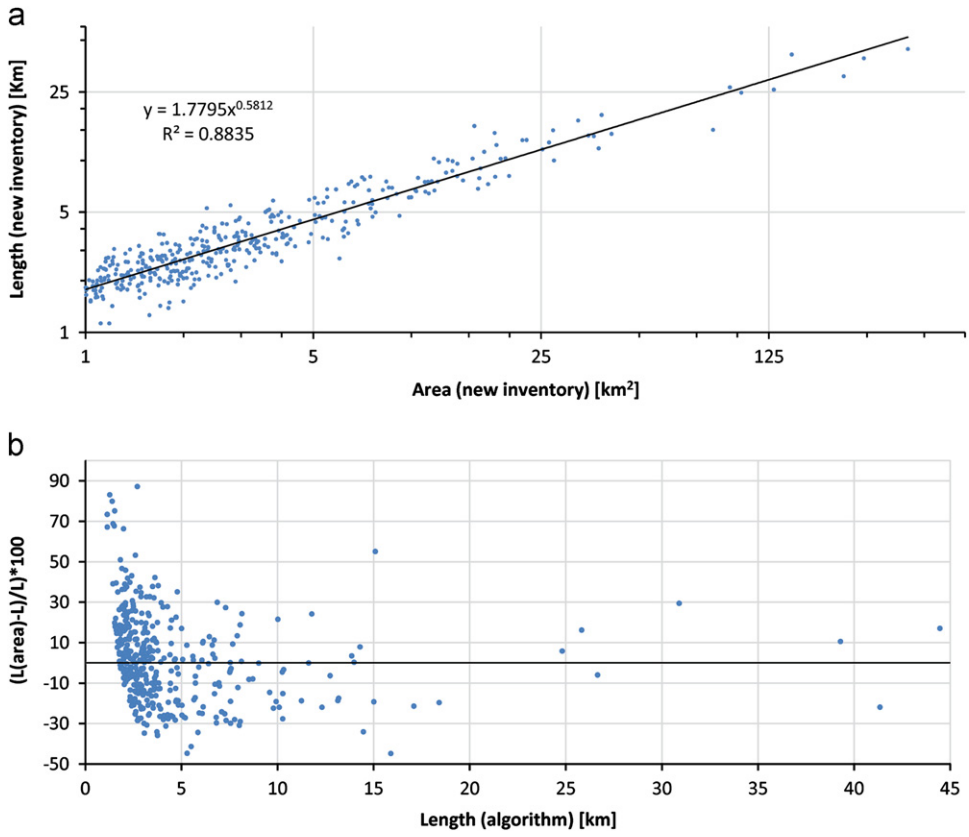

Fig. 7. (a) Log–log plot of glacier length vs. glacier area for a subset of the new Alaskan glacier inventory. (b) Relative differences of length as estimated from glacier area ($Length_{area}$) and length estimated from the algorithm ($Length_{FLA}$) vs. $Length_{FLA}$.

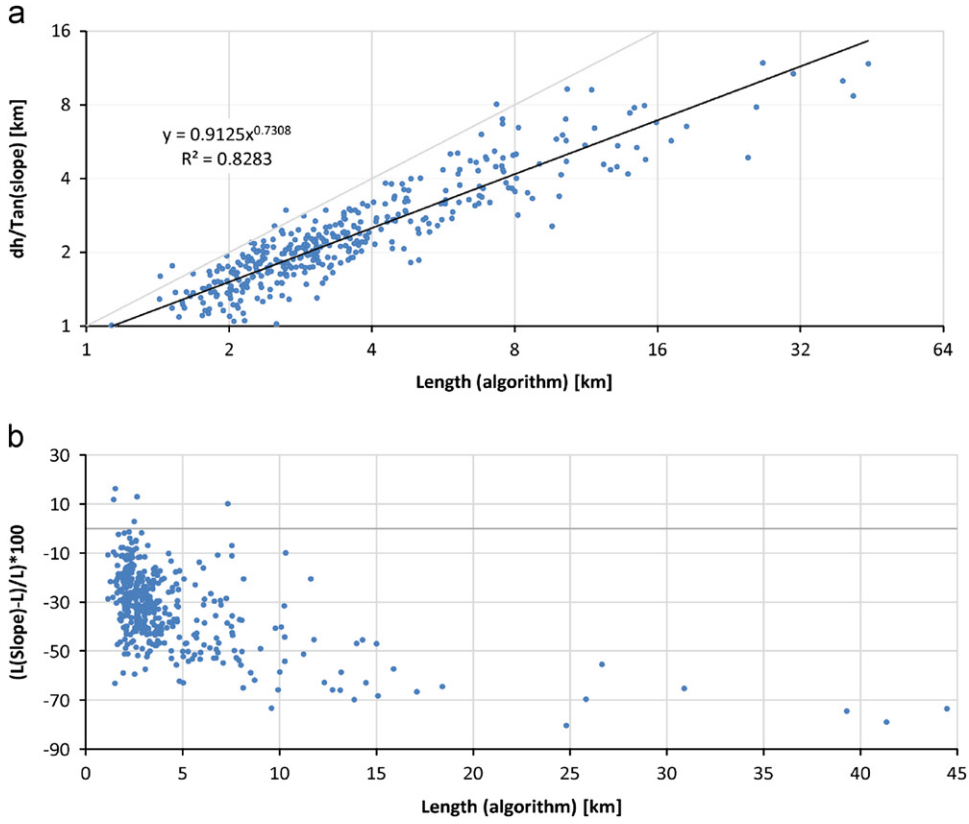

Fig. 8. (a) Glacier length as derived from elevation range and mean slope ($Length_{slope}$) vs. $Length_{FLA}$. (b) Relative differences of $Length_{slope}$ and $Length_{FLA}$ vs. $Length_{FLA}$.

Please cite this article as: Le Bris, R., Paul, F., An automatic method to create flow lines for determination of glacier length: A pilot study with Alaskan glaciers. Computers & Geosciences (2012), http://dx.doi.org/10.1016/j.cageo.2012.10.014

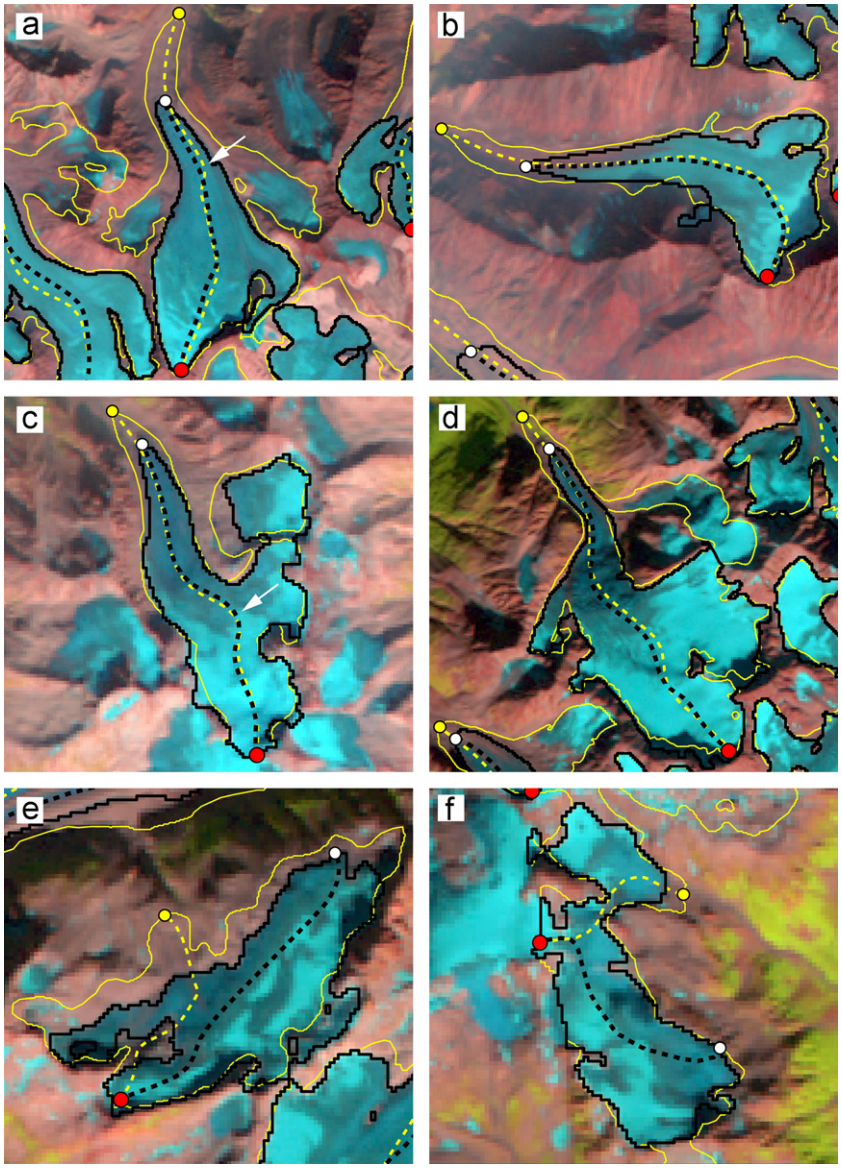

Fig. 9. Comparison of length change assessments. Images from (a)–(d) show examples with good agreement, whereas (e) and (f) are cases providing wrong results. Dotted lines in black refer to flow lines computed from the new Alaskan glacier inventory, and yellow lines (also dotted) are computed from the DLG outlines. White arrows in (a) and (c) indicate where glacier tributaries influence the shape of the lines. False color composite images (TM bands 543 as RGB) are displayed in the background.

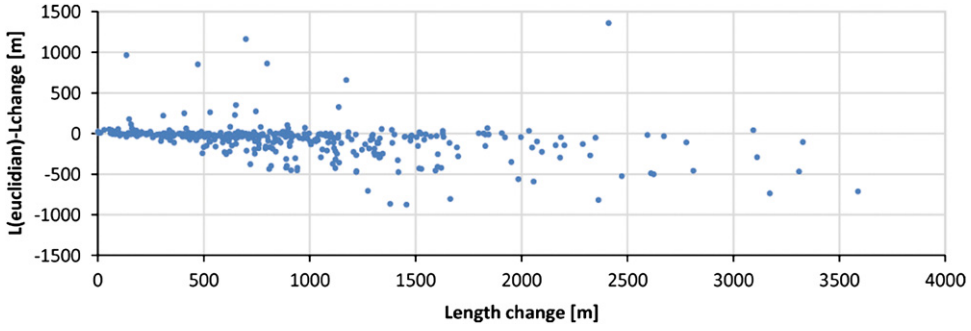

Fig. 10. A scatter plot illustrating the difference between the Euclidian distance of the two terminus position and their distance as derived from the respective segment of the FLA vs. length change.

computed from segments that are located in the middle of every glacier "slice" (see white arrows on Fig. 9a and c). Though this effect changes the shape of the line slightly, it has no significant influence on the total length.

6.2. Comparison with manual approaches

Manual digitizing is considered as being the most accurate approach to create flow lines. However, the overlay in Fig. 4 and

Please cite this article as: Le Bris, R., Paul, F., An automatic method to create flow lines for determination of glacier length: A pilot study with Alaskan glaciers. Computers & Geosciences (2012), http://dx.doi.org/10.1016/j.cageo.2012.10.014

the direct comparison of length values in Fig. 7 reveals that this is not really the case. For example, the digitized flow lines for a comparably simple shaped glacier depicted in Fig. 8b, reveals a rather high variability (between −7 and +19%) which is actually the largest for any of the 20 glaciers analyzed here. The length values of the FLA are only in 3 out of 20 cases outside the range of the manual digitizations and in these cases the algorithm failed because of very complex glacier geometry or due to the limitations of the method. On the other hand, the outliers stress the importance of a having a visual inspection of all flow lines generated by the FLA and applying a manual correction where required. To obtain comparable results, it is mandatory to provide starting and end points of the flow line. The clear drawbacks of the manual digitizations are the time consuming work for a large number of glaciers, the inconsistency of the digitization, and the point that the work needs to be repeated for other inventories (either past or future).

6.3. Computed length values and length changes

Comparing two glacier datasets from different sources is not straightforward, because the datasets could have been obtained from different techniques or methods (i.e. using remote sensing satellite data, airborne photographs, maps, automatic or manual digitizing) resulting in large potential mismatches. For example, even if the two datasets result from Landsat scenes, snow cover and cloud conditions could lead to differences in interpretation of the outline and hence to different flow lines. As many glaciers have experienced strong changes in their geometry in response to climate forcing during the past decades, it might be required to shift a former flow line to a different part of a glacier. In the case of a period dominated by glacier retreat, tributary glaciers might have been separated, or rock outcrops might have appeared somewhere on the glacier (e.g. Paul et al., 2007). Indeed, as the FLA is based on DEMs, a change in surface topography will also affect the resulting vector lines (e.g. when artefacts are present in the accumulation region of DEMs derived from optical sensors). However, the resulting changes in flow line position are small compared to changes resulting from changes of the outline.

7. Conclusions

This study presented a new and automated method called FLA to create glacier flow lines from only two input datasets (glacier outlines and DEM). The algorithm is based on open source software using the GDAL-OGR library and Python scripting. It uses a two dimensional geometry concept (glacier axis) to identify a series of center points in each glacier that are connected to give the flow line. Difficult issues such as the requirement to not cross the outline or internal polygons (e.g. from rock outcrops) are solved by the algorithm. The highest points as computed from the DEM and the outlines require, however, visual control and possibly correction. This is particularly important when glacier outlines from two inventories are used to perform change assessment.

We have created about 400 glacier flow lines for two points in time using the outlines from the DLG and a new inventory. Length changes were calculated for 388 common glaciers, indicating a weak dependence of length changes on original glacier length. The Euclidian distance between the two terminus positions gives values that are too small in most cases, and strong deviations point to glaciers that require visual control. A manual digitizing experiment revealed good visual agreement with the FLA computed flow lines and a quantitative comparison of the length values showed that for most of the cases they are within the variability of the values derived from the manual digitization. Comparison with length values derived from glacier area or simple topographic modeling (elevation range and slope) revealed statistically much poorer results. However, some manual intervention remains (e.g. shifting starting points, editing obviously wrong flow lines) necessary to create a high quality product. In any case, we conclude that automated computation with the FLA is very good alternative to a full manual digitization when it comes to large glacier samples and repeat application.

Acknowledgments

This study was performed in the framework of the ESA GlobGlacier project (21088/07/I-EC) and was partly also supported by the ESA Glaciers_cci project (4000101778/10/I-AM). Landsat scenes, DLG outlines, DRG maps and the DEM NED were obtained from the USGS (http://glovis.usgs.gov and http://seamless.usgs.gov). The ASTER GDEM is a product of Japan's Ministry of Economy, Trade and Industry (METI) and NASA and was downloaded from http://www.gdem.aster.ersdac.or.jp. We thank H. Frey for his help with the digitizing experiment and the two reviewers I. Evans and P. Leclercq for their very detailed and constructive comments.

References

Arendt, A., et al., 2012. Randolph Glacier Inventory [v1.0]: A dataset of global glacier outlines. Global Land Ice Measurements from Space, Boulder Colorado, USA. Digital Media.

Bahr, D.B., 1997. Width and length scaling of glaciers. Journal of Glaciology 43 (145), 557–562.

Bodansky, E., Gribov, A., Pilouk, M., 2002. Smoothing and compression of lines obtained by raster-to-vector conversion. Graphics Recognition Algorithms and Applications, 256–265.

Bolch, T., Menounos, B., Wheate, R., 2010. Landsat-based inventory of glaciers in western Canada, 1985–2005. Remote Sensing of Environment 114 (1), 127–137.

Citterio, M., Paul, F., Ahlstrøm, A.P., Jepsen, H.F., Weidick, A., 2009. Remote sensing of glacier change in West Greenland: accounting for the occurrence of surge-type glaciers. Annals of Glaciology 50 (53), 70–80.

De Berg, M., Cheong, O., Van Kreveld, M., 2008. Computational Geometry: Algorithms and Applications. Springer-Verlag, New York, Inc.

Denton, G.H., Field, W.O., 1975. Glaciers of the Alaska range. Mountain glaciers of the northern hemisphere. US Army Corps of Engineers 2, 573–620.

GCOS, 2003. Second Report on the Adequacy of the Global Observing Systems for Climate in Support of the UNFCCC. GCOS 82, WMO-TD/No. 1143.

Gesch, D.B., 2007. The National Elevation Dataset. The DEM user's manual. Second edition. American Society for Photogrammetry and Remote Sensing, Bethesda, Maryland, USA, 99–118 (Chapter 4).

Glasser, N.F., Harrison, S., Jansson, K.N., Anderson, K., Cowley, A., 2011. Global sea-level contribution from the Patagonian Icefields since the Little Ice Age maximum. Nature Geoscience 4 (5), 303–307.

Haeberli, W., Hoelzle, M., 1995. Application of inventory data for estimating characteristics of and regional climate-change effects on mountain glaciers: a pilot study with the European Alps. Annals of Glaciology 21, 206–212.

Hall, D.K., Bayr, K.J., Schöner, W., Bindschadler, R.A., Chien, J.Y.L., 2003. Consideration of the errors inherent in mapping historical glacier positions in Austria from the ground and space (1893–2001). Remote Sensing of Environment 86 (4), 566–577.

Hoelzle, M., Haeberli, W., Dischl, M., Peschke, W., 2003. Secular glacier mass balances derived from cumulative glacier length changes. Global and Planetary Change 36 (4), 295–306.

Klok, E.J., Oerlemans, J., 2004. Climate reconstructions derived from global glacier length records. Arctic, Antarctic, and Alpine Research 36 (4), 575–583.

Le Bris, R., Paul, F., Frey, H., Bolch, T., 2011. A new satellite derived glacier inventory for Western Alaska. Annals of Glaciology 52 (59), 135–143.

Leclercq, P.W., Oerlemans, J., 2011. Global and hemispheric temperature reconstruction from glacier length fluctuations. Climate Dynamics 38 (2012), 1065–1079.

Leclercq, P., Oerlemans, J., Cogley, J., 2011. Estimating the Glacier Contribution to Sea-Level Rise for the Period 1800–2005. Surveys in Geophysics 32 (4), 519–535.

Lemke, P., et al., 2007. Observations: changes in snow, ice and frozen ground. Climate Change, 337–383.

Please cite this article as: Le Bris, R., Paul, F., An automatic method to create flow lines for determination of glacier length: A pilot study with Alaskan glaciers. Computers & Geosciences (2012), http://dx.doi.org/10.1016/j.cageo.2012.10.014

Lüthi, M.P., Bauder, A., Funk, M., 2010. Volume change reconstruction of Swiss glaciers from length change data. Journal of Geophysical Research 115, F04022.

Lopez, P., Chevallier, P., Favier, V., Pouyaud, B., Ordenes, F., Oerlemans, J., 2010. A regional view of fluctuations in glacier length in southern South America. Global and Planetary Change 71, 85–108.

Manolopoulos, Y., Nanopoulos, A., Papadopoulos, A.N., Theodoridis, Y., 2005. R-Trees: Theory and Applications, Advanced Information and Knowledge Processing Series. Springer 195 pp.

Moore, A.W., 1991. An introductory tutorial on kd-trees. Computer Laboratory. University of Cambridge 20 pp.

Müller, F., Caflisch, T., Müller, G. (Eds.), 1977. Temporal Technical Secretariat for the World Glacier Inventory (TTS/WGI), ETH Zurich, Switzerland.

Nussbaumer, S.U., Zumbühl, H.J., 2011. The Little Ice Age history of the Glacier des Bossons (Mont Blanc massif, France): a new high-resolution glacier length curve based on historical documents. Climatic Change, 1–34.

Oerlemans, J., 2001. Glaciers and Climate Change. A.A. Balkema Publishers, 148 pp. ISBN 9026518137.

Oerlemans, J., 2005. Extracting a climate signal from 169 glacier records. Science 308 (5722), 675–677.

Oerlemans, J., Dyurgerov, M., van de Wal, R.S.W., 2007. Reconstructing the glacier contribution to sea-level rise back to 1850. The Cryosphere 1 (1), 59–65.

Oerlemans, J., 2008. Minimal Glacier Models. Igitur, Utrecht Publishing & Archiving Services, Universiteitsbibliotheek Utrecht, 90pp.

Paul, F., Kääb, A., Haeberli, W., 2007. Recent glacier changes in the Alps observed by satellite: consequences for future monitoring strategies. Global and Planetary Change 56 (1–2), 111–122.

Paul, F., et al., 2009. Recommendations for the compilation of glacier inventory data from digital sources. Annals of Glaciology 50 (53), 119–126.

Paul, F., Frey, H., Le Bris, R., 2011. A new glacier inventory for the European Alps from Landsat TM scenes of 2003: challenges and results. Annals of Glaciology 52 (59), 144–152.

Quinn, P., Beven, K., Chevallier, P., Planchon, O., 1991. The prediction of hillslope flow paths for distributed hydrological modeling using digital terrain models. Hydrological Processes 5 (1), 59–79.

Racoviteanu, A.E., Paul, F., Raup, B., Khalsa, S.J.S., Armstrong, R., 2009. Challenges and recommendations in mapping of glacier parameters from space: results of the 2008 Global Land Ice Measurements from Space (GLIMS) workshop, Boulder, Colorado, USA. Annals of Glaciology 50 (53), 53–69.

Raup, B., et al., 2007. Remote sensing and GIS technology in the Global Land Ice Measurements from Space (GLIMS) project. Computers & Geosciences 33 (1), 104–125.

Tsaparas, P., 1999. Nearest Neighbor Search in Multidimensional Spaces: Depth Oral Report, University of Toronto, Department of Computer Science, 53pp.

WGMS, 2008. Global Glacier Changes: Facts and Figures. Geneva: UNEP/WGMS, 45pp.

WGMS, 2009. In: Haeberli, W., Gärtner-Roer, I., Hoelzle, M., Paul, F., Zemp, M. (Eds.), Glacier Mass Balance Bulletin No. 10 (2006–2007). ICSU(WDS)/IUGG IACS)/UNEP/UNESCO/WMO, World Glacier Monitoring Service, Zürich.

Please cite this article as: Le Bris, R., Paul, F., An automatic method to create flow lines for determination of glacier length: A pilot study with Alaskan glaciers. Computers & Geosciences (2012), http://dx.doi.org/10.1016/j.cageo.2012.10.014

Paper III

Le Bris, R., Paul, F., 2012. *Glacier-specific elevation changes in western Alaska*. Annals of Glaciology *(submitted)*.

Glacier-specific elevation changes in western Alaska

R. Le Bris, F. Paul
Department of Geography, University of Zurich,
Winterthurerstrasse 190, CH-8057 Zurich, Switzerland
E-mail: rlebris@geo.uzh.ch

Submitted to Annals of Glaciology

ABSTRACT
Glaciers in Alaska strongly contribute to global sea-level rise. This contribution is best estimated by differencing digital elevation models (DEMs) from two points in time and converting the volume change to mass change, as the representativeness of the two glaciers with long-term mass balance measurements (Gulkana and Wolverine) for the entire region is not well known. Here we present the results of a glacier-specific assessment of elevation changes from c. 1962 to 2006 for 3100 glaciers in western Alaska that allows us to exclude calving glaciers (marine and lacustrine) from the sample and determine the representativeness of the two mass balance glaciers for the entire region and the land-terminating glaciers separately. Mean elevation changes for land-terminating, lake terminating and tide-water glaciers are -0.23 ±0.44 m yr^{-1}, -0.63 ±0.40 m yr^{-1} and -0.64 ±0.66 m yr^{-1}, respectively and -0.7 m yr^{-1} and -0.6 m yr^{-1} for the two benchmark glaciers. Their values do thus much better represent the calving glaciers and the overall mean (-0.63 ±1.14 m yr^{-1}) than the change of the land-terminating glaciers.

1. INTRODUCTION

Meltwater from glaciers in Alaska has already made a substantial contribution to sea-level rise in the past decades (Arendt *et al.* 2006; Forster *et al.* 2006; VanLooy *et al.* 2006; Berthier *et al.* 2010) and will likely continue to do so in the future (e.g. Radić and Hock 2010), assuming further increasing temperatures. However, the determination of the past contribution from all glaciers in Alaska is challenging, as the representativeness of the two glaciers with long-term mass balance measurements (Gulkana and Wolverine) for the entire region was not well known (Cogley 2005; Kaser *et al.* 2006). A simple extrapolation might not work as these glaciers are comparably small and cover a different elevation range than the large valley glaciers with low-lying tongues that essentially contribute to sea-level rise.

Shorter time-series of elevation changes for a selection of the largest glaciers are available from repeat laser profiling (e.g. Echelmeyer *et al.* 1996), but spatial extrapolation to the entire glacier is challenging (e.g. Arendt *et al.* 2002), might be biased (Berthier *et al.* 2010), and does not provide the overall changes. This shorcoming can be overcome by differencing two digital elevation models (DEMs) of sufficient accuracy and temporal separation (a few decades), and masking the changes with glacier extents (Forster *et al.* 2006; e.g. VanLooy *et al.* 2006; Paul and Haeberli 2008; Bolch *et al.* 2010). Nonetheless, for glaciers in Alaska it is also required to discriminate glaciers according to their type as many huge glaciers are of tide-water type or lake calving and a

substantial part of the volume change is thus due to glacier dynamics rather than surface mass balance (Pfeffer *et al.* 2008).

Hence, to properly determine the representativeness of the measured mass balance glaciers for the entire region, lake calving and tide-water glaciers need to be treated separately from the sample and the changes of the individual glaciers have to be assessed. This can be achieved by intersecting the drainage divides between individual glaciers as derived for the recently created glacier inventory for western Alaska (Le Bris *et al.* 2011) with the DEM differences calculated earlier (Schiefer *et al.* 2008; Berthier *et al.* 2010) and a separate assignment of calving and tidewater glaciers.

In this study we apply the above technique to a sample of 3180 glaciers in western Alaska to determine the representativeness of the two glaciers with long-term mass balance measurements (Gulkana and Wolverine) for this region. Special emphasis is given to the way of averaging mean elevation changes (per glacier or for the entire region) and the consideration of DEM artefacts (which might be reduced over low-contrast regions like snow and shadow) for calculating the mean values.

2. STUDY REGION, DATA SOURCES AND PROCESSING

Study region

The study region is located in the western Alaska Range including the Tordrillo, Chigmit, Katmai, and Chugach Mountains as well as the Kenai Peninsula. All types of glaciers are present in this region, from cirques to mountain and valley glaciers to iceclad-volcanos and ice caps. Few (36) but large glaciers are of calving or tidewater type (e.g. Columbia, with an area of 945 km^2). The recent glacier inventory of western Alaska includes more than 8800 glaciers larger than 0.02 km^2 covering a total area of 16 250 km^2, which is between 18% and 20% of the glacierized area of Alaska and neighboring Canada according to Cogley (2005) and Arendt and others (2002), respectively. Only 0.4% of the glaciers are larger than 100 km^2 but they account for 47% of the total area. Glaciers stretch from sea-level up to 4000 m a.s.l. and the large variability of mean elevations implies a significant decrease of precipitation from the coast towards the interior of Alaska (Le Bris *et al.* 2011).

Data and pre-processing

The glacier outlines used here are a subset of the Digital Line Graph (DLG) for Alaska. This vector dataset was compiled by the U.S. Geological Survey (USGS) by either manual or automated digitizing (USGS, 1988a) based on large-scale 7.5-minute topographic quadrangle maps (1:25,000 and 1:63,360 scales for Alaska). For quality control of the DLG outlines we compared them to the Digital Raster Graphic (DRG), which is a high-resolution scan of published paper maps (http://topomaps.usgs.gov/drg). This overlay revealed a systematic planimetric shift between the DLG and the DRG which might be due to effects of the georeferencing process. Furthermore, some outline mismatches (especially in the ablation part of glaciers) have been observed. We thus adjusted the displacement and manually edited a subset of the DLG glacier outlines (350 glaciers) according to the DRG maps (see S2).

The USGS National Elevation Dataset (NED) is a DEM derived from contour lines as given on the topographic maps from the 1950s (Gesch *et al.* 2009) and is used as the base for calculating elevation changes. For Alaska, the NED DEM is available at 2-arc-second postings (approximately 60 m). The absolute vertical accuracy of the quadrangle-based USGS 7.5-minute DEMs is reported to be 7 m (USGS, 1997). This product can be downloaded through the USGS Seamless Server (http://seamless.usgs.gov). We also used the Advanced Space-borne Thermal Emission and Reflection Radiometer (ASTER) global DEM (GDEM) that was compiled from all available stereo-pair images in the ASTER archive acquired between 2000 and 2007. The ASTER GDEM has a spatial resolution of 30 m (Hayakawa *et al.* 2008) and a vertical accuracy of about 7 to14 m (StDev) (ASTER 2009).

The elevation changes from 1962-2006 ($\Delta h/\Delta t$ raster maps) used here to determine glacier specific values were derived by Berthier and others (2010) and are based on the subtraction of two DEMs. The older one is the USGS NED and the more recent DEM was derived from the High Resolution Stereoscopic (HRS) sensor on-board SPOT 5 (Bouillon *et al.* 2006) and created within the framework of the International Polar Year (IPY) project SPIRIT descried by (Korona *et al.* 2009). This DEM has a 40 m cell size, a horizontal (geolocation) accuracy of 30 m, and a vertical accuracy between -5.5 and 3.5 m (compared to ICESat). Nonetheless, an elevation uncertainty of ±10 m is assumed over the entire studied area.

Individual glacier extents were derived by digital intersection with drainage divides from hydrological computations (watershed analysis) using the NED DEM and GIS tools following the approach by Bolch and others (2010). Hillshades from the DEM were created to visually check quality and artefacts.

3. METHODS

Due to data voids covering more than 20% of the area in the $\Delta h/\Delta t$ raster maps for the two mass balance glaciers (Gulkana and Wolverine) we had to determine elevation changes specifically for those two glaciers by differencing the NED DEM and the ASTER GDEM. To ease calculations, all elevation data sets were mosaiced into a single file. Mean elevation changes per glacier were calculated using zone statistics in the GIS software and divided by the number of years between the two DEMs to obtain comparable annual elevation change rates. Topographic map dates have an uncertainty of ±3.5 years which results in a total error of ±2.5 m (Arendt *et al.* 2006; Berthier *et al.* 2010).

As a first step of the statistical analysis, glaciers smaller than 0.05 m^2 and/or covered by more than 20% of their area by data voids are excluded. In a second step three types of glaciers are distinguished and marked in the attribute table: 0: land terminating, 1: lake terminating and 2: tide-water glaciers. Outside of data voids DEM artefacts can occur in areas of low contrast (e.g snow and steep slopes) and result in positive elevation changes (i.e mass gain). To reduce the influence of regions with positive changes, we further calculated mean changes from three different methods: (1) for the ablation areas only (regions below the mean elevation), (2) setting all positive elevation changes to 'no data', and (3) setting them to 0. Of course, in this region it is also possible that glaciers have

grown in their accumulation regions since the 1960s. But such an increase would result in a more homogenous spatial pattern of the changes () and is not compliant with the long-term mass balance measurements in the region. Mean values for the different samples were finally calculated from two methods of statistical averaging: (i) one mean value for the entire study region to determine the overall changes, and (ii) the arithmetic mean of all individual mean elevation change values. Due to the different cell sizes of the DEMs subtracted (30, 40 and 60 m), resampling effects and elevation dependent biases might occur in the difference grid (Svoboda and Paul 2010) that can be corrected by considering the maximum terrain curvature (Gardelle *et al.* 2012). However, we have not found any systematic elevation changes for terrain outside of glaciers (Fig. S1) and thus not corrected it. This is likely due to the very similar level of detail in all three DEMs as seen in a visual comparion of hillshades.

4. RESULTS

Elevation changes

In total, elevation changes were calculated for about 3180 Alaskan glaciers. The general tendency of glacier volume loss found here confirms earlier studies (e.g. Arendt *et al.* 2002; Berthier *et al.* 2010). Figure 1 shows colour coded glacier-specific mean elevation change values for three subsections of the study area. In these regions several small to medium sized glaciers experience a net increase in elevation if the difference values are used as they are. In some cases it is well possible that they are real rather than stemming from (more local) inaccuracies of the DEMs as a more detailed analysis of the spatial pattern of the positive changes revealed. In the Chugach Mts., Columbia Glacier exhibits the strongest mean thinning rate of -2.8 m yr^{-1}. The mean changes (using method i) for the entire study region are: -0.67 ±0.76 m yr^{-1}, with a mean value of -0.42 ±0.35 m yr^{-1} for the land terminating glaciers, -0.58 ±0.87 m yr^{-1} for lake terminating glaciers and -1.81 ±2.24 m yr^{-1} with and -0.60 ±0.90 m yr^{-1} without Columbia Glacier for the tide-water glaciers. Furthermore, Fig. 1 shows a strong variability of elevation changes even for glaciers originating from the same mountain summit.

Table 1 reveals the differences of the mean changes in dependence of the method used for averaging (i or ii) or the consideration of positive elevation values. For example, in the case of glaciers of type 1 (lake terminating), the mean loss is -0.58 m yr^{-1} if all cells are considered but -1.03 m yr^{-1} when only the ablation area is taken into account (method 1). Considering the entire region, the more detailed analysis of the mean elevation change values revealed a large spatial variability that is neither related to glacier size, nor to mean slope, exposition, or mean elevation.

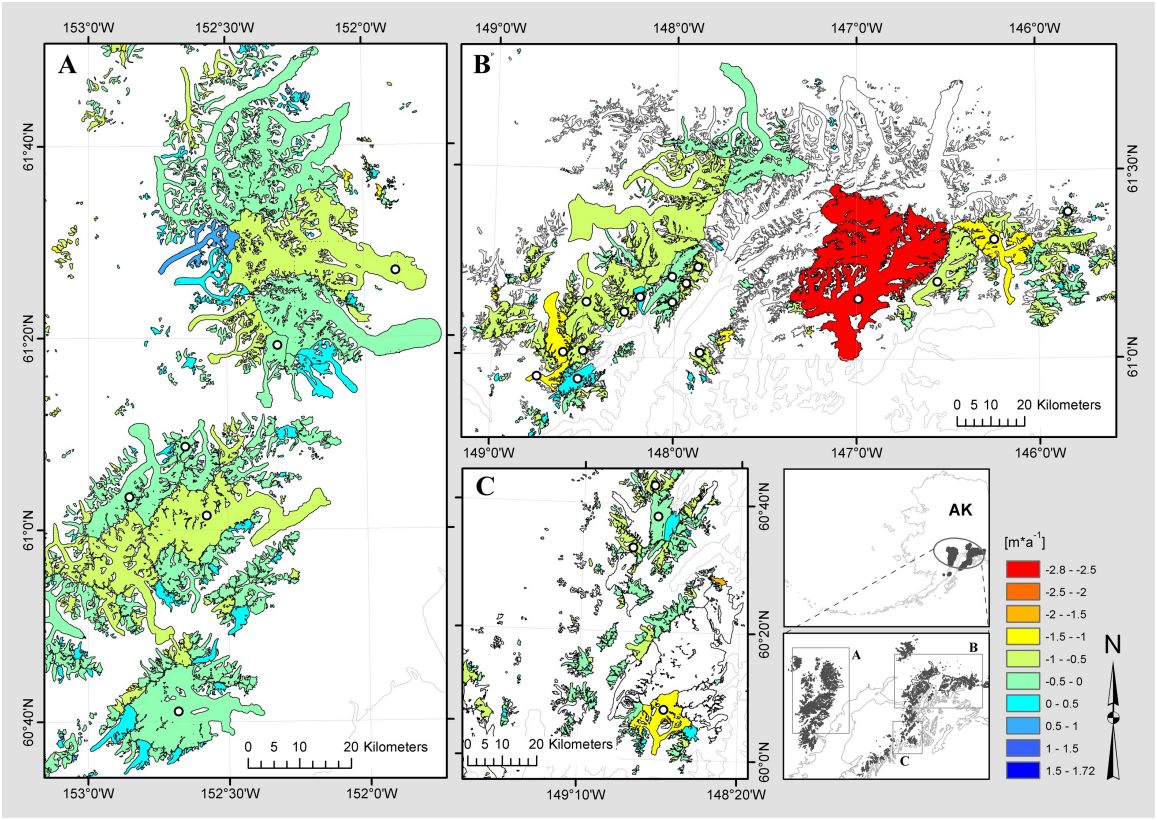

Fig.1. *Examples of specific mean elevation changes in (A) Tordrillo and Chigmit Mountains, (B) Chugach Mountains and (C) Kenai Peninsula. White dots indicate calving and tidewater glaciers. White glaciers represent those with more than 20% of data voids. Insets show the location of the mountains range in Alaska.*

Figure 2 illustrates the elevation changes averaged over 50 m elevation bins for the ten largest land terminating glaciers and the two benchmark glaciers Gulkana and Wolverine. For all glaciers the strongest elevation changes occurred at their lowest parts between 250 and 750 m.a.s.l. Between 1000 and 2000 m changes are rather similar for the largest glaciers, apart from Gulkana which has over large parts of its elevation range much stronger thickness losses than all other glaciers at this elevation. Towards higher elevations several glaciers show thickening (e.g. Caps glacier with up to 0.5 m a^{-1}) some show little change and some even increasing loss with altitude. However, some of these changes might be related to artefacts, implying that the values should not be over-interpreted.

In Fig. 3 seven glaciers illustrate the spatial distribution of elevation changes. Apart from Matanuska Glacier (D), all glaciers experienced moderate to strong elevation loss in the lower parts of their ablation areas, largely independent of their locations. For Gulkana (B), Wolverine (E) and in a less pronounced way also for Trimble glacier (F), surface lowering also occurred in the accumulation area. For Wolverine glacier the zone with elevation gain looks artificially constrained and might thus be due to DEM errors. Assuming that this region is indeed in error and setting it to no data, the mean elevation change decreases from -0.59 ±0.45 m yr^{-1} to -0.53 ±0.43 m yr^{-1}. Because we used the ASTER GDEM instead of the SPIRIT DEM for Wolverine and Gulkana glaciers, we compared both DEMs in regions of overlap to identify potential systematic differences on

stable terrain (Fig. S1). For flat terrain off-glaciers (with slopes less than 5°) the mean difference is 2.60 m (± 21.62 m), revealing that the GDEM can be used for our assessment (instead of the SPIRIT product).

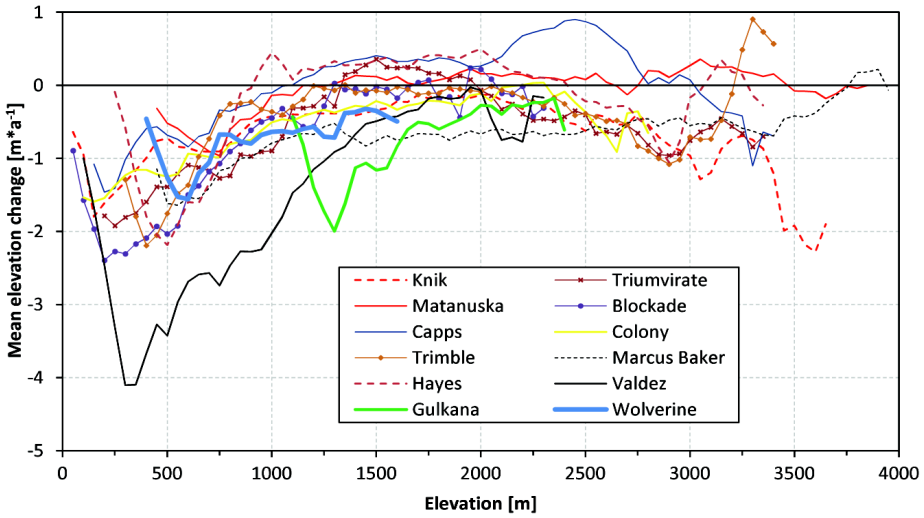

Fig.2. *Mean elevation changes with altitude for the 10 largest glaciers in 50 m elevation bins. Gulkana and Wolverine benchmark glaciers are also included.*

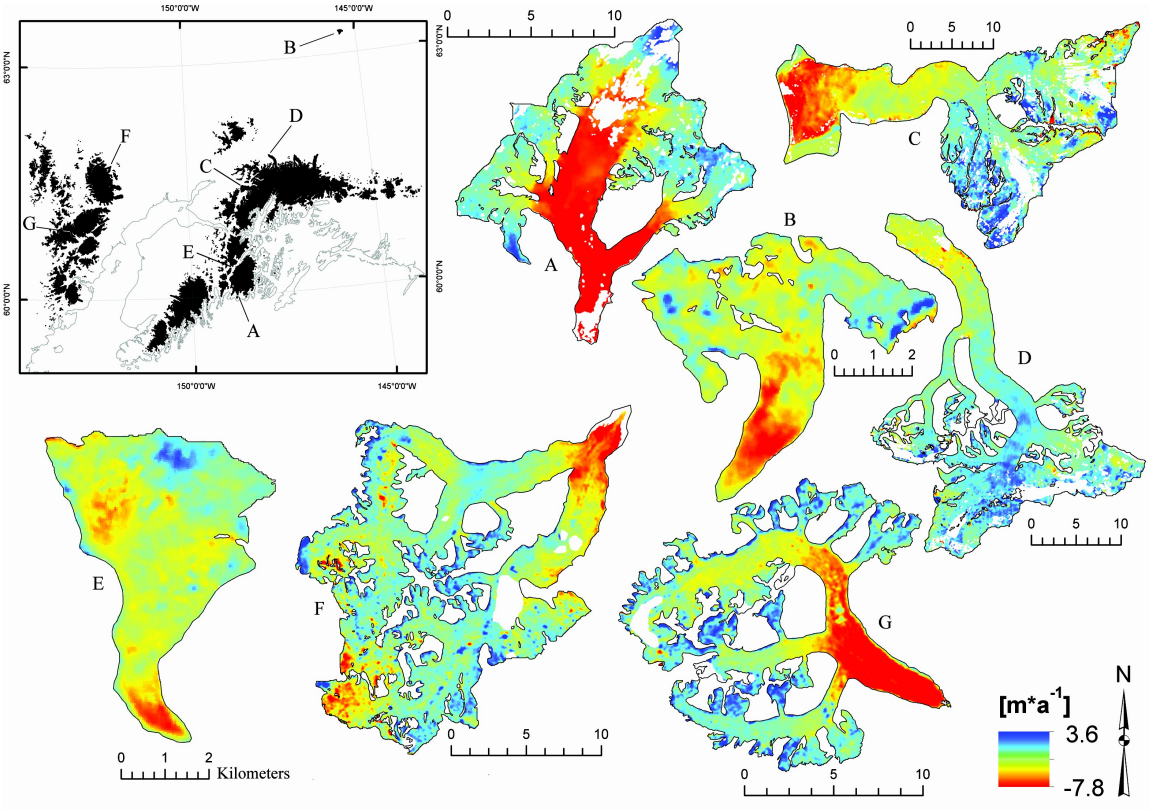

Fig.3. *Specific elevation changes for 7 glaciers. Glacier outlines correspond to the Digital Line Graph (DLG) inventory. White areas are no data. Inset shows location of the 7 glaciers. (A) Excelsior Glacier, (B) Gulkana Glacier, (C) Knik Glacier, (D) Matanuska Glacier, (E) Wolverine Glacier, (F) Trimble Glacier, (G) an unnamed glacier in the Chigmit Mts.*

Correction factors

When comparing the mean elevation changes of Gulkana and Wolverine glaciers (-0.7 and -0.6 m yr^{-1}) to the mean values of the three glacier types and the different ways of calculating them (Table 1), only the marine and lake terminating glaciers have similarly negative values (Fig. 4). The other land-terminating glaciers have much less negative mean values (-0.24 m yr^{-1}). In other words, extrapolating the mean elevation changes from the values measured at the two benchmark glaciers would overestimate the change of other land-terminating glaciers by a factor of 1/2.5 (for Wolverine) and 1/2.9 (for Gulkana). These ratios approximately hold for the three ways of excluding positive elevation changes in the calculation (see Table 1). On the other hand, the mean change of the two benchmark glaciers is very close to the mean of the entire region (including the calving ones and calculated with method i), i.e. their volume changes (an thus likely also their mass budgets) are indeed representative for the entire sample investigated. When the exceptionally strong elevation change of Columbia Glacier is excluded, the agreement is less good and uncorrected extrapolation would yield about 30% too negative mass budgets. However, these mean elevation rates should be interpreted prudently as they are not significantly different as indicated by the large standard deviations.

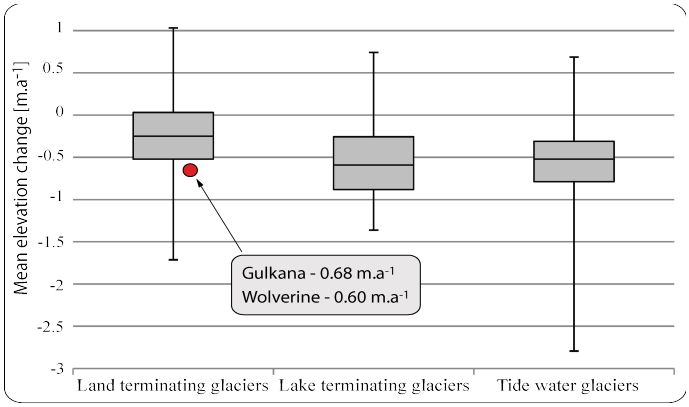

Fig.4. *Box plots show the mean elevation change per glacier types. Red dot shows values of the Gulkana and Wolverine glaciers.*

		Glacier type= 0		Glacier type= 1		Glacier type= 2		Gulkana	Wolverine
		n=1(i)	∑ glaciers(ii)	n=1(i)	∑ glaciers(ii)	n=1(i)	∑ glaciers(ii)		
Influence of artefacts	all cells	-0.420	-0.236	-0.582	-0.628	-1.809	-0.636	-0.677	-0.594
	1	-0.678	-0.330	-1.032	-1.036	-2.861	-0.936	-1.010	-0.761
	2	-0.687	-0.471	-0.896	-0.855	-2.120	-0.857	-0.781	-0.675
	3	-0.515	-0.368	-0.671	-0.698	-1.847	-0.697	-0.710	-0.617

Table 1. *Mean elevation change per glacier type calculated in two methods of statistical averaging: (i) the arithmetic mean of individual mean elevation change values, and (ii) one mean value for the entire study region. Lines 1 to 3 are the different ways of calculation that consider potential DEM's artefacts.*

5. DISCUSION

The large differences in the mean elevation changes of land-terminating vs. calving glaciers and the exclusion of Columbia Glacier from the sample demonstrated the importance of calculating glacier-specific changes for proper determination of climate change impacts. Though calculation of the sea-level contribution is important in itself (cf. Berthier *et al.*, 2010), this number cannot really be seen as a result of climate change when marine-terminating glaciers (with strongly decoupled dynamics) are largely responsible for the contribution. Moreover, glacier-specific values are also required to determine the representativeness of the reference glaciers for a larger region as shown by Paul and Haeberli (2008). As the measured glaciers are often comparably small and cover a different elevation range than the large valley glaciers (e.g. Fountain *et al.* 2009), differences could be large (as shown here) and related correction factors are required when using their values for upscaling. Interestingly, the two reference glaciers in this region are not representative for their type (land-terminating), but they are close to the mean for the entire region (method i and Columbia Glacier included). This finding is rather similar to the Alps, where the measured glaciers had partly also very negative values compared to other glaciers of the same size, but they represent the mean over the entire region nevertheless quite well as the (unmeasured) largest glaciers contribute most strongly to the overall change (Paul and Haeberli, 2008). The rough extrapolation scheme applied in the study by Kaser *et al.* (2006) (cf. also WGMS averaging) might thus have worked well for Alaska and maybe also for other regions (this remains to be shown).

Several uncertainties influence the quality of our results, among others: (a) the artefacts in the DEMs, (b) the unadjusted extent of most glaciers, (c) the use of the GDEM instead of the SPOT DEM for the two benchmark glaciers, and (d) uncorrected biases (e.g. due to different DEM resolutions). As we have already explained (c) and (d), some comments on (a) and (b) have to be made. To be reliable, the overall elevation changes should be larger than the accuracy of the two DEMs. This is certainly true for nearly all glaciers in the ablation region, but less so in the accumulation regions. Setting positive elevation changes to no data in this region is maybe the best way to exclude potentially wrong values from the analysis, as we cannot be sure whether they result from artefacts or represent real changes. In a very maritime climate such as in coastal Alaska it could be well possible that glaciers have increased in thickness in their accumulation region in a period of general retreat. Setting these positive values simply to zero might already introduce a bias, but as the mean values show (Table 1) the differences between the two methods of calculation are small.

To determine the influence of (b), we have corrected 350 glaciers according to the DRG and compared the mean mass budgets for the corrected and uncorrected extents (Fig. S2). This comparison revealed larger (non-systematic) deviations only for five glaciers, so that in the mean over the entire sample the influence of the missing correction is small. When the overall mass change is dominated by a few glaciers, the arithmetic mean of the individual values (method ii) gives indeed a much different mean value (less negative in this case). While the area-weighted values are important for the sea level contribution, the arithmetic mean better fits to the mean values of the direct measurements, as they are also arithmetically averaged. In any case, tidewater glaciers should be treated separately in related assessments. Further investigations of elevation changes vs. other glacier

parameters (i.e. size, mean elevation, elevation range, slope, and distance from the ocean) has not revealed any significant correlations (Fig. S3), indicating locally highly variable climatic regimes and glacier responses. Indeed, the large variability of elevation changes does not show any tendency neither with region nor glacier type. The reasons for the variability remain unexplained.

6. CONCLUSIONS

We have determined the representativeness of Gulkana and Wolverine glaciers for a large region in western Alaska using differencing of two DEMs from two points in time and the glacier outlines for a large part of western Alaska. The elevation changes were calculated for 3180 glaciers using two ways of statistical averaging, three ways to consider positive elevation changes in the accumulation area, and three types of glaciers. Glaciers with more than 20% of their area covered by data voids (in the $\Delta h/\Delta t$ raster maps) were excluded from the computations and over Gulkana and Wolverine Glaciers the ASTER GDEM was used to determine the changes.

Rates of elevation changes are -0.63 ±0.40 m yr^{-1} for both lake terminating and tide-water glaciers and -0.24 ±0.44 m yr^{-1} for land terminating glaciers. Thus, simple extrapolation of the mean elevation changes for Gulkana and Wolverine glaciers (-0.7 and -0.6 m yr^{-1}) would strongly overestimate the contribution from all other land-terminating glaciers and correction factors of 1/2.5 and 1/2.9 would be required, respectively. However, these two glaciers represent the mean value for other glacier types and the overall changes quite well, at least when Columbia Glacier is part of the sample (otherwise a 30% overestimation of mass loss would result). The simple extrapolation of the mass budgets from the two benchmark glaciers to the entire region as applied in previous studies might thus have worked rather well. The spatial variability across the study region can not easily be explained.

Acknowledgments
This study was funded by the ESA project Glaciers_cci (4000101778/10/I-AM) and the ice2sea programme from the European Union 7th Framework Programme, grant number 226375. Ice2sea contribution number 096. We thank Etienne Berthier for providing us with the mean elevation change raster maps of the study region.

REFERENCES

Arendt AA, Echelmeyer KA, Harrison WD, Lingle CS, Valentine VB (2002) Rapid Wastage of Alaska Glaciers and Their Contribution to Rising Sea Level. *Science* **297**(5580), 382–386.

Arendt A, Echelmeyer K, Harrison W, Lingle C, Zirnheld S, Valentine V, Ritchie B, Druckenmiller M (2006) Updated estimates of glacier volume changes in the western Chugach Mountains, Alaska, and a comparison of regional extrapolation methods. *J Geophys Res* **111**, .

ASTER G (2009) 'Validation Team. ASTER Global DEM Validation Summary Report.'

Berthier E, Schiefer E, Clarke GKC, Menounos B, Rémy F (2010) Contribution of Alaskan glaciers to sea-level rise derived from satellite imagery. *Nature Geoscience* **3**(2), 92–95.

Bolch T, Menounos B, Wheate R (2010) Landsat-based inventory of glaciers in western Canada, 1985-2005. *Remote Sensing of Environment* **114**(1), 127–137.

Bouillon A, Bernard M, Gigord P, Orsoni A, Rudowski V, Baudoin A (2006) SPOT 5 HRS geometric performances: Using block adjustment as a key issue to improve quality of DEM generation. *ISPRS Journal of Photogrammetry and Remote Sensing* **60**(3), 134–146.

Cogley JG (2005) Mass and Energy Balances of Glaciers and Ice Sheets. *Encyclopedia of Hydrological Sciencs Vol 4* 2555–2573.

Echelmeyer K, Harrison W, Larsen C, Sapiano J, Mitchell J, DeMallie J, Rabus B, Adalgeirsdottir G, Sombardier L (1996) Airborne surface profiling of glaciers: a case-study in Alaska. *Journal of Glaciology* **42**(142), 538–547.

Forster R, Ford ALJ, Bruhn R (2006) Surface elevation changes on the Bering Glacier, Alaska.

Fountain AG, Hoffman MJ, Granshaw F, Riedel J (2009) The'benchmark glacier'concept does it work? Lessons from the North Cascade Range, USA. *Annals of Glaciology* **50**(50), 163–168.

Gardelle J, Berthier E, Arnaud Y (2012) Impact of resolution and radar penetration on glacier elevation changes computed from DEM differencing. *Journal of Glaciology* **58**(208), 419.

Gesch D, Evans G, Mauck J, Hutchinson J, Carswell Jr WJ (2009) The National Map–Elevation. *US geological survey fact sheet* **3053**(4), .

Hayakawa YS, Oguchi T, Lin Z (2008) Comparison of new and existing global digital elevation models: ASTER G-DEM and SRTM-3. *Geophysical Research Letters* **35**(17), L17404.

Kaser G, Cogley JG, Dyurgerov MB, Meier MF, Ohmura A (2006) Mass balance of glaciers and ice caps: consensus estimates for 1961-2004. *Geophys Res Lett* **33**, 19.

Korona J, Berthier E, Bernard M, Rémy F, Thouvenot E (2009) SPIRIT. SPOT 5 stereoscopic survey of Polar Ice: reference images and topographies during the fourth International Polar Year (2007-2009). *ISPRS Journal of Photogrammetry and Remote Sensing* **64**(2), 204–212.

Le Bris R, Paul F, Frey H, Bolch T (2011) A new satellite-derived glacier inventory for western Alaska. *Annals of Glaciology* **52**(59), 135–143.

Paul F, Haeberli W (2008) Spatial variability of glacier elevation changes in the Swiss Alps obtained from two digital elevation models. *Geophysical Research Letters* **35**(21), L21502.

Pfeffer WT, Harper JT, O'Neel S (2008) Kinematic Constraints on Glacier Contributions to 21st-Century Sea-Level Rise. *Science* **321**(5894), 1340–1343.

Radić V, Hock R (2010) Regional and global volumes of glaciers derived from statistical upscaling of glacier inventory data. *Journal of Geophysical Research* **115**(F1), F01010 %U http://dx.doi.org/10.1029/2009JF001373.

Schiefer E, Menounos B, Wheate R (2008) An inventory and morphometric analysis of British Columbia glaciers, Canada. *Journal of Glaciology* **54**(186), 551–560.

Svoboda F, Paul F (2010) A new glacier inventory on southern Baffin Island, Canada, from ASTER data: I. Applied methods, challenges and solutions. *Annals of Glaciology* **50**, 11–21.

VanLooy J, Forster R, Ford A (2006) Accelerating thinning of Kenai Peninsula glaciers, Alaska. *Geophysical Research Letters* **33**(21), L21307.

U.S. Geological Survey, (1997) Part 1: General—Standards for digital elevation models, 11 p., URL: http://rockyweb.cr.usgs.gov/ nmpstds/acrodocs/dem/ 1DEM0897.PDF (last date accessed: 20 January 2006).

SUPPLEMENTARY MATERIAL

SM1 Uncertainties

Different potential sources of errors resulting from the variety of the input data used in this study needs to be taken into account. Uncertainties come mainly from elevation values of DEMs but also from glacier outlines. The date of topographic maps also account for a possible source of errors. As these errors are independent, they can be quadratically added yielding the overall uncertainty summarizes in equation (1):

$$\varepsilon = \pm\sqrt{a^2 + b^2 + c^2} \quad (1)$$

where (*a*) represents the error of mean elevation resulting from the corrected and uncorrected glacier outlines calculated as follow (2):

$$a = \frac{\pm\Delta h_{uncor} - \Delta h_{cor}}{\left(\frac{area_{uncor} + area_{cor}}{2}\right)} \quad (2)$$
$$= \pm 0.0003 \text{ m}$$

with Δh being the mean elevation.
Error (b) accounts for the sequential DEMs computation and includes vertical accuracies of NED DEM and SPOT5 DEM as described in (3):

$$b = \pm\sqrt{NED^2 + Spot5^2} \quad (3)$$
$$= \pm 5.9 \text{ m}$$

Since (a) is negligible and (c) equals ± 3.5 m (see above), ε is ± 4.9 m.

SM2 Figures

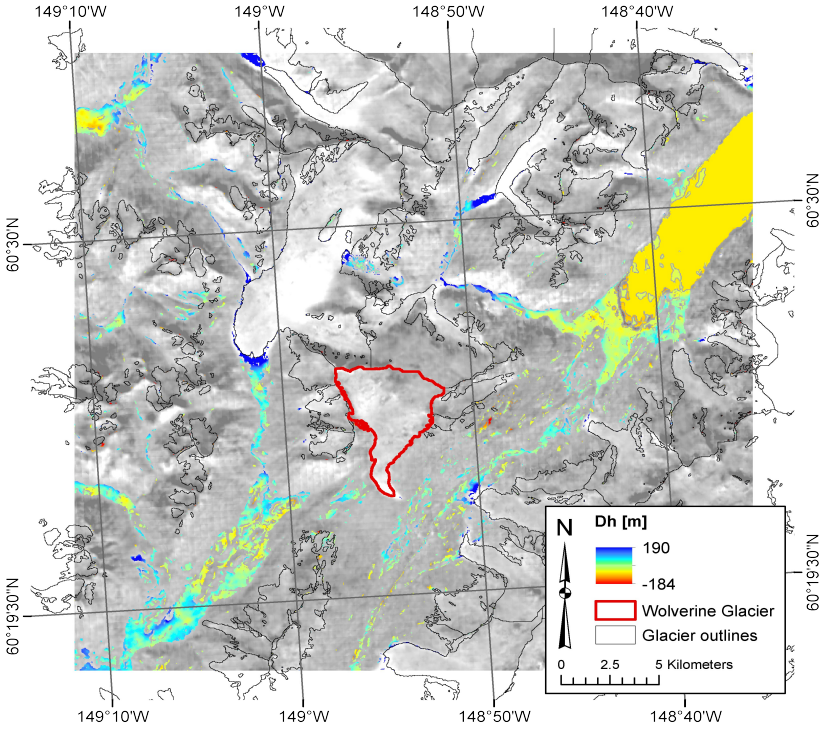

Fig.S1. *Elevation differences between NED and GDEM for flat terrain off-glaciers (with slopes less than 5°).*

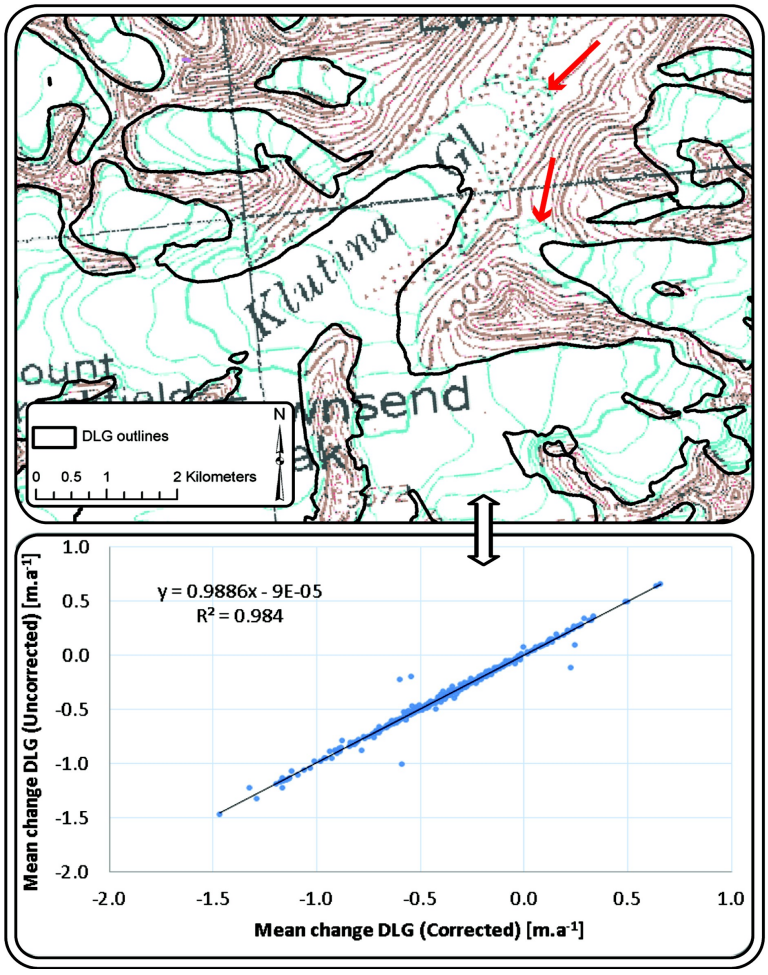

Fig.S2. *Elevation change for uncorrected DLG vs. corrected DLG glacier outlines. Red arrows on top of the picture show the glacier extents visible on the topographic map (DRG).*

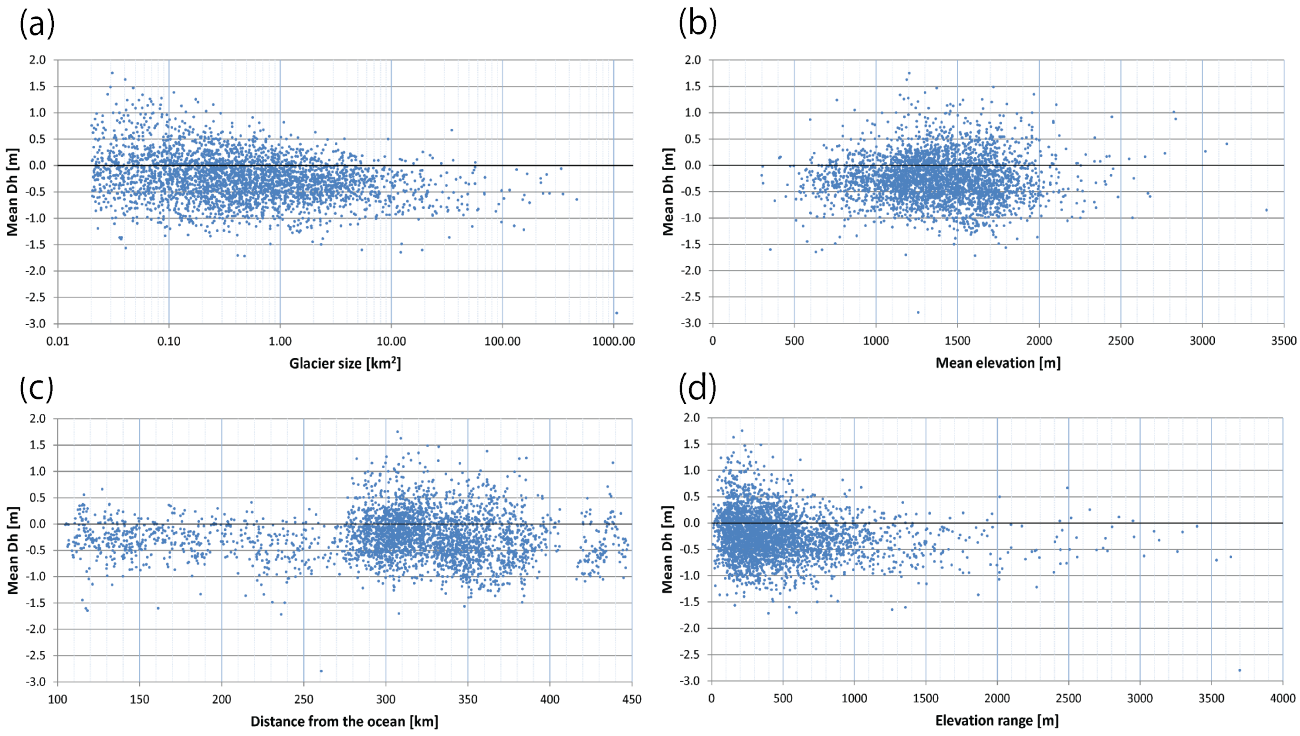

Fig.S3. *Elevation changes vs. others glacier parameters, respectively vs. glacier size (a), mean elevation (b), distance from the ocean (c) and elevation range (d).*

Part III

Appendix

A1: Quicklooks of all satellite scenes used in this study
A2: False Colour Composite
A3: Oblique views
A4: Steps of the watershed analysis
A5: Personal bibliography

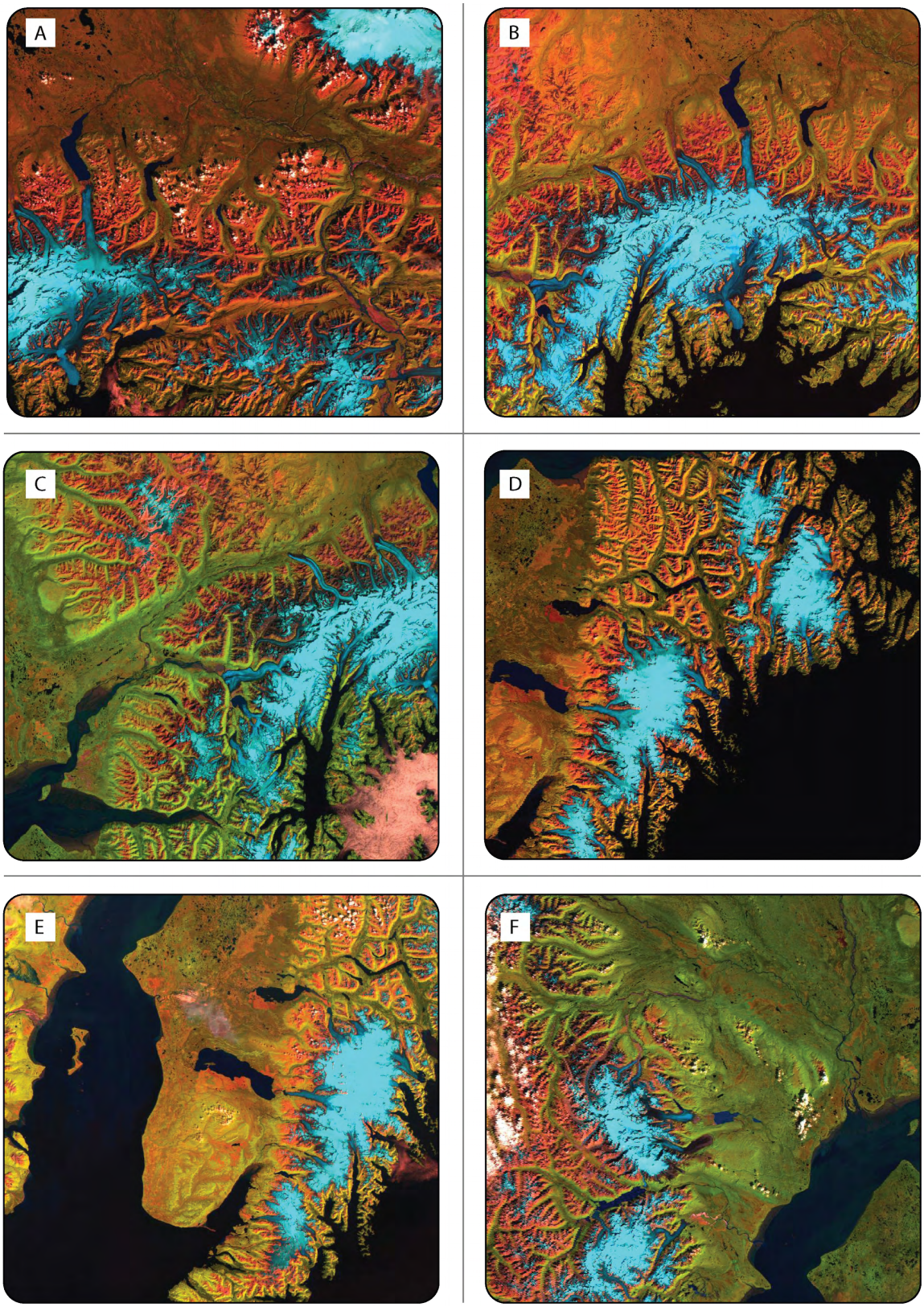
A
B
C
D
E
F

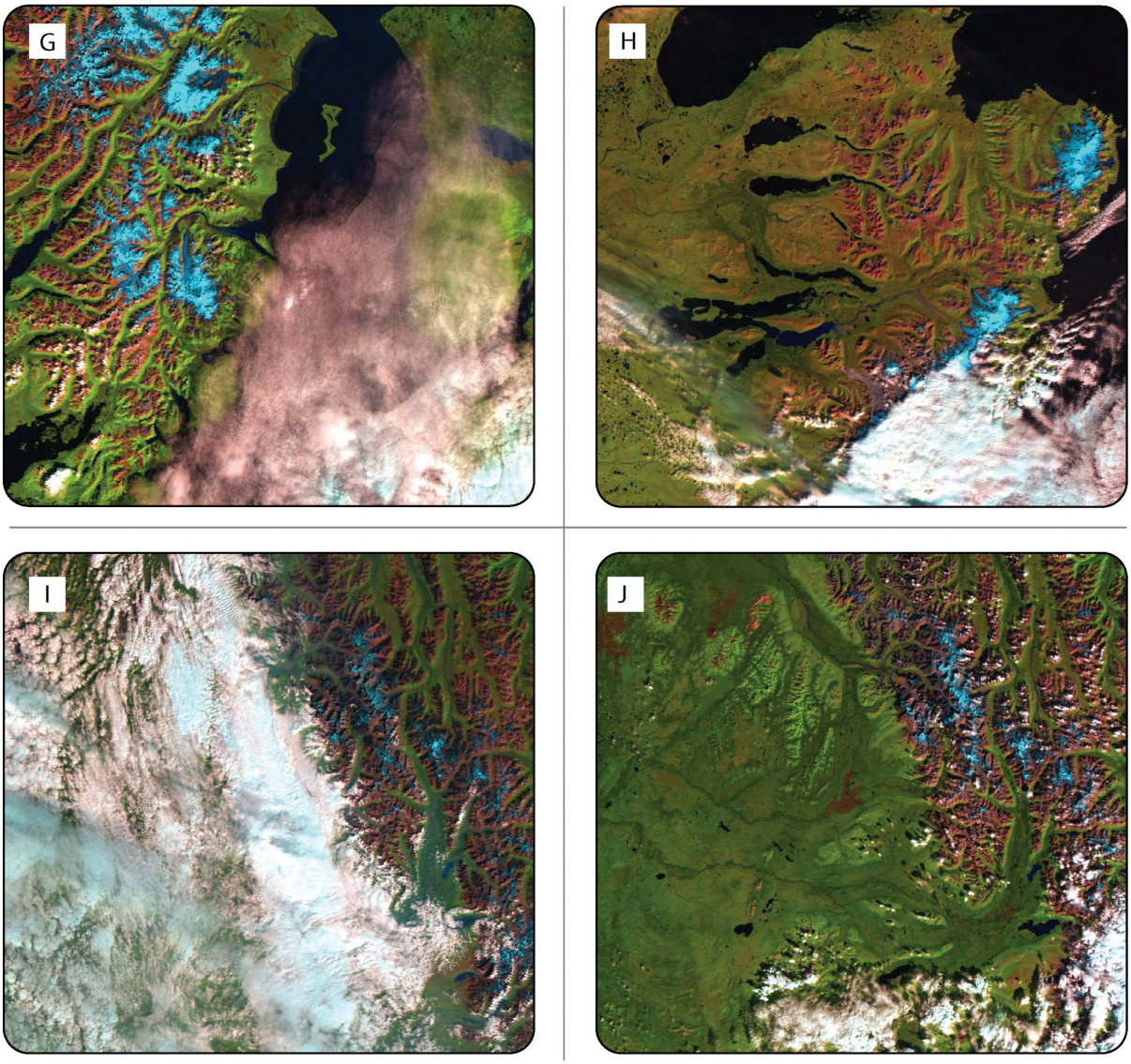

A1: Quicklooks of satellite scenes

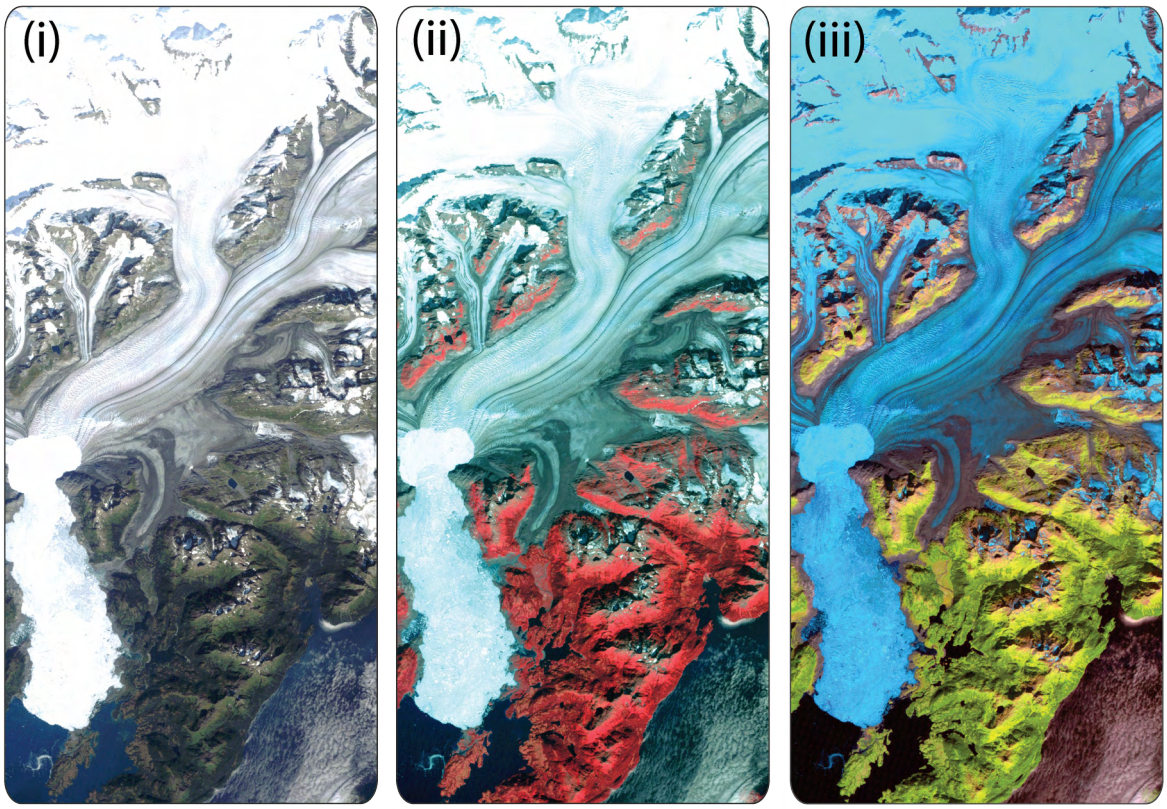

A2: False Colour Composite (FCC) of the eastern branch of the Columbia glacier (Chugach Mnts). (i), (ii) and (iii) are TM 3-2-1, TM 4-3-2 and TM 5-4-3 compositions as red, green and blue (RGB) respectively.

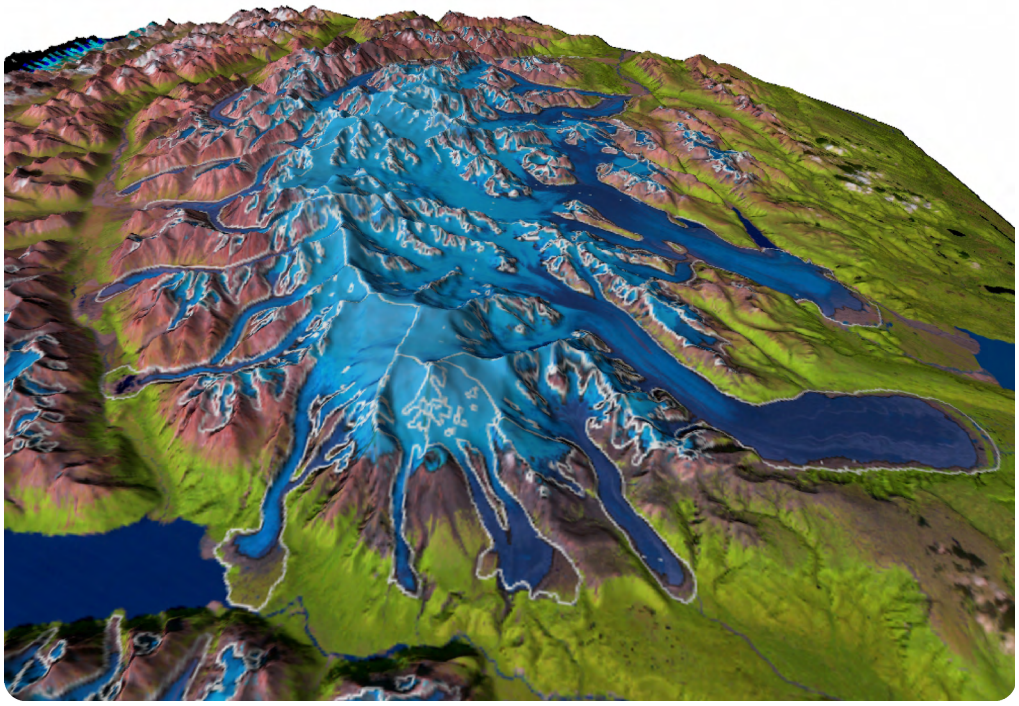

A3-1: Oblique view over the Tordrillo Mountains – Area change

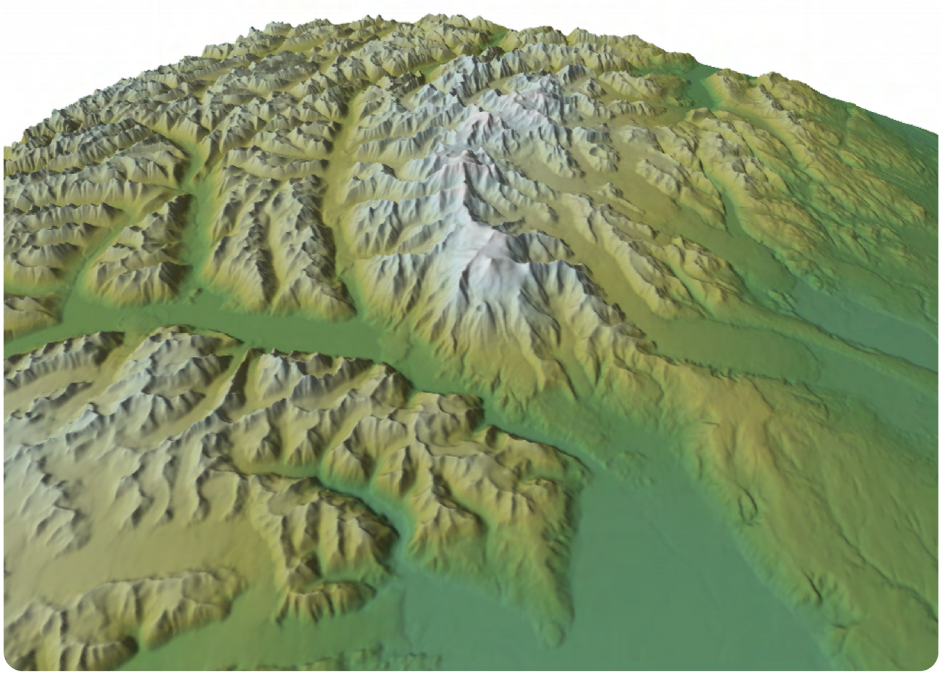

A3-2: Oblique view over the Tordrillo Mountains – DEM characteristics

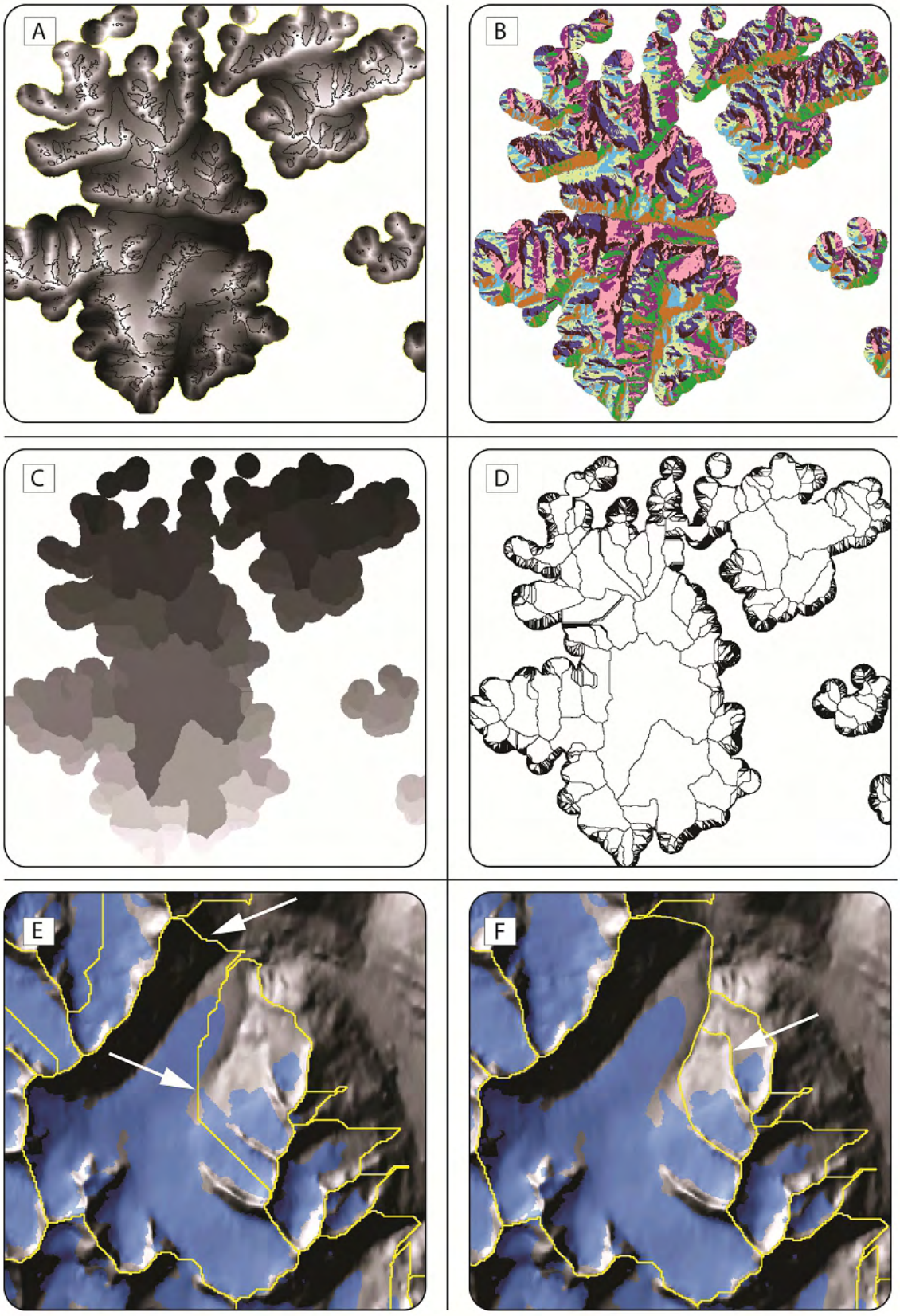

A4: Steps of the watershed analysis

Personal bibliography

- Peer reviewed articles

Le Bris, R. and Paul, F, 2012 (submitted). *Glacier-specific elevation changes in western Alaska.* Annals of Glaciology.

Le Bris, R. and Paul, F, 2012. *An automatic method to create flow lines for determination of glacier length: A pilot study with Alaskan glaciers.* Computer and Geosciences Journal.

Le Bris, R., Paul, F., Frey, H., Bolch, T., 2011. *A new satellite derived glacier inventory for Western Alaska.* Annals of Glaciology, 52(59), 135-143.

Berthier E, **Le Bris R**, Mabileau L, Testut L, Rémy F., 2009. *Ice wastage on the Kerguelen Islands (49° S, 69° E) between 1963 and 2006*. Journal of Geophysical Research.

Paul, F., N. Barrand, E. Berthier, T. Bolch, K. Casey, H. Frey, S.P. Joshi, V. Konovalov, **R. Le Bris**, N. Mölg, G. Nosenko, C. Nuth, A. Pope, A. Racoviteanu, P. Rastner, B. Raup, K. Scharrer, S. Steffen and S. Winsvold (in press) 2011. *On the accuracy of glacier outlines derived from remote sensing data.* Annals of Glaciology, 54 (63).

Rastner, P., T. Bolch, **Le Bris, R**., N. Mölg, H. Machguth and F. Paul, 2012. *The first complete glacier inventory for the whole of Greenland.* The Cryosphere Discussions, 6, 2399-2436

Paul, F., Frey, H. and **Le Bris, R**. 2011. *A new glacier inventory for the European Alps from Landsat TM scenes of 2003: Challenges and results.* Annals of Glaciology, 52 (59), 144-152.

- Conference presentations

Le Bris, R and Paul, F. *Correction factors for extrapolating measured mass balances to all glaciers in Alaska.* IGS, International Symposium on Glaciers and ice sheets in a warming climate, University of Alaska Fairbanks, Alaska, USA, 25.06.2012.

Le Bris, R and Paul, F. *A semi-automatic method to create central glacier flow lines: A pilot study with Alaskan glaciers.* European Geosciences Union General Assembly 2012, Vienna, Austria, 22.04.2012.

Le Bris, R. *A semi-automatic method to create central glacier flow lines: A pilot study with Alaskan glaciers.* 16th Alpine Glaciology Meeting, ETH Zürich, Switzerland, 02.02.2012.

Le Bris, R. *Glacier mapping using remote sensing satellite data*. Seminar presentation at the City College of New York, New York, USA, 08.04.2011.

Le Bris, R., Frey, H., Paul, F., Bolch, T. *A new glacier inventory for Western Alaska.* IGS International Symposium, Earth's Disappearing Ice Drivers, Responses and Impacts. A celebration of the 50th Anniversary of the Byrd Polar Research Center. Byrd Polar Research Center, Columbus, Ohio, USA, 17.08.2010.

Le Bris, R., Frey, H., Paul, F., Bolch, T. *Nouvel inventaire des glaciers de l'ouest Alaska créé à partir d'images satellites.* Journées de la Section de Glaciologie-Nivologie de la Société Hydrologique de France (SHF), Grenoble, 31.03-01.04.2010.

Le Bris, R., Berthier, E., Mabileau, L., Testut, L., and Rémy, F. *Ice wastage on the Kerguelen Islands (49°S, 69°E) between 1963 and 2006*. 7th Swiss Geoscience Meeting, Neuchâtel, 20.11.2009.

- Report

Le Bris, R. MSc thesis title: *Glaciologie de la calotte Cook aux Kerguelen*. Université de Caen, France, 2007.

- Technical report

Arendt, A., T. Bolch, J.G. Cogley, A. Gardner, J.-O. Hagen, R. Hock, G. Kaser, W.T. Pfeffer, G. Moholdt, F. Paul, V. Radić, L. Andreassen, S. Bajracharya, M. Beedle, E. Berthier, R. Bhambri, A. Bliss, I. Brown, E. Burgess, D. Burgess, F. Cawkwell, T. Chinn, L. Copland, B. Davies, H. De Angelis, E. Dolgova, K. Filbert, R. Forester, A. Fountain, H. Frey, B. Giffen, N. Glasser, S. Gurney, W. Hagg, D. Hall, U.K. Haritashya, G. Hartmann, C. Helm, S. Herreid, I. Howat, G. Kapustin, T. Khromova, C. Kienholz, M. Koenig, J. Kohler, D. Kriegel, S. Kutuzov, I. Lavrentiev, **R. Le Bris**, J. Lund, W. Manley, C. Mayer, E. Miles, X. Li, B. Menounos, A. Mercer, N. Moelg, P. Mool, G. Nosenko, A. Negrete, C. Nuth, R. Pettersson, A. Racoviteanu, R. Ranzi, P. Rastner, F. Rau, B.H. Raup, J. Rich, H. Rott, C. Schneider, Y. Seliverstov, M. Sharp, O. Sigurðsson, C. Stokes, R. Wheate, S. Winsvold, G. Wolken, F. Wyatt, N. Zheltyhina. 2012, *Randolph Glacier Inventory [v2.0]: A Dataset of Global Glacier Outlines. Global Land Ice Measurements from Space, Boulder Colorado, USA. Digital Media.*

Acknowledgements

Mes premiers remerciements vont à Frank Paul qui a été mon superviseur durant cette thèse. Je ne pourrai jamais suffisamment exprimer ma gratitude envers lui tant son aide mais surtout son enthousiasme et son immense compétence scientifique m'ont porté. Je ne pense pas que l'on puisse avoir un meilleur superviseur. Mille mercis à Frank pour tout ce qu'il m'a apporté et appris.

Je tiens à remercier Wilfried Haeberli pour m'avoir permis d'intégrer son équipe, pour son aide à travers ses conseils et son soutien. Une thèse est souvent un long chemin qui peut être épuisant. Wilfried, par son humanisme a eu ce talent de toujours être là au bon moment pour nous remotiver lorsque le doute s'installe. J'ai toujours trouvé en lui une écoute attentive et bienveillante ainsi qu'une source de connaissance glaciologique intarissable.

Bien que cette thèse représente les résultats de mon travail scientifique, je n'aurais pas pu réaliser seul ce projet. L'analyse que j'ai menée sur les changements des glaciers en Alaska s'appuie en effet sur des concepts et techniques développés précédemment par d'autres scientifiques. À cet égard, la collaboration avec mes collègues durant ces années a été des plus précieuses et des plus stimulantes. J'ai particulièrement apprécié l'émulation qui s'est créée avec Holger Frey sur le projet GlobGlacier pour l'aspect recherche mais aussi en "dehors" par -32°C au Svalbard notamment. Je n'oublierai jamais que nous avons marché ensemble dans les traces de Dark Vador:-)

J'aimerais également remercier chaleureusement ceux qui ont successivement partagé notre grand bureau toujours avec bonne humeur et entraide à savoir, Isabelle Gärdner-Roer, Stefanie Gubler, Andreas Hasler et Nico Mölg. Comment ne pas exprimer aussi ma gratitude à Philipp Rastner et Tobias Bolch pour leur amitié et notre collaboration sur la cartographie des glaciers ainsi qu'à Jeannette Nötzli et Christian Huggel également pour leur amitié et leur support. Un grand merci à Andreas Linsbauer avec qui nous avons traversé la dernière année de notre thèse jusqu'à la soutenance avec un encouragement mutuel et sincère. Merci à toute l'équipe 3G pour avoir créé un environnement de travail inspirant et chaleureux.

Un immense merci à Michèle pour son soutien indéfectible et ses encouragements. Toutes ses heures à discuter ensemble ont été indéniablement une des clés pour que j'achève ma thèse. Merci à tous mes amis et notamment à Pierre, Manuel, Sophie, Samuel.

Merci à toi Silke, en qui je trouve bien plus que du soutien.

Et comment avancer sans sa famille ? Merci à vous tous qui m'avez toujours soutenu, encouragé et conforté dans mes choix bien que ceux-ci m'aient souvent conduit loin de vous. Monique et Jean-Michel, sans vous je n'y serais pas arrivé, merci infiniment! Remerciements particuliers à mon oncle, à ma grand-mère et à ma mère.

À ma mère, je dédie cette thèse.